EVALUATING LAND-COVER CHANGE EFFECTS ON RUNOFF AND RECHARGE IN KAWELA, MOLOKA‘I, HAWAI‘I

A THESIS SUBMITTED TO THE GRADUATE DIVISION OF THE UNIVERSITY OF HAWAI‘I AT MĀNOA IN PARTIAL FULFILLMENT OF THE REQUIREMENTS FOR THE DEGREE OF

MASTER OF SCIENCE

IN

NATURAL RESOURCE AND ENVIRONMENTAL MANAGEMENT

MAY 2013

By

Sarah N. Rosa

Thesis Committee:

Ali Fares, Chairperson
Aly El-Kadi
Delwyn Oki

Keywords: Hydrological modeling, land-cover change, runoff, recharge, Moloka‘i, Hawai‘i

Acknowledgements

Mahalo nui loa to my committee members, Dr. Ali Fares, Dr. Aly El-Kadi, and Dr. Delwyn Oki, for helping me navigate through the thesis process. This study would not have been possible without their patience and guidance. I would also like to acknowledge Kolja Rotzoll for his help in downloading and processing the rainfall datasets used in the study. Without his persistence and perseverance the radar rainfall data would not have been incorporated into the study. Thank you to Jim Jacobi of the USGS for providing vegetation maps of the Kawela watershed and Ed Misaki of the Nature Conservancy for allowing us to access the Kamakou Nature Preserve. In addition, I would like to thank Steve Markstrom, Lauren Hay, Steve Regan, and Roland Viger of the USGS Precipitation-Runoff Modeling research group for their help in setting up the model. Lastly, I would like to thank my ʻohana, friends, and co-workers at the USGS PIWSC for their support throughout this process.

Abstract

The Precipitation Runoff Modeling System (PRMS), a modular, physically based, distributed-parameter modeling system, was used to develop a watershed model for Kawela, Moloka‘i to evaluate the impact of changing watershed characteristics on surface-water runoff and groundwater recharge. Available spatial information was processed in a geographic information system (GIS) environment and assigned to the delineated hydrologic response units (HRUs) within the watershed. PRMS simulates different parts of the hydrological cycle based on a set of user-defined modules, and each component of the hydrological cycle is computed by empirical relations or process algorithms. For each HRU, an energy and a water balance is computed; the sum of all of the HRU's water-budget components produces the watershed's total hydrological response. The model was manually calibrated using a climatic adjustment coefficient and this calibration resulted in a reasonable match between simulated and observed hydrographs and flow volumes. To further minimize any differences between the simulated and observed streamflow values, the model was automatically calibrated using PEST (Parameter ESTimation) software. The simulated total runoff volume was within 8.7 percent over the entire simulation period (04/01/2006-03/31/2010). Simulation results for the four-year period indicate that 91 percent of the precipitation that falls on the watershed is partitioned into evapotranspiration (43 percent) and groundwater recharge (48 percent). A much smaller percentage of rainfall is partitioned into runoff (8 percent) that is measured at the outlet of the watershed. The calibrated model was used to assess different watershed restoration and degradation scenarios and evaluate the hydrological system's sensitivity to changes in land cover. Compared to the current land cover, the tested land-cover change scenario of vegetation denudation resulted in a smaller

component of fog-drip, which translated to a 4 percent decrease in precipitation and consequently only a 1 percent increase in the amount of precipitation partitioned into runoff. However, vegetation restoration decreases runoff by 16 percent, which, by inference, would lead to reduced sediment loading of the nearshore environment. The amount of precipitation partitioned into recharge changed by less than 5 percent in both scenarios. PRMS is a helpful management tool that can be used to evaluate changes in runoff and recharge under different land-cover change scenarios.

TABLE OF CONTENTS

Page

LIST OF TABLES

LIST OF FIGURES

Figure **Page**

Chapter 1

INTRODUCTION

1.1 Background

The U.S Geological Survey's (USGS) Ridge to Reef project on the south shore of the island of Moloka'i in the Kawela watershed has been studying the link between watershed degradation and the degradation of the downstream nearshore reef environment since 1999 (Field et al., 2008). The main goal of this interdisciplinary project is to thoroughly understand the ecological connections within the watershed, and create a set of much needed tools to aid stakeholders in making their decisions regarding critical watershed and nearshore management issues.

In the past decade, multiple studies have been published and a variety of mapping efforts and field measurements concentrated on southern Moloka'i were recorded (Barnhardt et al., 2005; Bothner et al., 2006; Calhoun and Field, 2008; Carr and Nipper, 2003; Engels et al., 2004; Ogston et al., 2004; Presto et al., 2006; Roberts, 2001; Rodgers, et al., 2005; Stock and Tribble, 2010; Storlazzi et al., 2004). Extensive mapping, biological assessments, and sediment studies of the coastal communities of South Moloka'i (including Kawela) are summarized by Field et al. (2008). Geospatial datasets, including airborne and ground-based Light Detection and Ranging (LiDAR) topography and QuickBird imagery (Stock et al., 2009; Field et al., 2008), were also generated for the watershed and nearby areas. Since 2004, a USGS stream-gaging station in Kawela has been monitoring streamflow and sediment loads leaving the watershed to the coastal waters (U.S. Geological Survey, 2010a). Maps of geomorphic processes, infiltration rates, and plant communities have been prepared for the watershed and the surrounding areas (Stock et al., 2009; Price et al., 2007; Price et al., 2009). In 2007, an

experimental site on the Kawela ridge was established to measure rainfall, infiltration, runoff, erosion rate, and sediment transport. In 2008, a second site was established nearby and fenced to exclude ungulates. Vegetation surveys are currently (2013) being conducted at both sites by the USGS as a part of the USGS's Ridge to Reef project. In 2008, a study was started to determine the effect of plant roots on soil cohesion and determine how both native and invasive plants affect erosion. An annual water budget for Molokaʻi was created by the State of Hawaiʻi (1990), a monthly water budget was created by Shade (1997), and an updated water budget for the island is currently being formulated by the USGS. A numerical groundwater model for Molokaʻi (Oki, 1997) has been used to evaluate different withdrawal distributions (Oki, 2006). A refined groundwater model of central and southern Molokaʻi is currently being developed by the USGS.

Watershed models have been developed for other areas in Hawaiʻi to simulate the hydrology, sediment transport, climate change, and land-cover changes in Hawaiian watersheds. Shade (1984) used a distributed routing rainfall-runoff model (Dawdy et al., 1978) to simulate event-based runoff and sediment transport in Moanalua, Oʻahu resulting in errors of 35 percent or less for 50 percent of the events modeled. The successful application of the model to Moanalua indicated its applicability to a sub-tropical watershed and transferability potential (Shade, 1984). Sahoo et al. (2006) used the physically distributed modeling system MIKE SHE (DHI, 2003) to predict streamflow in Mānoa-Palolo, Oʻahu watersheds resulting in correlation coefficients greater than 0.7 between the measured and simulated streamflow. The results of the modeling indicated potential for use in Hawaiian watersheds with future refinements in input data (Sahoo et al., 2006). Polyakov et al. (2007) used the continuous, distributed

watershed model AnnAGNPS (Binger and Theurer, 2005) to simulate runoff and soil erosion in Hanalei, Kaua‘i resulting in annual simulations of runoff within 7 percent of the annual measured runoff and accurate simulations of monthly runoff (R^2=0.90) and sediment loads (R^2=0.85). The results of this study indicated that AnnAGNPS is mostly applicable for annual simulations of runoff and sediment loads in Hawaiian watersheds. Cheng (2007) used the distributed model N-SPECT (National Oceanic and Atmospheric Administration, 2004) to simulate runoff and sediment in the Hanalei, Kaua‘i and Hālawa, O‘ahu watersheds resulting in annual runoff volumes within 10 percent of observed values and unrealistic sediment amounts due to an unsuitable sediment delivery equation for Hawaiian watersheds. The results of this study indicated that N-SPECT is suitable to model annual runoff, but should not be used to simulate sediment transport for Hawaiian watersheds. Apple (2008) used the spatially distributed HSPF model (Bicknell et al., 2005) to simulate runoff and sedimentation in Kāne‘ohe, O‘ahu resulting in acceptable simulations of runoff for as fine as a weekly temporal resolution (R=0.89-0.93) and sedimentation on an annual basis (+/-38 percent). The results of this study indicated that HPSF is suitable for simulating runoff at various temporal scales, but should only be used on an annual time step to simulate sedimentation in Hawaiian watersheds. Safeeq and Fares (2011) used the physically distributed modeling system DHSVM (Wigmosta et al., 1994) to simulate the effects of climate change on the hydrology of the Mākaha, O‘ahu watershed. Results of this study indicated that DHSVM is suitable for simulating the hydrology of Hawaiian watersheds and the potential impact of climate-change scenarios on the streamflow and evapotranspiration of Hawaiian watersheds on a monthly and annual basis. Models that accurately predict runoff in Hawaiian watersheds on an annual, monthly, or even weekly time step exist. Models that

accurately predict runoff at a daily time step for Hawaiian watersheds are still needed. To best understand sediment discharge from Hawaiian watersheds, models that are capable of accurately simulating runoff at finer time scales are needed.

No rainfall-runoff models have been previously developed for the Kawela watershed study area (Figure 1), and therefore the watershed-scale rainfall-runoff process has not been sufficiently studied. A daily hydrological model of the watershed must be constructed to synthesize the available hydrological data to evaluate how changes to the watershed affect the amount of freshwater discharge, and by inference sediment transport, to the nearshore environment.

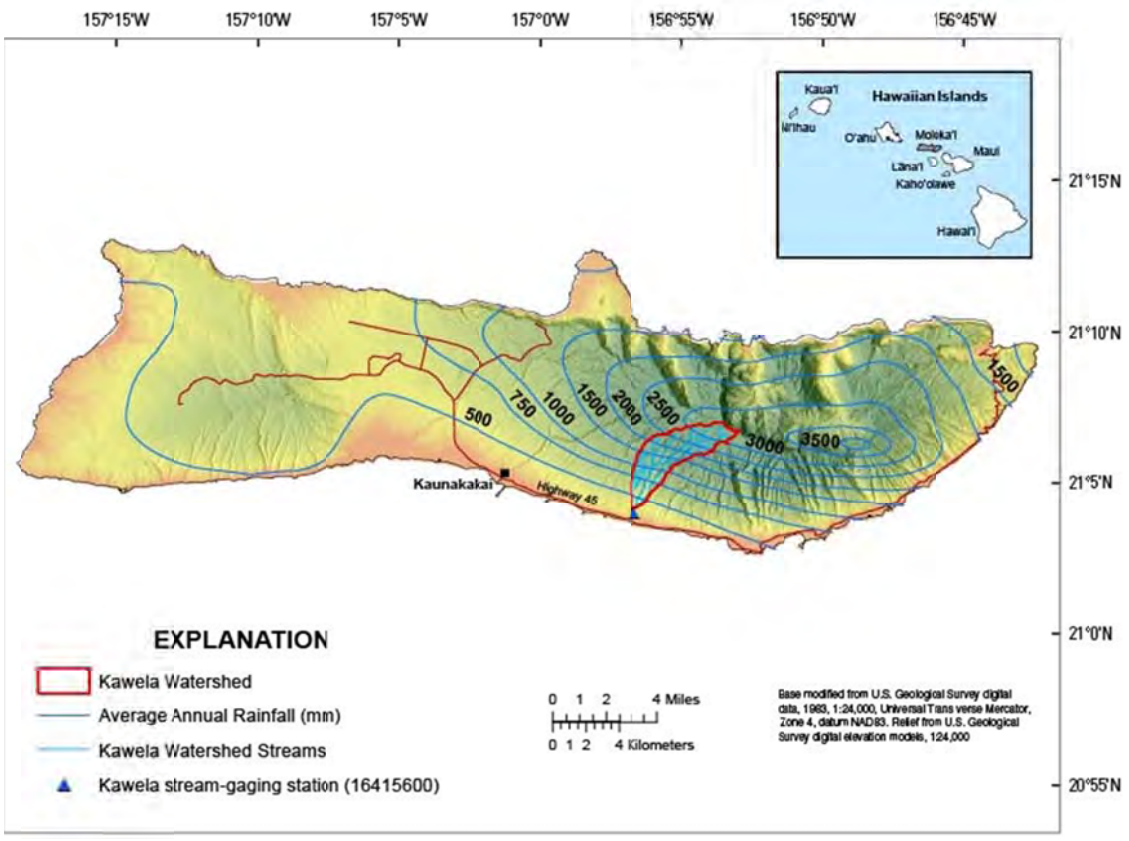

Figure 1. Location of the Kawela watershed and USGS Kawela stream-gaging station (16415600), Moloka‘i, Hawai‘i (contours of average annual rainfall modified from Giambelluca et al. (2012))

1.2 Purpose and Scope

The goal of this study is to evaluate the effect of land-cover changes on the hydrology (e.g., streamflow, runoff, groundwater recharge) of Kawela watershed. This goal will be met by (1) developing and evaluating the performance of a rainfall-runoff model, Precipitation-Runoff Modeling System (PRMS) (Leavesley et al., 1983), in simulating the hydrology of Kawela watershed, Moloka‘i, and (2) simulating selected land-cover changes with the model.

The PRMS model will serve as a management tool for stewards of this watershed and others that are hydrologically similar. Eventually, although not in the scope of this project, the model could be coupled with a sediment transport model to determine the effect of different land-use changes on the amount of sediment transported to the nearshore reef environment.

Chapter 2

DESCRIPTION OF STUDY AREA

The island of Moloka‘i has an area of approximately 673 square kilometers (km^2) making it the fifth largest island in the Hawaiian archipelago located in the middle of the Pacific Ocean. The island is about 63 kilometers (km) long and 16 km across at its widest point (Figure 1). Kawela watershed is located on the southern part of the island and east of the town of Kaunakakai. Kawela watershed has an area of approximately 13.73 km^2 with the northern drainage divide at the ridge of the East Moloka‘i volcano (an extinct shield volcano) at an altitude of 1,383 m and the outlet of the watershed at the USGS Kawela Gulch stream-gaging station (16415600) near the coast at an altitude of 14 m. The watershed is deeply incised by two main tributaries, West Fork Kawela Stream and East Fork Kawela Stream, that converge above the Kawela Gulch gaging station. Two surface-water diversions, one on each main fork of Kawela Stream, divert water in the upper perennial reaches of the stream. However, surface-water discharge measurements above and below the diversions and/or a visual inspection of the diversion system confirmed that only a small amount of flow is currently being diverted from the watershed, and therefore the diversions do not substantially affect the amount of flow measured at the gaging station at the outlet of the watershed. Runoff from the watershed may flow past the USGS stream-gaging station and discharge into the nearshore reef environment of Moloka‘i's south shore.

2.1 Climate

The climate of Moloka‘i is characterized by persistent cool northeasterly trade winds and mild temperatures throughout the year. The steep volcanic island topography produces spatial gradients for many of the components of climate, including rainfall,

solar radiation, humidity, and wind (Juvik and Juvik, 1998.) In Hawai‘i, two prominent features affect climate variability: the El Niño Southern Oscillation (ENSO) and the Pacific Decadal Oscillation (PDO) (Christensen et al., 2007; Giambelluca et al., 2008). Seasonal or inter-annual variability is driven by ENSO with drier periods during El Niño and wetter periods during La Niña. Typically, the dry summer season is from May to September and the rainy winter season is from October to April. Decadal variations in temperature in Hawai‘i historically have been closely coupled to the PDO, but recently temperature and the PDO have become decoupled (Giambelluca et al., 2008). Statewide streamflow trend analyses and interannual and interdecadal rainfall variations have shown that the climate in Hawai‘i is getting drier (Oki, 2004; Chu and Chen, 2005).

On Moloka‘i, prevailing northeasterly trade winds force warm moisture-laden air up the northeast side, or windward side, of the East Moloka‘i volcano causing the air to cool and condense resulting in cloud formation and an orographic rainfall pattern, with more rain typically falling at higher altitudes. The Kawela watershed study area is located in the leeward rain shadow of the East Moloka‘i volcano. Due to the orographic nature of rainfall in the watershed, the average annual amount of rainfall varies spatially within the watershed from about 3,300 millimeters (mm) near the headwaters to 380 mm near the coast (Figure 1). The long-term (1978-2007) average annual rainfall for Kawela watershed is 1,798 mm (Giambelluca et al., 2012). However, because of the mountain range’s parallel orientation to the prevailing trade winds, the maximum observed rainfall is less than other locations at the same altitude within Hawai‘i (Giambelluca et al., 1986). Leeward sides of the Hawaiian Islands, including the south shore of Moloka‘i, receive a high percentage of their annual rainfall from frontal storms approaching from the southwest, locally known as Kona storms. In the fall and winter months, Kona storms and

some storms arriving from the north bring heavy localized rainfall to areas like Kawela and can produce large amounts of surface-water runoff.

The upper forested part of Kawela watershed is often covered in clouds and therefore receives an added amount of precipitation, known as fog drip, through constant cloud mist or fog. In places like the upper part of Kawela watershed where fog persists the amount of water intercepted by vegetation may add a significant amount of precipitation input to the water budget (Juvik and Ekern, 1978).

2.2 Geology

The geology underlying Kawela watershed is comprised of the East Moloka‘i Volcanics and sedimentary deposits (Figure 2). The East Moloka‘i Volcanics is comprised of a lower member of shield-stage tholeiitic basalt and an upper member of postshield-stage alkalic basalt from the Pleistocene and Pliocene. The upper member forms a thin layer over the lower member, about 150 meters thick at the upper watershed divide and 15 meters thick at the lower sections of the watershed, making it the dominant surficial rock type in Kawela watershed. The lower member of the East Moloka‘i Volcanics is exposed in the two main stream channels of the West Fork Kawela Stream and the East Fork Kawela Stream. In general, the lower member of the East Moloka‘i Volcanics is considered more permeable than the upper member (Mink and Lau, 1992; Stearns and Macdonald, 1947). The coastal sedimentary deposits and sedimentary deposits, which extend slightly into the lower reaches of Kawela Stream, are classified as alluvium and dated to the Holocene (Stearns and Macdonald, 1947).

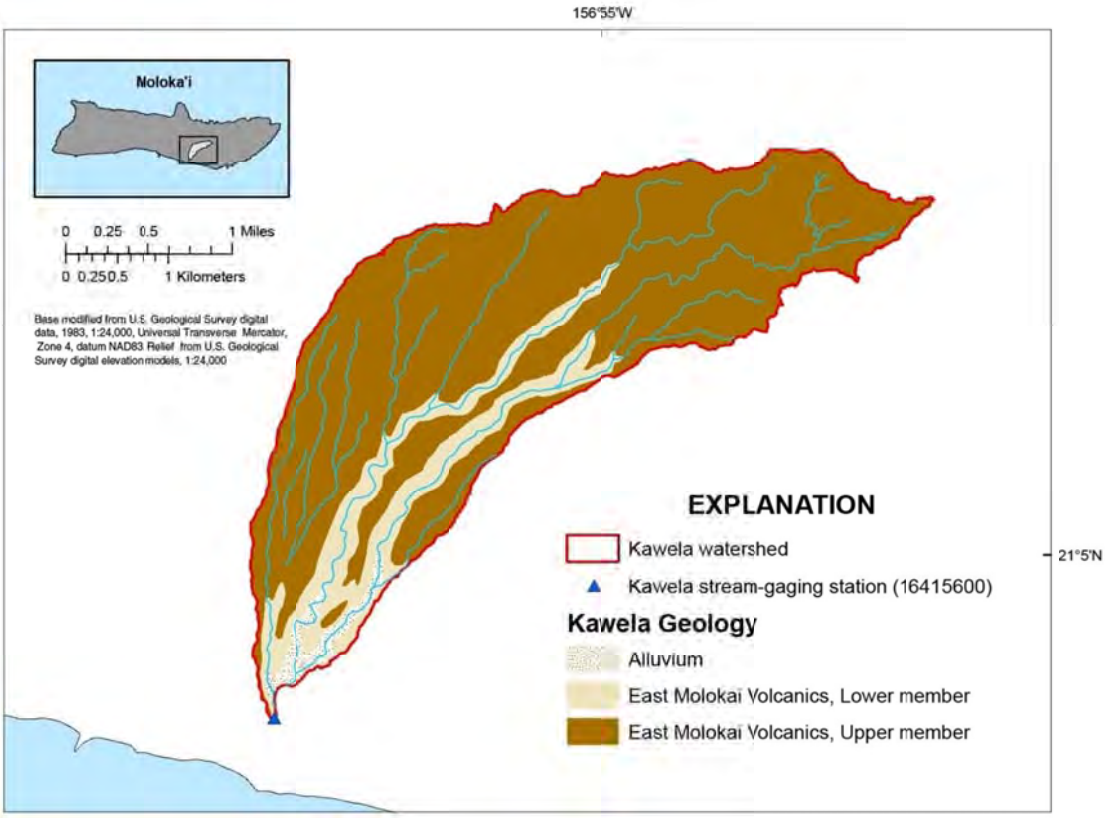

Figure 2. Surficial geology in the Kawela watershed, Moloka‘i, Hawai‘i (modified from Sherrod et al. (2007)).

2.3 Soils

In 2006, the Natural Resources Conservation Service published the U.S. General Soil Map (STATSGO2) with descriptions of the hydrological properties of soils for Moloka‘i. Kawela watershed is dominated by rocky, rough, and stony soil series that have a limited amount of soil water storage capacity (Table 1, Figure 3). The majority of the watershed is covered in soils that are either classified as highly erodible land or potentially highly erodible land. Only a small part of the watershed in the incised mid-to-lower reaches of the stream valleys is not classified as highly erodible land. In other areas of the watershed are small pockets of Kahanui gravelly silty clay, Naiwa silty clay loam, Niuli‘i silty clay loam, Olelo silty clay, Oli silt loam, Olokui silty clay loam, and Amalu peaty silty clay (Table 1).

Table 1. Average available water capacity of soils in the Kawela watershed, Moloka‘i, Hawai‘i.

[Average values were calculated using data from Natural Resources Conservation Service (2006) U.S. General Soil Map (STATSGO2)]

Soil Series	Available Water Capacity (cm per cm of soil)
Kahanui (gravelly silty clay)	0.11
Naiwa (silty clay loam)	0.10
Niuli‘i (silty clay loam)	0.13
Olelo (silty clay)	0.11
Oli (silt loam)	0.13
Olokui (silty clay loam)	0.19
Amalu (peaty silty clay)	0.24
Rock Land	0.14
Rock outcrop	0.00
Rough broken land	0.15
Rough mountainous land	0.14
Stony alluvial land	0.06
Tropaquods	0.19
Very stony land	0.09
Very stony land, eroded	0.09

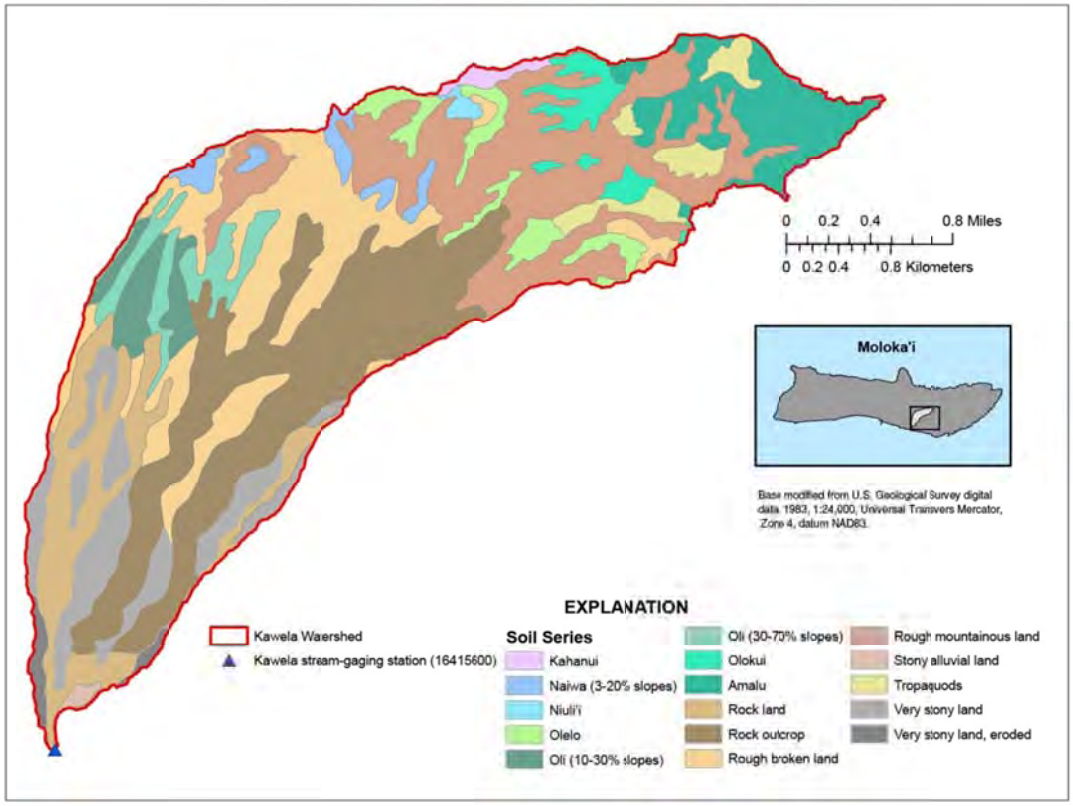

Figure 3. Soil series underlying Kawela watershed, Moloka‘i, Hawai‘i (modified from the Natural Resources Conservation Service (2006) U.S. General Soil Map (STATSGO2)).

2.4 Vegetation

Kawela watershed has been altered over the years due to Native Hawaiian settlement, plantation-scale agricultural development, spreading of invasive plants, expanding ungulate populations, and some residential development at the lower altitudes. The Native Hawaiian settlement of Moloka‘i some 1,400 years ago resulted in land-use changes associated with clearing and farming activities and the introduction of many crops for cultivation (Field et al., 2008; Weisler and Kirch, 1985). After European contact in the 1770s, a dramatic shift in land use resulted from the introduction of grazing animals (goats, sheep, pigs, horses, and cattle) and commercial farming (Field et al., 2008). These introduced grazing animals began the denudation of vegetation in Hawaiian landscapes that continues to present day (Field et al., 2008). Clearing of the land in the 1800s for sugarcane plantations also left lasting changes to the environment of southeastern Moloka‘i (Field et al., 2008).

Efforts have been undertaken to halt and reverse some of the destructive effects that the land-use changes have had on the environment and overall watershed processes of Moloka‘i. A cloud forest fenced off in the upper one-third of the watershed dominated by a closed mesic or wet ‘ohia lehua (*Metrosideros polymorpha*) forest and mixed mesic native shrubs survives and is being managed by the Nature Conservancy. The middle third of the watershed consists of bare areas, sparse grass or shrub cover, and ‘a‘ali‘i (*Dodonaea viscosa*) shrub land. The stream channels are dominated by kiawe (*Prosopis pallida*) with an alien grass understory, and the lower one third of the basin is dominated by a sparse distribution of alien grasses and ‘ilima (*Sida fallax*) shrubs (Jacobi, 2011a). The vegetation in the middle of the watershed and at the coast is being heavily grazed by

ungulates (Stock and Tribble, 2010). The current distribution of trees, shrubs, grasses, and bare ground areas is shown in Figure 4 (Jacobi, 2011a).

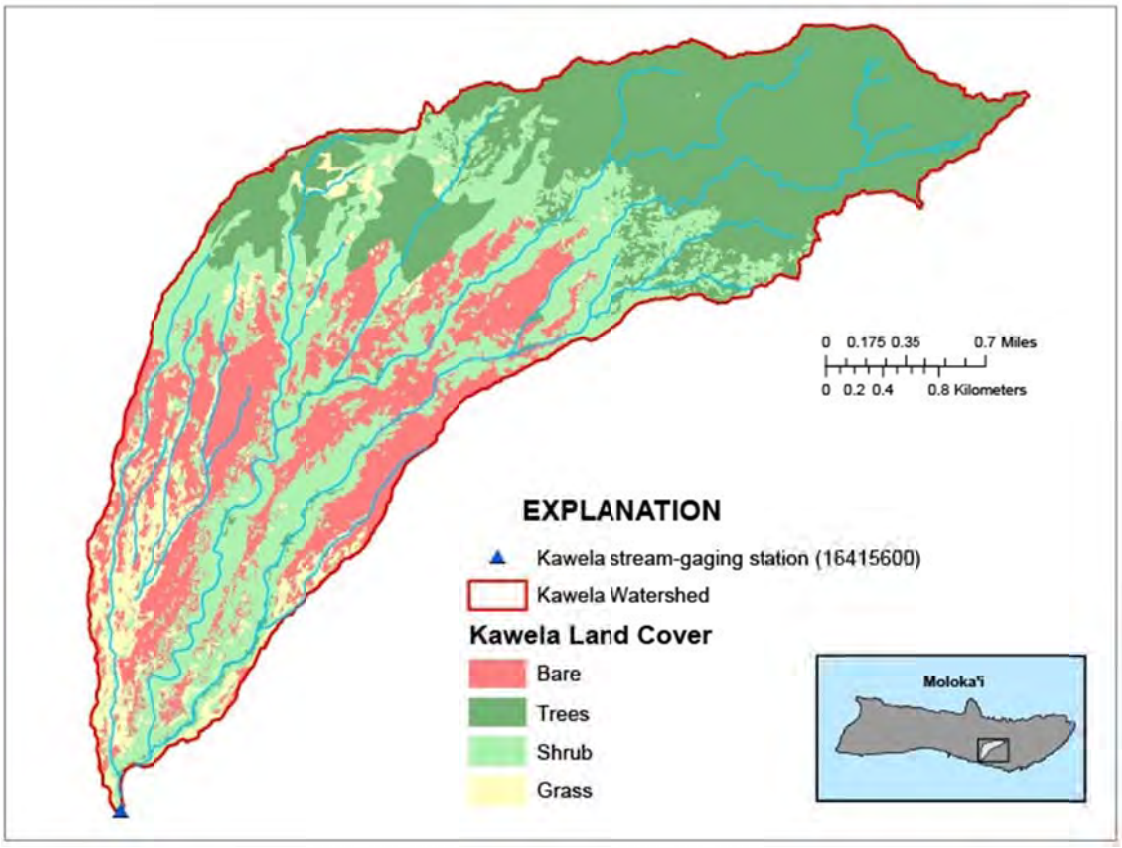

Figure 4. Current distribution of generalized vegetation classes and bare areas in the Kawela watershed, Moloka‘i, Hawai‘i (modified from Jacobi (2011a)).

2.5 Runoff Characteristics

The USGS Kawela Gulch stream-gaging station 16415600 (U.S. Geological Survey, 2010 a), in operation from October 1, 2004 to September 30, 2011, collected discharge and suspended-sediment data for Kawela watershed. For the period of record, the flow that is equaled or exceeded 90 percent of the time (Q_{90}) is 0 cubic meters per second (m^3sec^{-1}). The Q_{90} flow is commonly used to characterize low flows in a stream. The flow that is equaled or exceeded 50 percent of the time (Q_{50} or median flow) is also 0 m^3sec^{-1} for the period of record. For the period of record, flow that is equaled or exceeded

10 percent of the time (Q_{10}) is 0.21 m^3sec^{-1}. The mean annual flow for the period of record, October 1, 2004 to September 30, 2011 (8 years), is 0.08 m^3sec^{-1}. The highest annual mean flow, 0.13 m^3sec^{-1}, occurred in water year (12-month period from October 1 through September 30) 2008, while the lowest annual mean flow of 0.05 m^3sec^{-1} occurred in water year 2009. The Kawela Stream, like several other streams on the southern leeward coast of Moloka‘i, is only perennial in its upper reaches mainly due to seepage loss of the stream water before it reaches the stream-gaging station. The Kawela Gulch stream-gaging station indicates that near the ocean, the stream only flows about 30 percent of the time (Figure 5). The runoff characteristics in Kawela watershed are greatly influenced by the seasonal rainfall pattern. Flow in the upper reaches of Kawela during the dry summer months is sustained by base flow (groundwater input to the stream) resulting in a relatively constant flow. Kawela streamflow is flashy due to the relatively small drainage area, steep terrain, and intense rainfall in the wet winter. Currently, surface-water diversions are maintained by Moloka‘i Properties Limited (commonly referred to as Moloka‘i Ranch) on both the East and West Forks of Kawela Stream, although these diversions do not substantially affect the discharge measured at the outlet of the watershed by the Kawela Gulch stream-gaging station.

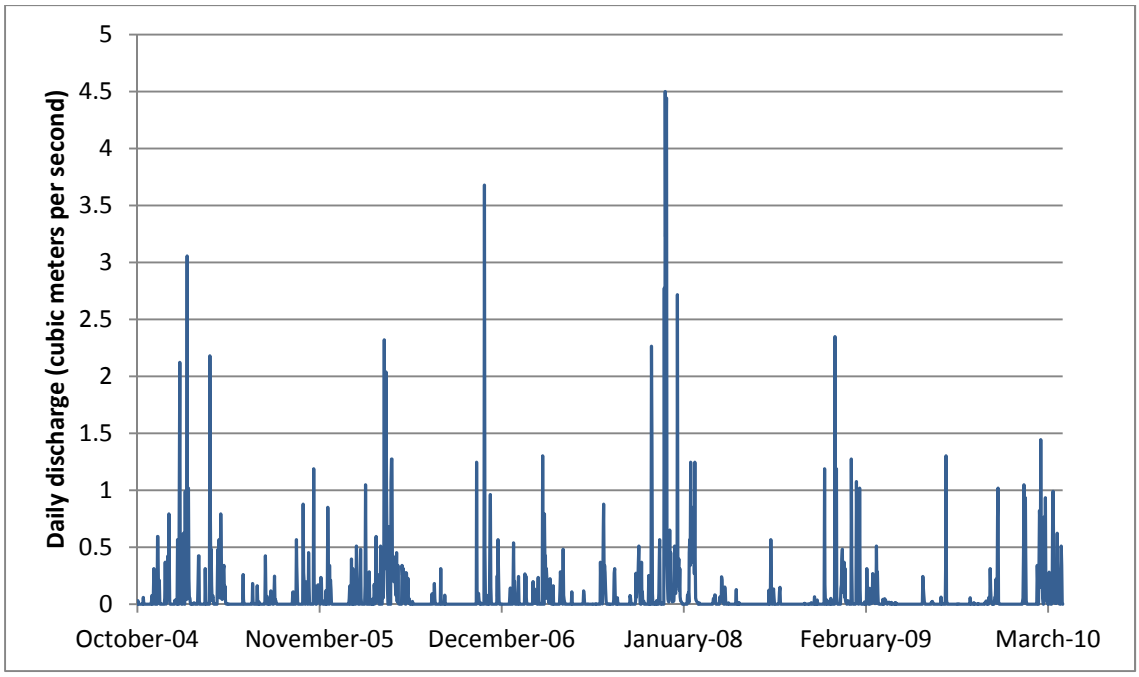

Figure 5. Daily mean discharge for USGS stream-gaging station 16415600 Kawela Gulch near Moku, Moloka‘i, Hawai‘i from 10/01/2004 to 4/25/2010.

Chapter 3

RAINFALL-RUNOFF MODEL

3.1 Precipitation-Runoff Modeling System (PRMS)

The PRMS software is well documented (Leavesley et al., 1983; Leavesley and Stannard, 1995; Markstrom et al., 2008) and has been used in various studies for water-resources research (Yeung, 2004), long-term precipitation trend analysis (Bae et al., 2008), flood analysis (Goode et al., 2010), and prediction of the hydrological response to climate and land-use changes (Chang and Jung, 2010; Legesse et al., 2003; Notter et al., 2007). The software, developed by the USGS (Leavesley et al., 1983), is a modular, physically based, distributed-parameter modeling system that was developed as a tool to evaluate the impact of changing watershed characteristics on surface-water runoff and recharge of a watershed. The model can be run in either a daily mode using daily time steps or a storm mode using hourly time steps (Leavesly et al., 1983). For this study, PRMS was run in the daily mode using daily datasets for the Kawela watershed.

PRMS simulates different parts of the hydrological cycle through a set of inter-connected user-defined modules (Table 2, Figure 6). Each component of the hydrological cycle in PRMS is computed by empirical relations or process algorithms. By taking into account watershed characteristics, including slope, aspect, altitude, land cover, soil type, and temperature and rainfall distribution, the watershed can be divided into homogeneous units called hydrologic response units (HRUs). These HRUs are assumed to be homogeneous with regard to their physical properties and hydrological response. PRMS must implement these HRUs to have distributed-parameter capabilities and account for the spatial variability within a watershed. To account for heterogeneity within a given HRU, area-weighted averages are calculated for each characteristic within

a HRU. For each of these units, an energy and water balance is computed and then the HRU water-budget components are summed to produce the entire watershed's hydrological response (Markstrom et al., 2008).

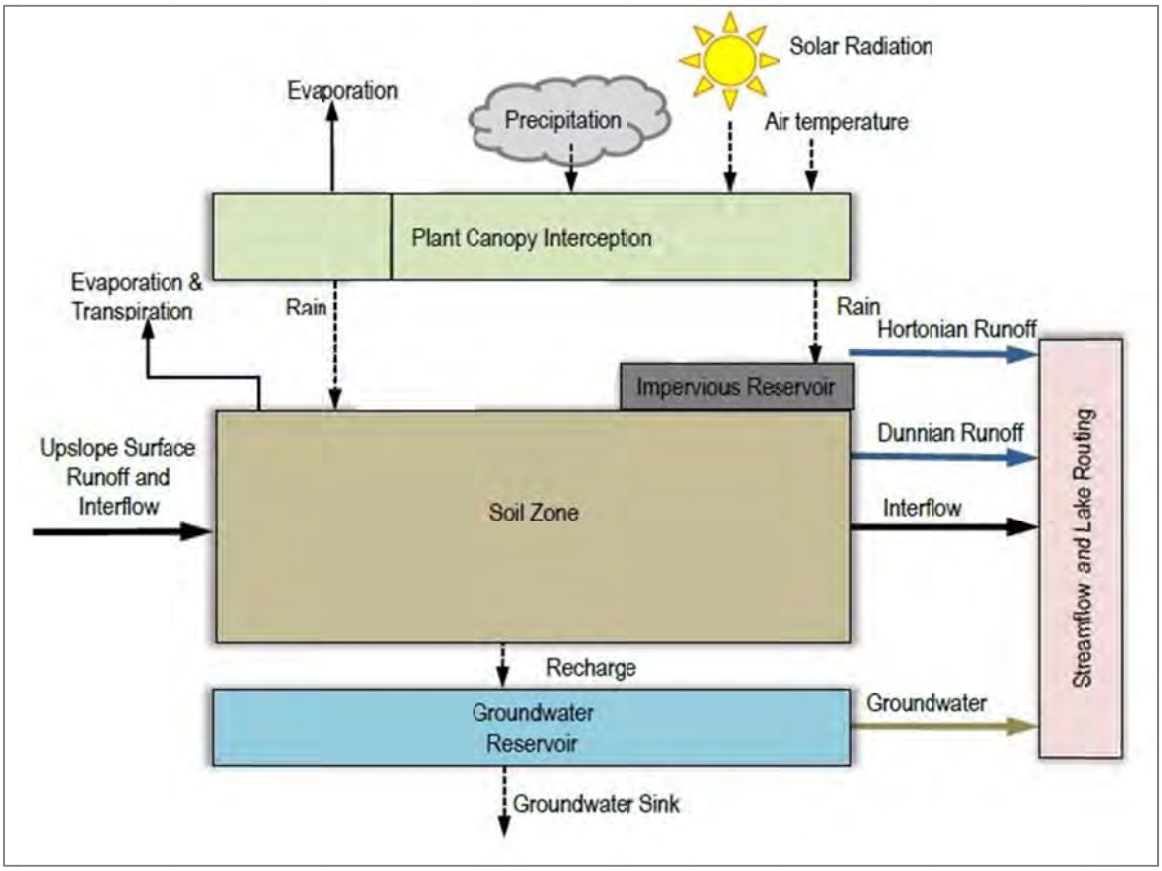

Figure 6. Hydrological processes simulated by the Precipitation-Runoff Modeling System (modified from Markstrom et al. (2012)).

Table 2. Descriptions of modules used for the PRMS Kawela model.
[Table modified from Markstrom et al. (2012). HRU: Hydrologic response unit]

Module Name	Description
	Basin-definition process
basin	Defines shared watershed-wide and HRU physical parameters and variables.
	Cascading-flow process
cascade	Determines computational order of the HRUs and groundwater reservoirs for routing flow downslope.
	Solar-table process
soltab	Compute potential solar radiation and sunlight hours for each HRU for each day of year; modification of soltab_prms.
	Time-series data process
obs	Reads and stores observed data from all specified measurement stations.
	Combined climate-distribution process
xyz_dist	Determines the form of precipitation and distributes precipitation and temperature to each HRU using a multiple linear regression of measured data from a group of measurement stations or from atmospheric model simulation.
	Solar-radiation distribution process
ddsolrad	Distributes solar radiation to each HRU and estimates missing solar radiation data using a maximum temperature per degree-day relation.
	Transpiration-period process
transp_frost	Determines whether the current time step is in a period of active transpiration by the killing-frost method.
transp_tindex	Determines whether the current time step is in a period of active transpiration by the temperature-index method.
	Potential-evapotranspiration and total precipitation process
climate_hru	Reads distributed values of potential evapotranspiration and total precipitation (rainfall and fog drip) directly from files.
	Canopy-interception process
intcp	Computes volume of intercepted precipitation, evaporation from intercepted precipitation, and throughfall that reaches the soil.
	Surface-runoff process
srunoff_smidx	Computes surface runoff and infiltration for each HRU using a nonlinear variable-source-area method allowing for cascading flow.
	Soil-zone process
soilzone	Computes inflows to and outflows from soil zone of each HRU and includes inflows from infiltration, groundwater, and upslope HRUs, and outflows to gravity drainage, interflow, and surface runoff to downslope HRUs
	Groundwater process
gwflow	Sums inflow to and outflow from PRMS groundwater reservoirs; outflow can be routed to downslope groundwater reservoirs and stream segments.
	Streamflow process
strmflow	Computes daily streamflow as the sum of surface runoff, shallow-subsurface flow, detention-reservoir flow, and groundwater flow.
	Summary process
basin_sum	Computes daily, monthly, yearly, and total flow summaries of volumes and flows for all HRUs.

3.2 Data

PRMS requires precipitation, and minimum and maximum air temperature data that can be generated with the USGS Downsizer application (Ward-Garrison et al., 2009) by compiling data from available climate-station records into a data file recognized by PRMS. USGS streamflow data stored in the National Water Information System (NWIS) for the Kawela Gulch stream-gaging station (16415600) were also downloaded using the USGS Downsizer and used to calibrate PRMS based on the measured daily streamflow. The USGS Downsizer program automates the quality-assurance/quality-control (QA/QC) checks while formatting the data into an appropriate file that can be used with PRMS (Ward-Garrison et al., 2009). The data file compiled by the USGS Downsizer was then supplemented with other precipitation data that were either not in the database used by the Downsizer (NEXRAD-derived rainfall data) or were collected after the September 30, 2009 cut-off date in the version of the Downsizer used to assemble the PRMS data file.

3.2.1 Streamflow Data

Daily streamflow data from the Kawela Gulch stream-gaging station (16415600), operated by the USGS since October 2004, were used to calibrate the PRMS Kawela watershed model. The Kawela Gulch stream-gaging station is 305 m upstream of Highway 45 and 8 km southeast of Kaunakakai town at latitude 21°04'11.9"N, longitude 156°56'54.0"W. Measured daily streamflow was used directly without any adjustments. Records from Kawela Gulch stream-gaging station are rated poor due to the small diversions in the upper stream reaches, although these diversions likely do not substantially affect the measured discharge at the gaging station. A poor rating means that the daily discharges have less than a "fair" accuracy rating. A "fair" accuracy rating is

defined as having about 95 percent of the discharges within 15 percent of the true discharge value.

3.2.2 Climate Data

Temperature

Minimum and maximum temperature data used in the PRMS Kawela model (Figure 7) were downloaded from four climate stations across the island (Table 3); they were compiled from available climate-station records using the USGS Downsizer application (Ward-Garrison et al., 2009). The location, altitude, operator, and period of record used in the model for each climate station are described in Table 3.

Table 3. Climate stations used in the PRMS Kawela model
[NWS: National Weather Service, NOAA: National Oceanic and Atmospheric Administration]

Station	Longitude (Decimal Degrees)	Latitude (Decimal Degrees)	Altitude (meters)	Operator	Period of Record Used in Model
Molokaʻi AP (Airport) 524	-157.0921847	21.1551500	136	NWS	10/01/04-04/25/10
Kepuhi Sheraton 550.2	-157.2430153	21.1926503	43	NOAA	10/01/04-04/30/08
Kalaupapa 563	-156.9805185	21.1884809	9	NOAA	10/01/04-07/31/06
Puʻu O Hoku Ranch 542.1	-156.7471853	21.1467991	216	NOAA	10/01/04-11/30/08

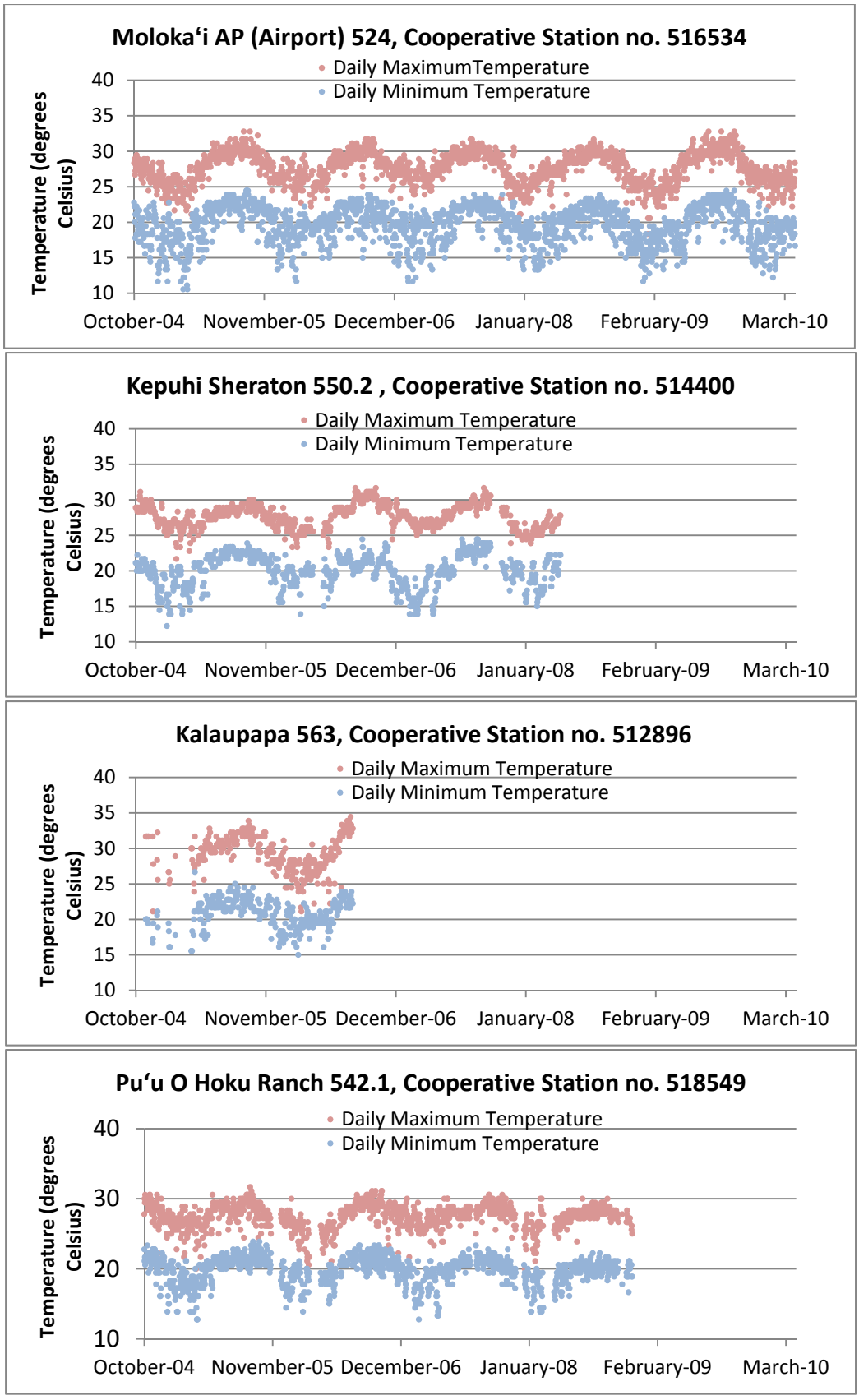

Figure 7. Daily minimum and maximum temperature data used in the PRMS Kawela model.

Rainfall

Rainfall data in the form of rain-gage data and Next-Generation Radar (NEXRAD) estimated data were available for the island of Moloka‘i. An analysis (Rotzoll and El-Kadi, 2012) comparing the rain-gage data and NEXRAD-derived rainfall data over the Kawela watershed indicated a poor correlation between radar and gage rainfall rates, particularly at low rates. Differences in the NEXRAD-derived rainfall and rain-gage data could be due to the size of the radar polygons (1 km^2), the binning of the radar rainfall in variable increments, and the uncertainty in the measured rain-gage data due to mechanical issues or reporting errors. The analysis determined that NEXRAD-derived rainfall data would be a promising rainfall input for a rainfall-runoff model, but that it would be best to limit use of radar rainfall to supplement areas without a dense network of rain gages or for times when rain-gage data are not available (Rotzoll and El-Kadi, 2012). Due to the sparse network of rain gages and lack of rain gages located near the headwaters of the watershed a combination of NEXRAD-derived rainfall and rain-gage data was used to estimate rainfall for Kawela watershed. The NEXRAD-derived rainfall data were available for the entire span of the modeled period and were downloaded from the National Climatic Data Center (2007), and for each of the 32 NEXRAD polygons that covered Kawela watershed a daily rainfall amount was calculated. The NEXRAD-derived rainfall data originally were in the form of reflectivity (Ref) and were converted to rainfall (L) using the following standard calibration equation: $L=250*Ref^{1.2}$ (National Weather Service, 2010). Daily rainfall data from five rain gages from areas surrounding the watershed and correlated to streamflow in Kawela watershed were also available, however only one of the rain gages was actually located within Kawela watershed, the USGS Kawela Ridge to Reef gage (Kawela Field Site), at

an altitude of 685.8 m (Table 4, Figure 8). Both the radar data and rain-gage data used in the PRMS Kawela model were downloaded and processed by Rotzoll and El-Kadi (2012). Daily rainfall for the five rain gages and 32 radar bin centroids are shown in Figures 9 and 10 respectively.

Table 4. Rain-gaging stations used in the PRMS Kawela model
[Data from Rotzoll and El-Kadi (2012). USGS: U.S. Geological Survey, RAWS: Remote Automated Weather Stations , NOAA: National Oceanic and Atmospheric Administration]

Station	Longitude (Degrees)	Latitude (Degrees)	Altitude (meters)	Operator	Period of Record Used in Model
Kawela Field Site	-156.926	21.094	686	USGS	10/03/07-04/18/10
Kawela Fan	-156.950	21.064	2	Bill Feeter	10/01/04-12/31/07
Kamiloloa	-156.947	21.115	833	RAWS	10/01/04-04/25/10
Kānoa Beach	-156.963	21.069	6	Doug Macmillan	10/01/04-04/25/10
Kaunakakai	-157.018	21.094	21	NOAA	10/01/04-03/31/10

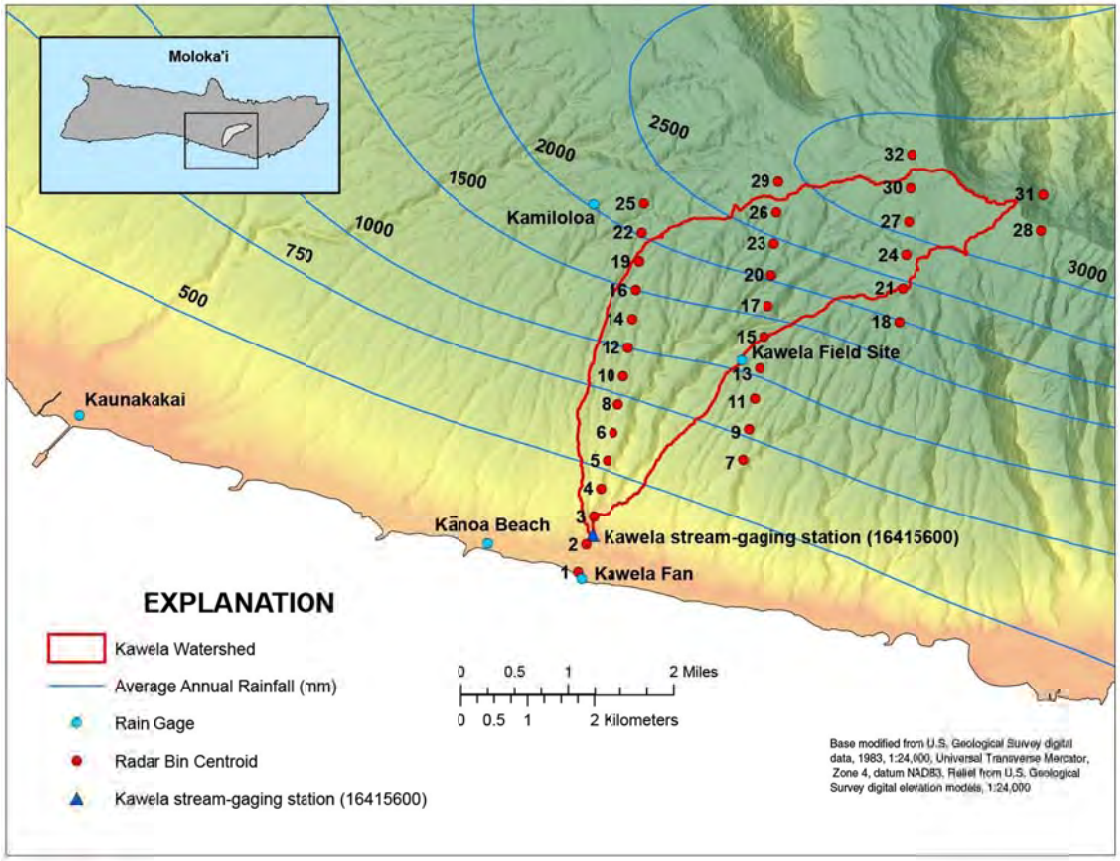

Figure 8. Location of rain gages and centroids of each radar bin used as rainfall input data to the PRMS Kawela model.

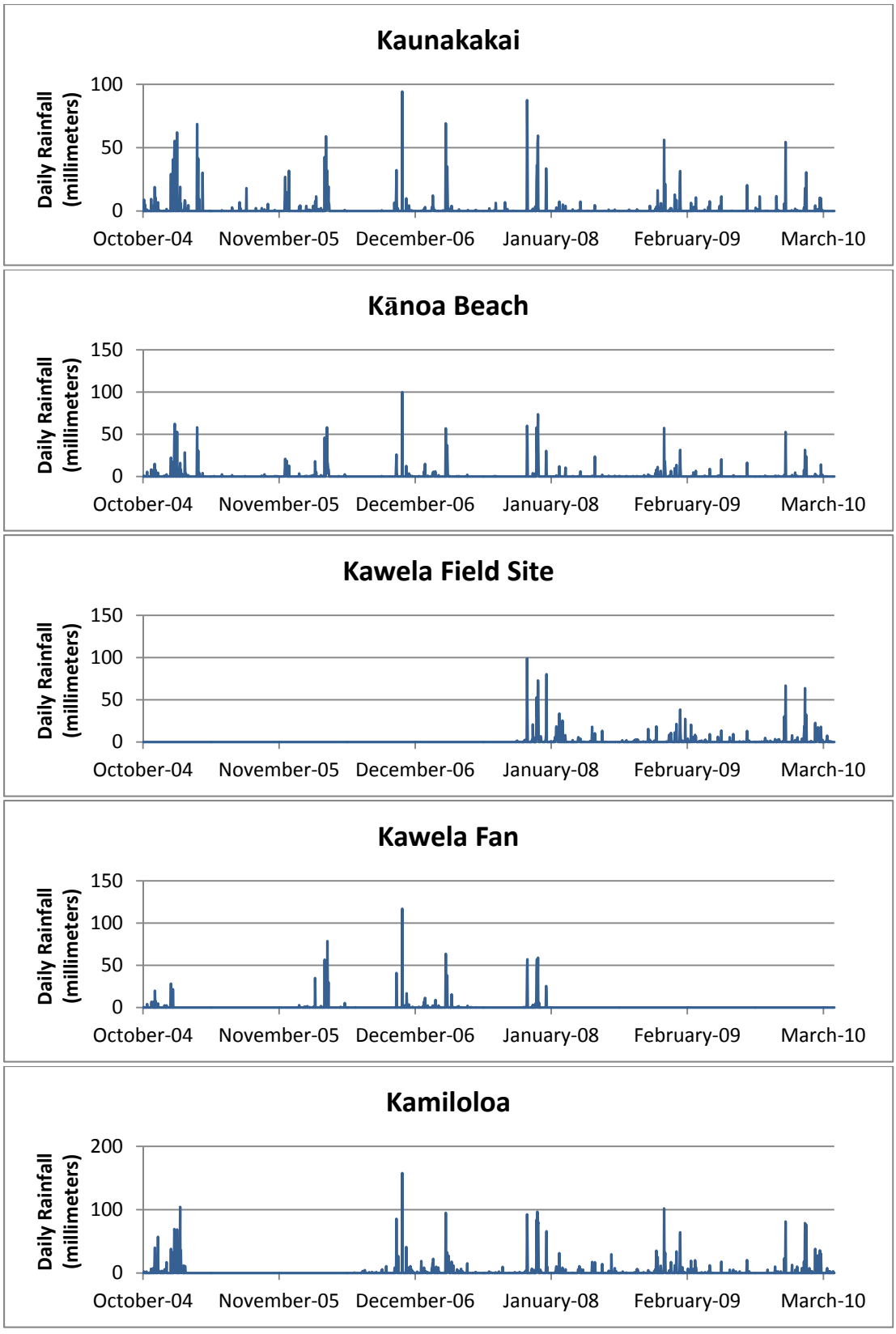

Figure 9. Daily rainfall data for Kawela area rain gages.

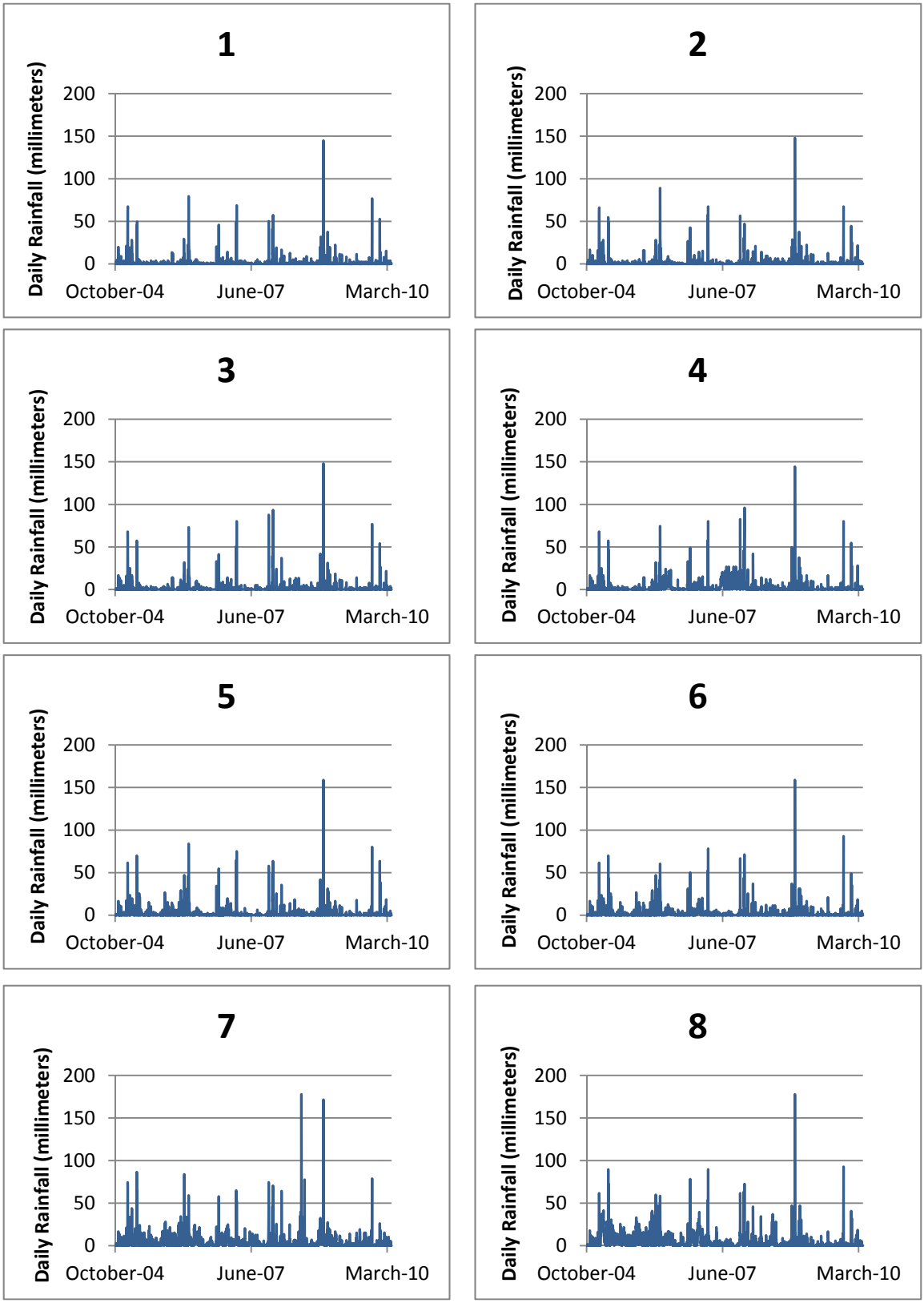

Figure 10. Daily radar rainfall at each radar polygon centroid.

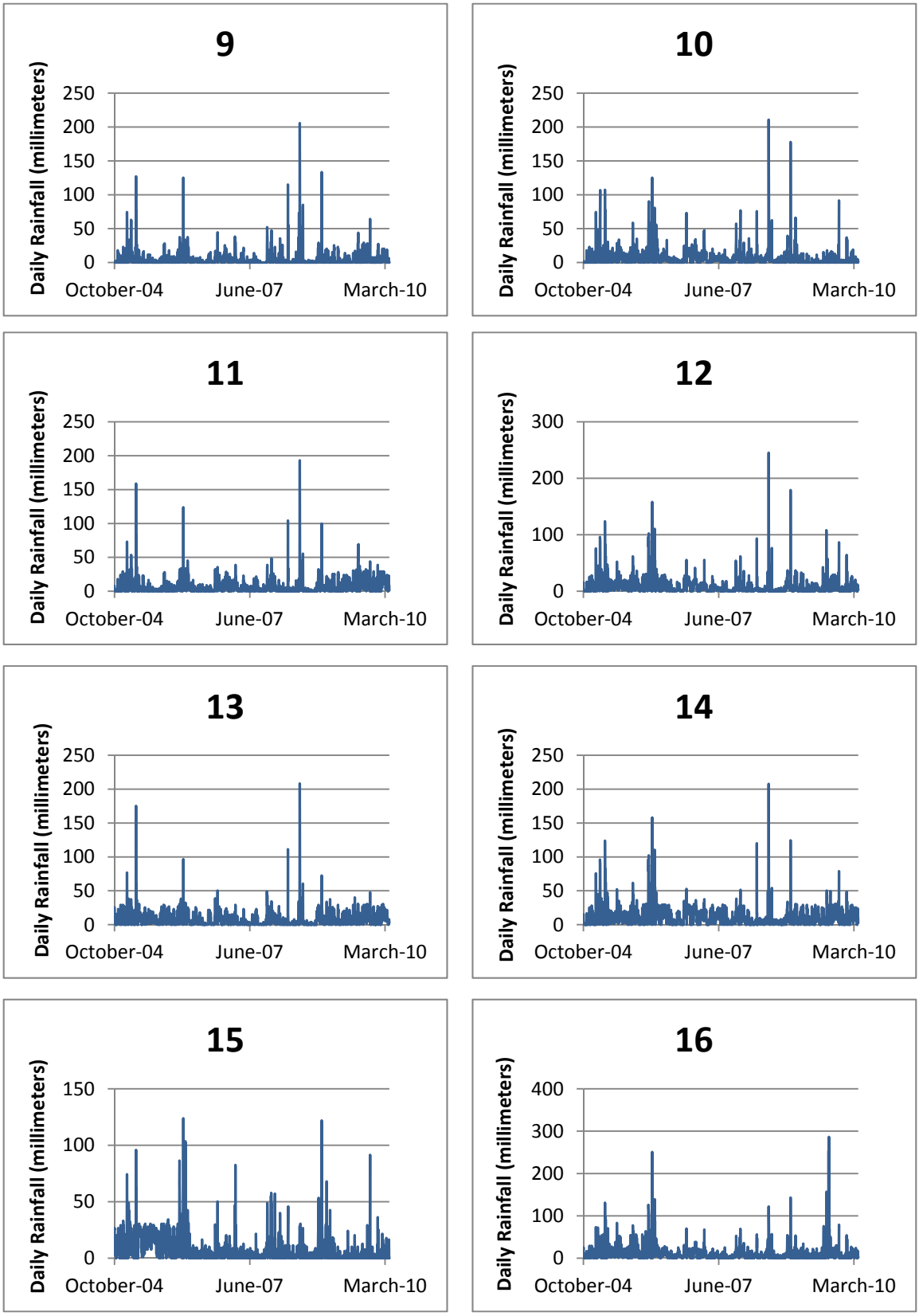

Figure 10. Daily radar rainfall at each radar polygon centroid–Continued.

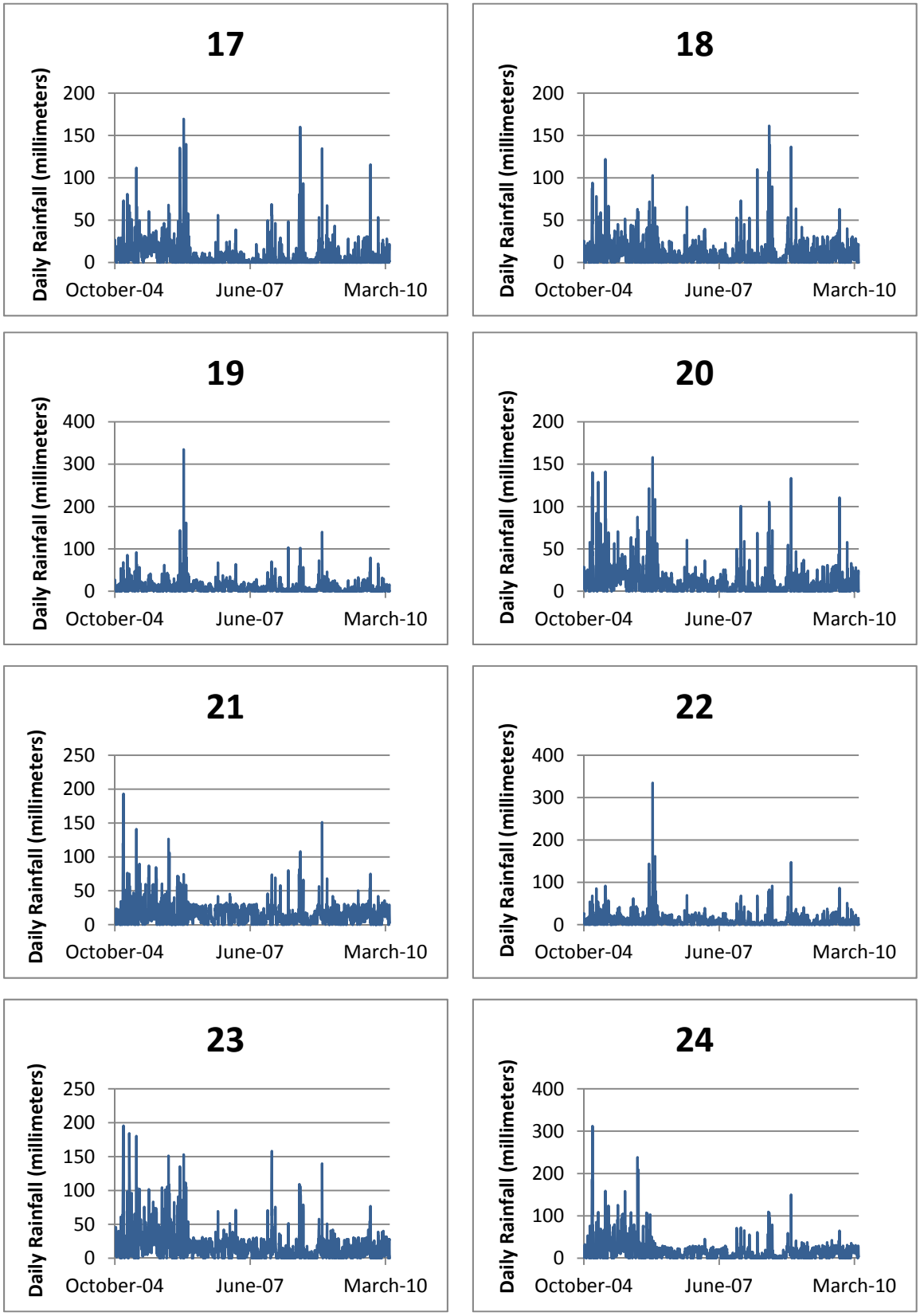

Figure 10. Daily radar rainfall at each radar polygon centroid–Continued.

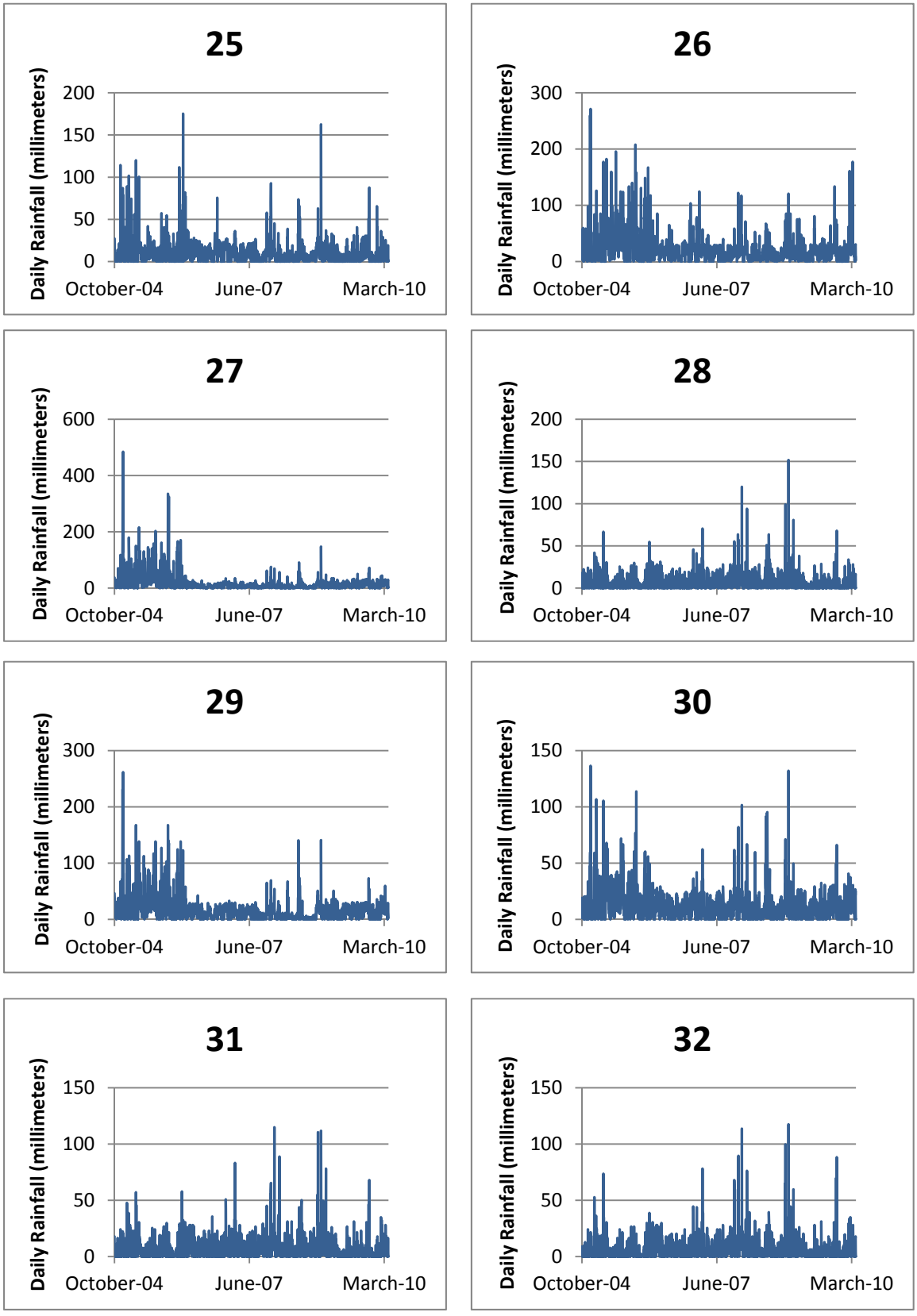

Figure 10. Daily radar rainfall at each radar polygon centroid–Continued.

Due to the sparse network of rain gages, limited rainfall data within the watershed, and lack of rain gages located near the headwaters of the watershed a combination of NEXRAD-derived rainfall and rain-gage data was used to estimate rainfall for Kawela watershed. A daily mean-field bias correction was used to correct the radar rainfall estimates at each of the 32 polygon centroids (Figure 8 and 10) using rain-gage data (Smith et al., 2012). The daily observations from the 5 rain gages surrounding Kawela watershed (Table 4, Figure 5) were used to apply the daily mean-field bias correction using the following equation:

$$B_i = \frac{\sum_{j \in Si} G_{ij}}{\sum_{j \in Si} R_{ij}} \quad (1)$$

where G_{ij} is the daily cumulative rainfall for day i from gage j, R_{ij} is the daily cumulative rainfall for day i from the radar pixel containing gage j, and S_i is the index of rain gages for which both rain gage and radar have positive rainfall accumulations for the day (Smith et al., 2012). To apply the bias correction, B_i is multiplied by each daily radar rainfall value at each of the 32 polygon centroids overlapping Kawela watershed. The bias correction was applied if at least one radar-rain gage pair with positive rainfall was available. No correction was applied if no pairs were available. Rainfall estimated from NEXRAD data and corrected with data from the five Kawela area rain gages using the mean-field bias correction was used as input for the final Kawela watershed model (Figure 11).

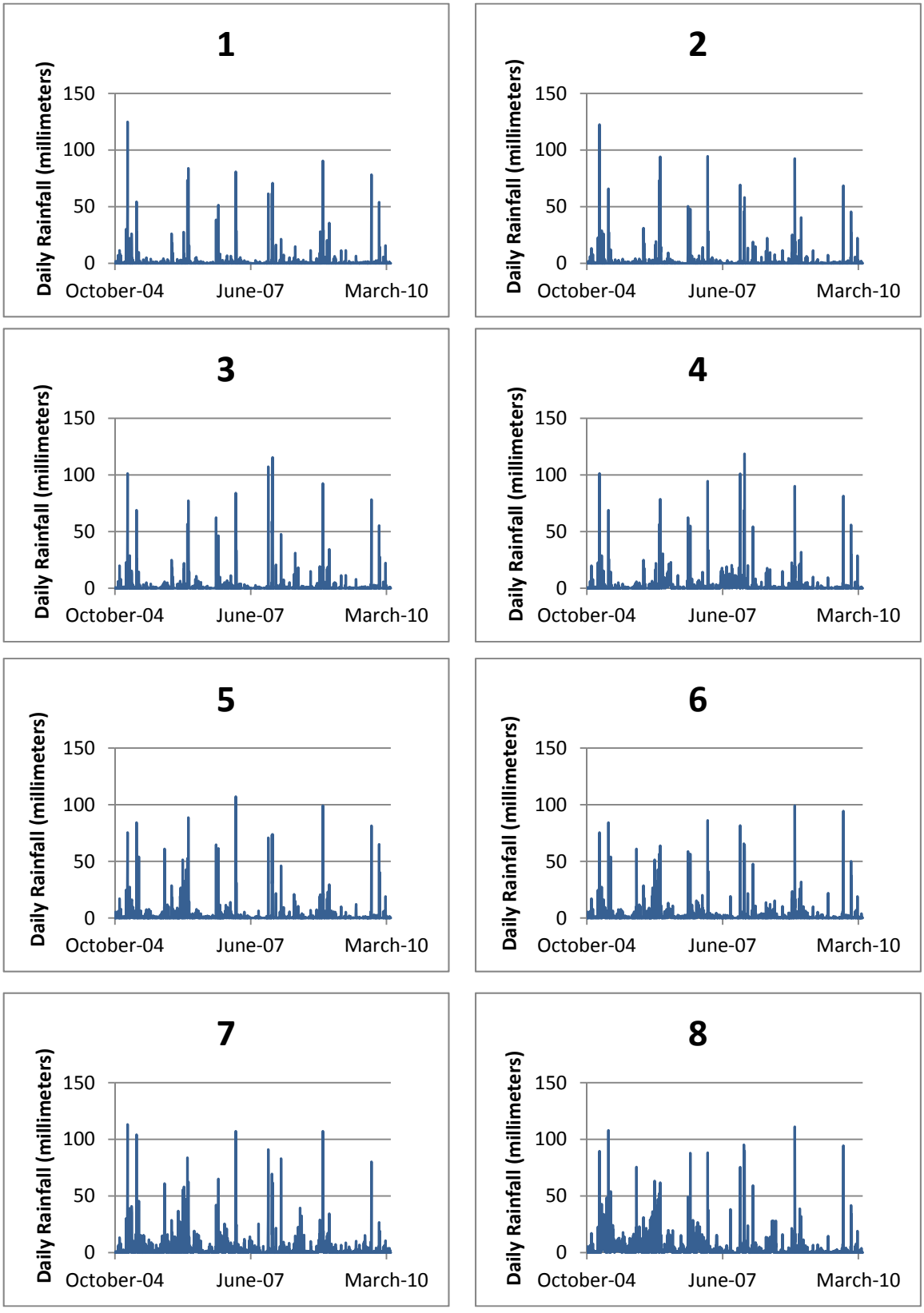

Figure 11. Daily mean-field bias corrected rainfall used in the PRMS Kawela model.

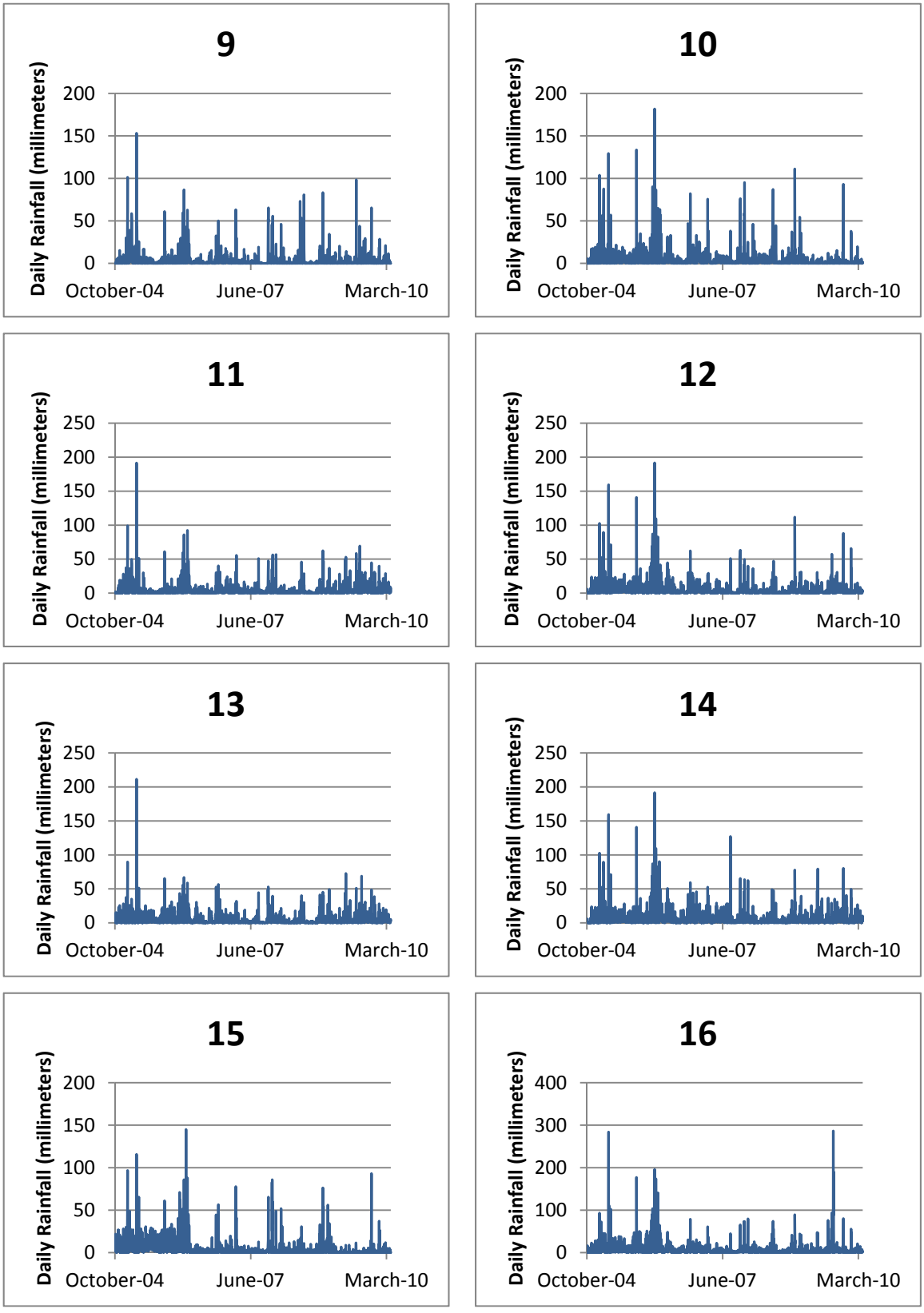

Figure 11. Daily mean-field bias corrected rainfall used in the PRMS Kawela model–Continued.

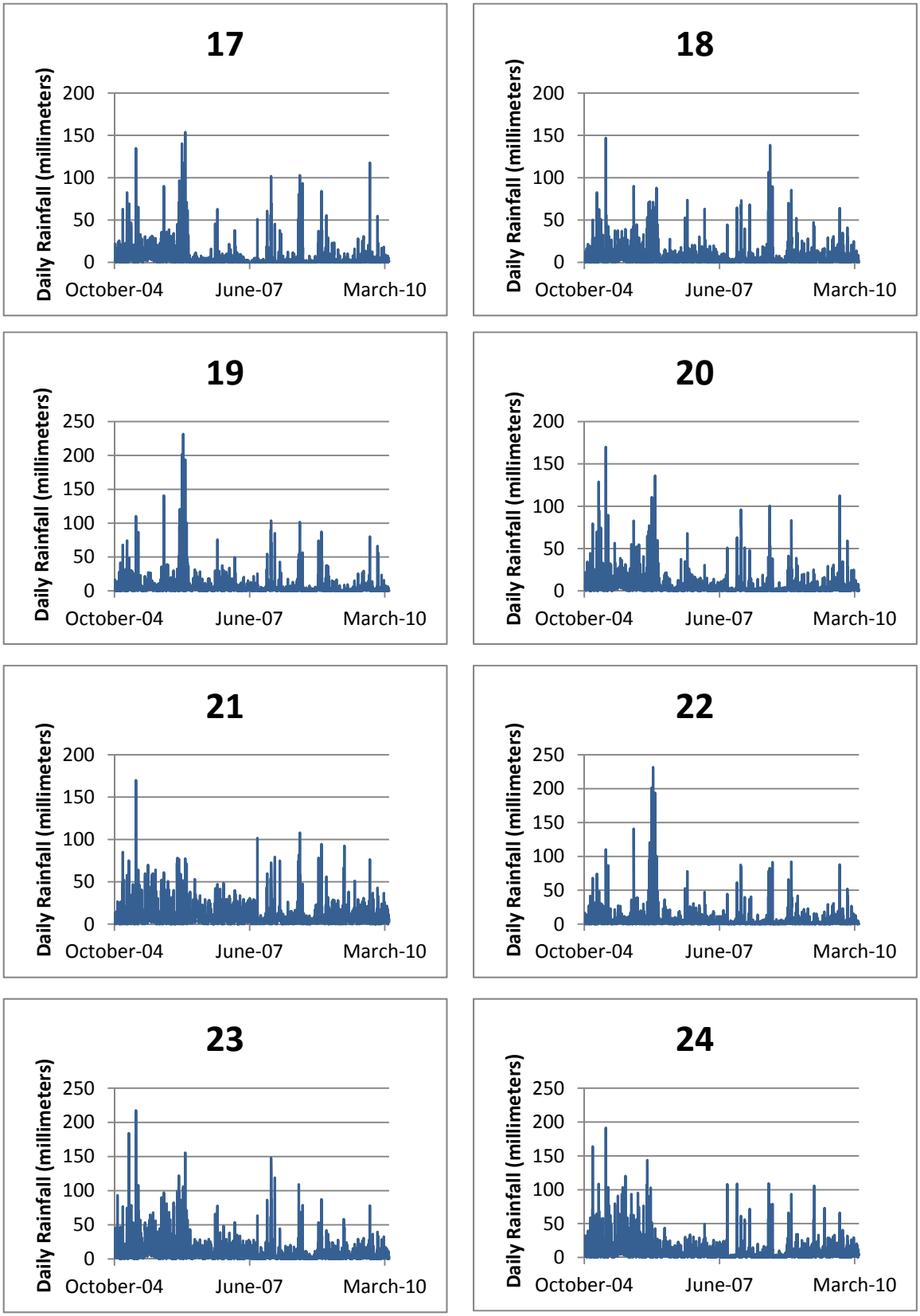

Figure 11. Daily mean-field bias corrected rainfall used in the PRMS Kawela model–Continued.

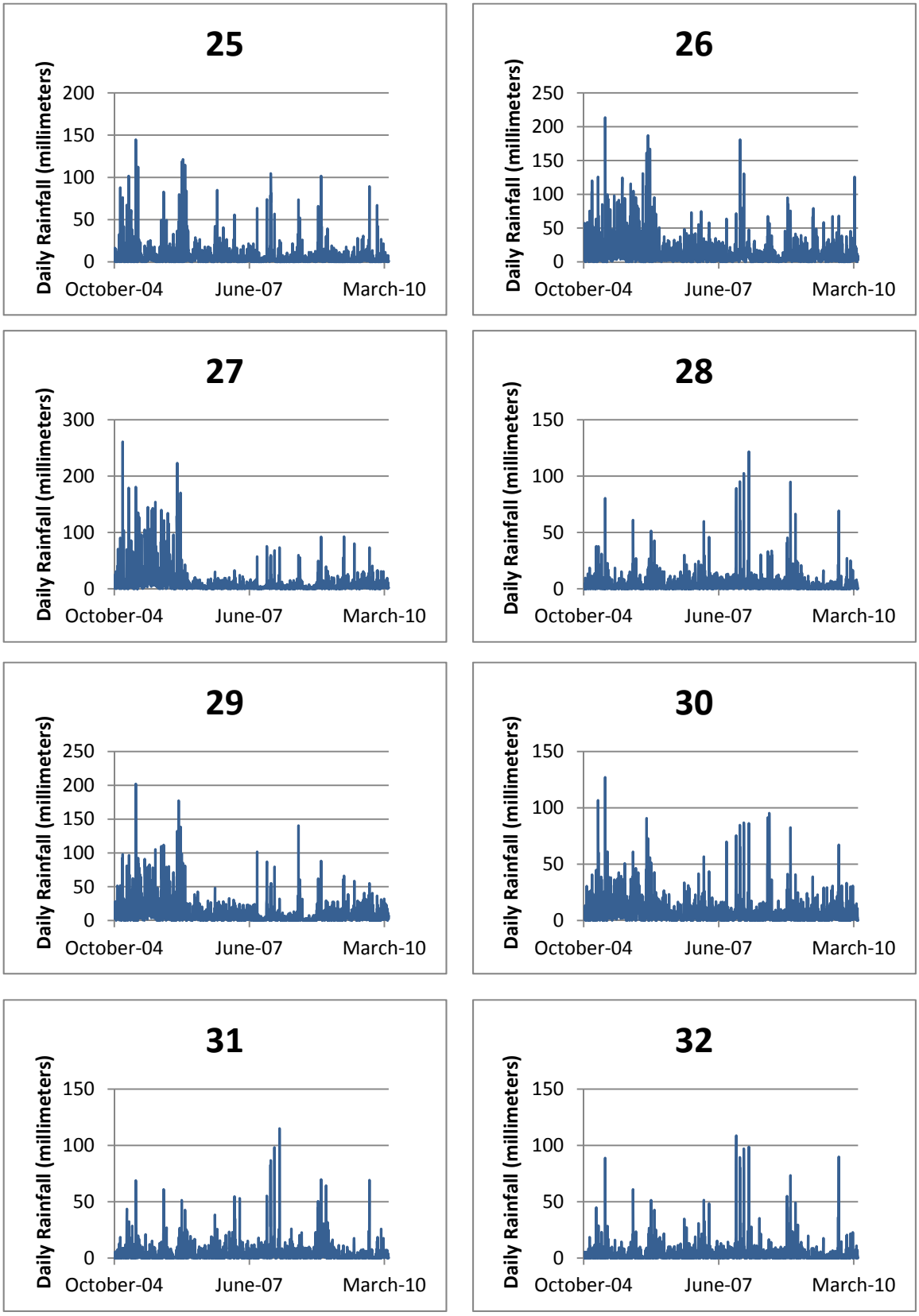

Figure 11. Daily mean-field bias corrected rainfall used in the PRMS Kawela model–Continued.

Fog Drip

Fog drip (interception) was only calculated for HRUs that are located at altitudes of at least 763 meters and with land-cover designations of either trees or shrubs, which is consistent with the approach of Engott (2011). Fog interception was incorporated as an added precipitation input using the climate-by-HRU module (*climate_hru*), which reads in files of climate variables by HRU (Markstrom et al., 2012). After rainfall is distributed to each of the HRUs using a separate PRMS module (*xyz_dist*), which will be described later, these values of distributed rainfall are then read out to a climate-by-HRU precipitation file that can be adjusted for added fog drip by HRU. The calculated precipitation for each HRU is then multiplied by the fog-adjustment factors for each HRU where fog is assumed to occur.

The fog adjustment was calculated using an equation that multiplies a fog interception-to-rainfall ratio and a fog-catch efficiency for the specified land-cover type within the HRU. There are no fog interception-to-rainfall ratios for leeward Moloka‘i; however fog interception-to-rainfall ratios for other leeward Hawaiian slopes like the leeward slopes of Mauna Loa and Hualālai have been determined (Engott, 2011). Fog interception-to-rainfall ratios of 0.02, 0.12, and 0.21 were used in the fog-drip calculation for HRUs located in the 762-914 meter, 915-1,219 meter, and 1,220-1,524 meter altitude ranges, respectively. HRUs with a tree land-cover classification were assigned a fog-catch efficiency of 1 and HRUs with shrubs were assigned a fog-catch efficiency of 0.5, reflecting the lower stature of shrubs relative to trees. Calculated fog-drip adjustments for each relevant HRU within Kawela watershed are summarized in Table 5. The locations of the numbered HRUs referred to in Table 5 are shown in Figure 12.

Table 5. Calculated fog-drip adjustment for relevant HRUs within Kawela watershed.

HRU	COV_TYPE	Catch Efficiency	Fog Interception-to-Rainfall Ratio	Fog Adjustment
4	Trees	1	0.02	0.02
5	Trees	1	0.02	0.02
12	Shrubs	0.5	0.02	0.01
14	Shrubs	0.5	0.12	0.06
15	Shrubs	0.5	0.02	0.01
16	Shrubs	0.5	0.02	0.01
17	Shrubs	0.5	0.02	0.01
19	Trees	1	0.12	0.12
20	Trees	1	0.12	0.12
21	Shrubs	0.5	0.02	0.01
25	Trees	1	0.12	0.12
26	Shrubs	0.5	0.02	0.01
27	Trees	1	0.12	0.12
28	Trees	1	0.02	0.02
29	Shrubs	0.5	0.02	0.01
32	Trees	1	0.12	0.12
36	Trees	1	0.12	0.12
37	Trees	1	0.12	0.12
38	Trees	1	0.12	0.12
40	Trees	1	0.12	0.12
41	Trees	1	0.12	0.12
43	Trees	1	0.12	0.12
47	Shrubs	0.5	0.02	0.01
50	Trees	1	0.12	0.12
51	Shrubs	0.5	0.12	0.06
52	Shrubs	0.5	0.02	0.01
55	Shrubs	0.5	0.02	0.01
59	Trees	1	0.12	0.12
63	Shrubs	0.5	0.02	0.01
64	Trees	1	0.12	0.12
65	Trees	1	0.21	0.21
67	Shrubs	0.5	0.02	0.01
70	Trees	1	0.12	0.12
71	Trees	1	0.12	0.12
73	Trees	1	0.12	0.12
74	Trees	1	0.12	0.12
75	Trees	1	0.21	0.21
75	Trees	1	0.21	0.21
77	Shrubs	0.5	0.02	0.01
78	Trees	1	0.12	0.12
79	Trees	1	0.21	0.21
80	Trees	1	0.12	0.12
81	Trees	1	0.21	0.21
83	Trees	1	0.21	0.21
84	Trees	1	0.12	0.12
85	Trees	1	0.21	0.21
86	Trees	1	0.21	0.21

Table 5. Calculated fog-drip adjustment for relevant HRUs within Kawela watershed–Continued.

HRU	COV_TYPE	Catch Efficiency	Fog Interception-to-Rainfall Ratio	Fog Adjustment
87	Trees	1	0.21	0.21
96	Trees	1	0.12	0.12
97	Trees	1	0.12	0.12
98	Trees	1	0.21	0.21
99	Trees	1	0.21	0.21

Evapotranspiration

Potential evapotranspiration (ET) was calculated externally from PRMS with a Java script using the Penman-Monteith daily reference evapotranspiration equations based on the minimum temperature, maximum temperature, net radiation, and wind speed (Monteith, 1965). Fares (2008) states that the Penman-Monteith model is probably the most suitable ET model for tropical island watershed studies due to the importance of wind intensity and its effect on ET. Other hydrological studies in Hawai‘i (for example, Safeeq and Fares, 2012; Mair and Fares, 2010) have used the Penman-Monteith method to determine potential ET. Daily potential ET was computed using precipitation, minimum temperature, maximum temperature, the latitude of the centroid for each HRU as a proxy for the net radiation, and a default value of wind speed (Snyder and Eching, 2002). The calculated daily potential ET data for each HRU were compiled into one data file for all of the HRUs in Kawela watershed and read in as a climate-by-HRU file with the *climate_hru* module. The actual ET is then computed by PRMS as a function of the potential ET, HRU soil type, water available in the soil zone, and storage capacity of the soil zone.

3.2.3 Physiographic Data

A 5-meter digital elevation model (DEM) re-sampled up from a 1-meter LIDAR dataset was used to determine the physical watershed characteristics, including basin

area, altitude, slope, and aspect for each HRU using a geographic information system (GIS) (U.S. Geological Survey, 2010b). The 2001 National Land Cover Data set and impervious-surface data produced by the Multi-Resolution Land Characteristics Consortium (MRLC, 2001) were used as the initial land-cover input to PRMS. A vegetation-distribution map for Kawela watershed based on pre-human conditions was used as one of the vegetation-change scenarios (Jacobi, 2011b). In PRMS, land cover is classified as one of the following four general categories: trees, shrubs, grass, or bare ground. Physical soil properties were derived from the U.S. General Soil Map (STATSGO2) (Natural Resources Conservation Service, 2006). Surface geology for the study area was derived from Sherrod et al. (2007.) The spatial variation of the physical watershed characteristics for Kawela watershed was determined using GIS techniques and these sets of physiographic data.

3.3 Model Development

PRMS is a distributed-parameter model, and therefore the PRMS Kawela model must be defined by the boundary of the watershed and comprised of many discrete HRUs. PRMS simulates different parts of the hydrological cycle based on a set of user-defined modules. Model development requires the delineation of the watershed and HRUs and the selection of appropriate PRMS modules suitable for simulating this environment.

3.3.1 Watershed Delineation

The drainage boundary of Kawela watershed was delineated from the 5-meter DEM using the USGS Kawela Gulch stream-gaging station (16415600) as the outlet of the watershed and the automated “area of interest” delineation procedure in the GIS

Weasel (Viger and Leavesley, 2007). The Kawela watershed above the Kawela stream-gaging station delineated using the GIS Weasel is shown in Figure 12.

3.3.2 Delineation of Hydrologic Response Units

HRUs for Kawela watershed were also delineated using the automated delineation procedure in the GIS Weasel (Viger and Leavesley, 2007). A topological delineation approach was used initially to discretize the watershed resulting in many irregularly shaped polygons representing hill slopes and flow planes in Kawela watershed. Annual precipitation, vegetation cover, soils, and geology maps of Kawela were then used to combine or split the purely topological HRUs to better represent the physical characteristics of the watershed. The automated GIS Weasel delineation and revisions based on the watershed physiographic data resulted in 99 HRUs used to model the Kawela watershed in PRMS (Figure 12).

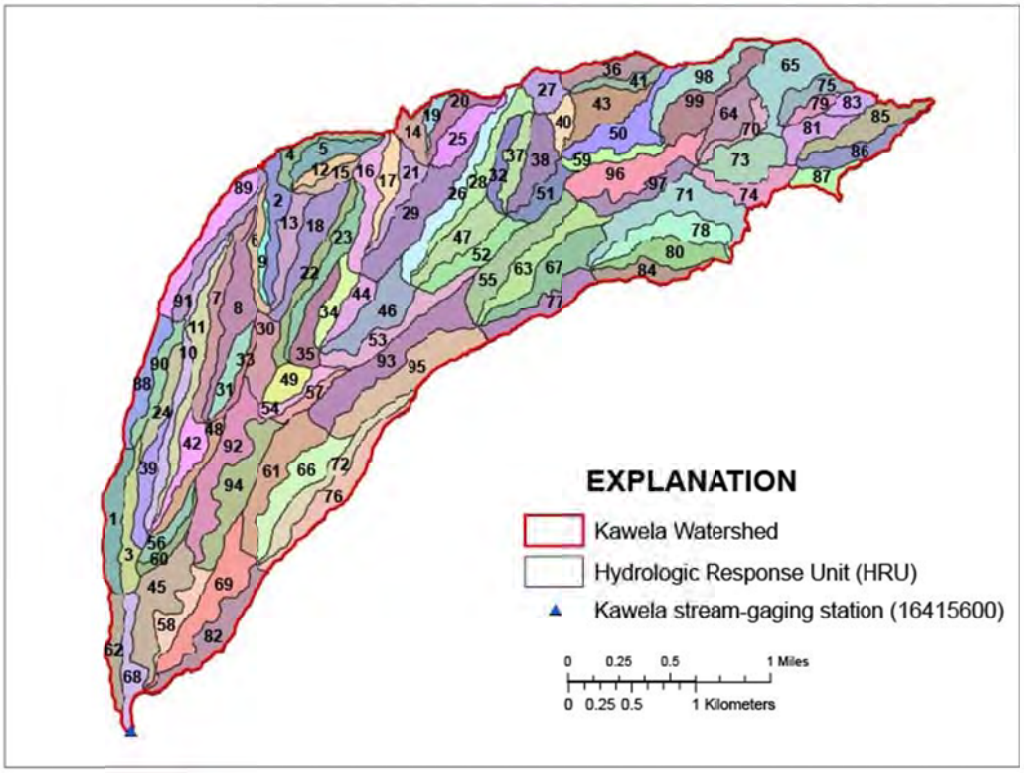

Figure 12. The GIS Weasel delineation of the Kawela watershed and the 99 HRUs used in the PRMS Kawela model.

Table 6. List of parameters used in the PRMS Kawela model Moloka‘i, Hawai‘i.

[Abbreviation: PRMS, Precipitation-Runoff Modeling System. HRU, Hydrologic Response Unit.] Parameter units are specified in the format that PRMS requires.

PRMS Model Parameter	Description of parameter
Distributed (HRU-dependent) parameters	
CAREA_MAX	Maximum possible area contributing to surface runoff (in decimal fraction of HRU area)
COV_TYPE	Plant cover type for HRU (bare soil, grasses, shrubs, or trees)
COVDEN_SUM	Summer plant cover density for plant type on HRU as a decimal fraction
COVDEN_WIN	Winter plant cover density for plant type on HRU as a decimal fraction
FASTCOEF_LIN	Linear flow-routing coefficient for fast interflow
FASTCOEF_SQ	Non-linear flow-routing coefficient for fast interflow
HRU_AREA	Area of HRU (acres)
HRU_ASPECT	Aspect of HRU (degrees azimuth)
HRU_ELEV	Mean land-surface altitude of HRU (meters)
HRU_PERCENT_IMPERV	Decimal fraction of HRU area that is impervious
HRU_SLOPE	HRU slope, specified as change in vertical length divided by change in horizontal length
HRU_X	Longitude (X) for HRU in albers projection
HRU_Y	Latitude (Y) for HRU in albers projection
IMPERV_STOR_MAX	Maximum retention storage for HRU impervious area (inches)
PREF_FLOW_DEN	Decimal fraction of the soil zone available for preferential flow
RAD_TRNCF	Transmission coefficient for short-wave radiation through winter plant canopy (decimal fraction)
SAT_THRESHOLD	Maximum volume of water per unit area in the soil zone (inches)
SLOWCOEF_LIN	Linear flow-routing coefficient for slow interflow
SLOWCOEF_SQ	Non-linear flow-routing coefficient for slow interflow
SMIDX_COEF	Coefficient in non-linear contributing area algorithm (for computing surface runoff)
SMIDX_EXP	Exponent in non-linear contributing area algorithm (for computing surface runoff)
SOIL_MOIST_INIT	Initial value of available water in the capillary reservoir (inches)
SOIL_MOIST_MAX	Maximum available capillary water-holding capacity of soil zone in an HRU (inches)
SOIL_RECHR_INIT	Initial value in capillary reservoir where evaporation and transpiration can occur simultaneously (inches)
SOIL_RECHR_MAX	Maximum quantity of water in the capillary reservoir where evaporation and transpiration can occur simultaneously (inches)
SOIL_TYPE	HRU soil type (sand, loam, or clay)
SOIL2GW_MAX	Maximum value of soil-water excess routed directly to PRMS ground-water reservoir (inches)
SRAIN_INTCP	Maximum summer rain storage in the plant canopy for plant type on HRU (inches)
WRAIN_INTCP	Maximum winter rain storage in the plant canopy for plant type on HRU (inches)
Selected temperature and rainfall related parameters	
MAX_LAPSE	Monthly maximum air temperature regression coefficient for longitude, latitude, and altitude
MIN_LAPSE	Monthly minimum air temperature regression coefficient for longitude, latitude, and altitude
PPT_ADD	Calculated mean of precipitation for watershed
PPT_DIV	Calculated standard deviation of precipitation for watershed
PPT_LAPSE	Precipitation regression coefficient for longitude, latitude, and altitude, respectively by month

Table 6. List of parameters used in the PRMS Kawela model Moloka‘i, Hawai‘i–Continued.

[Abbreviation: PRMS, Precipitation-Runoff Modeling System. HRU, Hydrologic Response Unit.]

Selected temperature and rainfall related parameters	
PSTA_ELEV	Altitude of each measurement station that measures precipitation
PSTA_FREQ_NUSE	Defines measurement stations used to determine if precipitation is occurring in watershed
PSTA_MONTH_PPT	Monthly average precipitation at each measurement station
PSTA_NUSE	Defines which measurement stations will be used in the distribution regression of precipitation
PSTA_Y	Latitude (Y) for each measurement station that measures precipitation in albers projection
RAIN_ADJ	Monthly factor as a decimal fraction used to adjust rain at the HRU
TMAX_ADD	Calculated mean of maximum air temperature for watershed
TMAX_ADJ	Adjustment to maximum air temperature for HRU, estimated on basis of slope and aspect
TMAX_DIV	Calculated standard deviation of maximum air temperature for watershed
TMIN_ADD	Calculated mean of minimum air temperature for watershed
TMIN_ADJ	Adjustment to minimum air temperature for HRU, estimated on basis of slope and aspect
TMIN_DIV	Calculated standard deviation of minimum air temperature for watershed
TSTA_ELEV	Altitude of each measurement station that measures air temperature
TSTA_MONTH_MAX	Monthly average maximum air temperature at measurement station
TSTA_MONTH_MIN	Monthly average minimum air temperature at each measurement station
TSTA_NUSE	Defines which measurement stations will be used in distribution regression of air temperatures
TSTA_X	Longitude (X) for each measurement station that measures air temperature in albers projection
TSTA_Y	Latitude (Y) for each measurement station that measures air temperature in albers projection
X_ADD	Calculated mean of measurement station longitude (X) coordinates for watershed
X_DIV	Calculated standard deviation of measurement station longitude (X) coordinates for watershed
Y_ADD	Calculated mean of measurement station latitude (Y) coordinates for watershed
Y_DIV	Calculated standard deviation of measurement station latitude (Y) coordinates for watershed
Z_ADD	Calculated mean of measurement station altitude (Z) coordinates for watershed
Z_DIV	Calculated standard deviation of measurement station altitude (Z) coordinates for watershed
Groundwater and sub-surface routing related parameters	
GWFLOW_COEF	Linear coefficient to route water in groundwater reservoir to streams
GWSINK_COEF	Linear coefficient to route water in groundwater reservoir to ground-water sink
GWSTOR_INIT	Initial storage in groundwater reservoir (inches)
SSR2GW_EXP	Exponent in the equation used to compute gravity drainage to PRMS ground-water reservoir
SSR2GW_RATE	Linear coefficient in the equation used to compute gravity drainage to PRMS groundwater reservoir
SSRMAX_COEF	Maximum amount of gravity drainage to PRMS groundwater reservoir
SSSTOR_INIT	Initial storage in PRMS subsurface reservoir or gravity reservoir

Table 7. Physical characteristics of hydrologic response units for Kawela watershed.
Parameter definitions are shown in Table 6.

HRU	COV_TYPE	HRU_AREA (acres)	HRU_ASPECT (degrees azimuth)	HRU_ELEV (meters)	HRU_PERCENT_IMPERV	HRU_SLOPE	SOIL_TYPE
1	Shrubs	36.8	181.7	260	0.00	0.333	Loam
2	Shrubs	30.1	176.4	799	0.00	0.484	Loam
3	Shrubs	29.9	248.8	226	0.00	0.384	Loam
4	Trees	18.4	201.0	879	0.00	0.403	Loam
5	Trees	23.0	333.9	905	0.00	0.453	Loam
6	Shrubs	21.9	169.3	743	0.00	0.459	Loam
7	Shrubs	38.7	182.6	612	0.00	0.434	Loam
8	Shrubs	50.8	269.9	644	0.00	0.418	Loam
9	Shrubs	9.4	266.8	730	0.00	0.497	Loam
10	Shrubs	40.2	187.5	481	0.00	0.403	Loam
11	Shrubs	42.3	278.0	549	0.00	0.391	Loam
12	Shrubs	12.0	233.4	896	0.00	0.466	Loam
13	Shrubs	29.0	285.9	763	0.00	0.582	Loam
14	Shrubs	19.0	160.5	1009	0.00	0.531	Loam
15	Shrubs	13.1	328.6	906	0.00	0.543	Loam
16	Shrubs	35.1	174.0	888	0.00	0.672	Loam
17	Shrubs	23.1	277.8	905	0.00	0.613	Loam
18	Shrubs	45.0	214.9	788	0.00	0.573	Loam
19	Trees	9.4	265.3	1029	0.00	0.432	Clay
20	Trees	20.2	233.5	1058	0.00	0.410	Loam
21	Shrubs	24.6	189.3	913	0.00	0.751	Loam
22	Shrubs	28.0	207.6	705	0.00	0.637	Loam
23	Shrubs	35.1	295.0	765	0.00	0.606	Loam
24	Shrubs	22.0	206.8	464	0.00	0.336	Loam
25	Trees	28.7	292.2	1041	0.00	0.524	Loam
26	Shrubs	43.8	188.5	951	0.00	0.623	Loam
27	Trees	21.1	124.9	1119	0.00	0.199	Loam
28	Trees	39.2	309.5	1006	0.00	0.554	Loam
29	Shrubs	67.1	298.3	895	0.00	0.658	Loam
30	Shrubs	32.3	180.1	540	0.00	0.767	Loam
31	Grass	21.0	221.3	543	0.00	0.356	Loam
32	Trees	19.3	176.2	1024	0.00	0.547	Loam
33	Grass	10.4	285.0	535	0.00	0.403	Loam
34	Shrubs	21.0	186.5	666	0.00	0.868	Loam
35	Shrubs	29.0	226.3	616	0.00	0.609	Loam
36	Trees	25.6	253.2	1146	0.00	0.383	Loam
37	Trees	21.1	273.9	1032	0.00	0.493	Loam
38	Trees	36.8	198.1	1037	0.00	0.530	Loam
39	Shrubs	26.7	258.4	327	0.00	0.354	Loam
40	Trees	17.0	164.7	1087	0.00	0.609	Loam
41	Trees	15.1	333.4	1159	0.00	0.437	Loam
42	Shrubs	26.9	201.6	393	0.00	0.376	Loam
43	Trees	41.1	292.5	1125	0.00	0.485	Loam
44	Shrubs	20.6	308.8	681	0.00	0.822	Loam
45	Shrubs	61.4	198.4	156	0.00	0.532	Loam
46	Shrubs	48.8	209.6	680	0.00	0.779	Loam
47	Shrubs	38.6	204.3	879	0.00	0.873	Loam
48	Shrubs	21.5	300.0	349	0.00	0.443	Loam
49	Shrubs	18.7	314.8	470	0.00	0.928	Loam
50	Trees	43.5	237.6	1118	0.00	0.435	Loam
51	Shrubs	24.5	329.8	999	0.00	0.638	Loam
52	Shrubs	32.3	338.8	858	0.00	0.941	Loam
53	Shrubs	42.7	337.2	648	0.00	0.861	Loam

Table 7. Physical characteristics of hydrologic response units for Kawela watershed–Continued.
Parameter definitions are shown in Table 6.

HRU	COV_TYPE	HRU_AREA (acres)	HRU_ASPECT (degrees azimuth)	HRU_ELEV (meters)	HRU_PERCENT_IMPERV	HRU_SLOPE	SOIL_TYPE
54	Shrubs	13.8	261.6	531	0.00	0.546	Loam
55	Shrubs	53.5	186.3	901	0.00	0.924	Loam
56	Bare	16.9	230.4	263	0.00	0.314	Loam
57	Shrubs	13.2	310.2	541	0.00	0.394	Loam
58	Shrubs	27.9	302.3	137	0.00	0.683	Loam
59	Trees	17.5	15.1	1078	0.00	0.758	Loam
60	Shrubs	12.0	300.0	251	0.00	0.308	Loam
61	Shrubs	62.7	186.7	362	0.00	0.788	Loam
62	Shrubs	22.8	159.8	122	0.00	0.443	Loam
63	Shrubs	46.9	328.4	909	0.00	0.841	Loam
64	Trees	34.1	211.7	1218	0.00	0.356	Loam
65	Trees	57.2	219.8	1252	0.00	0.293	Loam
66	Shrubs	50.2	317.9	341	0.00	0.802	Loam
67	Shrubs	52.2	228.2	942	0.00	0.536	Loam
68	Shrubs	29.5	253.2	78	0.00	0.410	Loam
69	Shrubs	62.6	202.9	176	0.00	0.506	Loam
70	Trees	15.8	315.1	1206	0.00	0.336	Loam
71	Trees	73.0	253.2	1113	0.00	0.380	Loam
72	Shrubs	42.5	218.4	414	0.00	0.391	Loam
73	Trees	45.2	232.3	1185	0.00	0.396	Loam
74	Trees	32.6	16.1	1164	0.00	0.451	Loam
75	Trees	21.2	295.7	1250	0.00	0.239	Loam
76	Shrubs	49.6	292.1	426	0.01	0.412	Loam
77	Shrubs	35.2	344.6	903	0.00	0.812	Loam
78	Trees	44.1	351.9	1094	0.00	0.485	Loam
79	Trees	11.2	260.2	1248	0.00	0.247	Loam
80	Trees	38.4	271.9	1093	0.00	0.458	Loam
81	Trees	26.6	282.2	1230	0.00	0.282	Loam
82	Shrubs	48.0	316.9	141	0.00	0.598	Loam
83	Trees	14.0	301.2	1300	0.00	0.234	Loam
84	Trees	24.9	350.7	1055	0.01	0.518	Loam
85	Trees	40.2	241.2	1292	0.00	0.532	Loam
86	Trees	29.4	321.2	1262	0.00	0.265	Loam
87	Trees	20.1	328.6	1230	0.00	0.181	Loam
88	Shrubs	27.0	183.8	487	0.00	0.434	Loam
89	Shrubs	40.0	205.0	750	0.00	0.468	Loam
90	Shrubs	23.1	290.9	494	0.00	0.437	Loam
91	Shrubs	29.0	295.8	715	0.00	0.466	Loam
92	Shrubs	64.3	175.6	338	0.00	0.831	Loam
93	Shrubs	80.3	200.1	594	0.00	1.026	Loam
94	Shrubs	61.0	306.9	324	0.00	0.776	Loam
95	Shrubs	74.3	346.8	604	0.00	1.008	Loam
96	Trees	60.2	225.3	1068	0.00	0.644	Loam
97	Trees	26.1	357.3	1060	0.00	0.731	Loam
98	Trees	43.1	216.7	1217	0.00	0.352	Loam
99	Trees	46.5	302.6	1199	0.00	0.372	Loam

3.3.3 Model Parameterization

PRMS uses distributed and non-distributed model parameters. Distributed parameters vary by HRU whereas non-distributed parameters describe the entire watershed. Major distributed and non-distributed parameters used are described in Table 6. Physical distributed parameters were derived from the USGS DEM, the 2001 National Land Cover Data set, and the STATSGO soils dataset using the parameterization methods in the GIS Weasel (Viger and Leavesley, 2007). Major physical characteristics of all HRUs are listed in Table 7.

3.3.4 Modules Used

A detailed description of each PRMS module available and the equations used by these modules to represent each hydrological process can be found in Markstrom et al. (2008) and a draft report detailing updates to PRMS (Markstrom et al., 2012). The modules used in this model are briefly described in Table 2. Module descriptions and equations taken directly from Markstrom et al. (2008, 2012) are shown in italicized text below. The units in this thesis have been converted to the International System of Units (SI units); however PRMS requires the units listed in Table 6 for the reported equations below. To be consistent with Markstrom et al. (2008, 2012) the required units for PRMS were not changed in the equations presented in this thesis.

Precipitation and temperature data were distributed using the *xyz_dist* module. The *xyz_dist* module uses a three-dimensional multiple-linear regression based on latitude, longitude, and altitude of climate stations to distribute temperature and precipitation data to each HRU. Parameters used in each module that are shown in all capitals and bold throughout the text are defined in Table 6.

*Multiple linear regression parameters (**PPT_LAPSE**$_{direction,month}$, **MAX_LAPSE**$_{direction,month}$, and **MIN_LAPSE**$_{direction,month}$) for the three independent variables in the equation (xsta, ysta, and zsta) are computed for each month using monthly mean values from the climate stations located in or near the watershed. The general equation below describes a plane in three-dimensional space with multiple linear regression parameters or "slopes" (lapse) intersecting the climate variable (CV) axis at b_0.*

$$CV = (lapse_x \cdot x_{sta}) + (lapse_y \cdot y_{sta}) + (lapse_z \cdot z_{sta}) + b_0$$

*where $lapse_x$, $laspse_y$, and $lapse_z$ are the appropriate values of **PPT_LAPSE**$_{direction,month}$, **MAX_LAPSE**$_{direction,month}$, and **MIN_LAPSE**$_{direction,month}$ depending on which climate variable is being computed.*

*The climate variable precipitation (hru_ppt_{HRU}) is selected to illustrate how the above equation is used. The procedure is identical for calculation of maximum and minimum temperature ($tmaxf_{HRU}$ and $tminf_{HRU}$). First, mean daily precipitation (ppt_mean) and corresponding mean location (x_mean, y_mean, and z_mean) are calculated from a set of stations specified by the parameter **PSTA_NUSE**$_{sta}$. Any station which does not have valid data is dropped from this calculation. Consequently, a different set of stations can be used each day. If none of the stations have data available on a particular day, then the mean monthly value is used (parameter **PSTA_MONTH_PPT**$_{sta,month}$). With these values, b_0 is computed according to:*

$$b_0 = ppt_{mean} - (\boldsymbol{PPT\_LAPSE}_{x,month} \cdot x_{mean}) - (\boldsymbol{PPT\_LAPSE}_{y,month} \cdot y_{mean}) - (\boldsymbol{PPT\_LAPSE}_{z,month} \cdot z_{mean})$$

Then, the precipitation amount for an HRU can be computed according to:

$$hru\_ppt_{HRU} = (\boldsymbol{PPT\_LAPSE}_{x,month} \cdot HRU\_X_{HRU} + \boldsymbol{PPT\_LAPSE}_{x,month} \cdot HRU\_Y_{HRU} + \boldsymbol{PPT\_LAPSE}_{x,month} \cdot HRU_{Z_{HRU}}) + b_0$$

*All dependent and independent variables used in the regression are transformed by subtracting the mean (parameters **PPT_ADD**, **X_ADD**, **Y_ADD**, and **Z_ADD**) and dividing by the standard deviation (parameters **PPT_DIV**, **X_DIV**, **Y_DIV**, and **Z_DIV**) to remove the effects of units, magnitude, and inconsistency in specification of the origin. The multiple linear regression parameters (**PPT_LAPSE**$_{direction,month}$) must be determined using these normalized values.*

The minimum temperature, maximum temperature, and precipitation distributed by the *xyz_dist* module to each of the modeled HRUs and summarized for the Kawela watershed are shown in Figure 13.

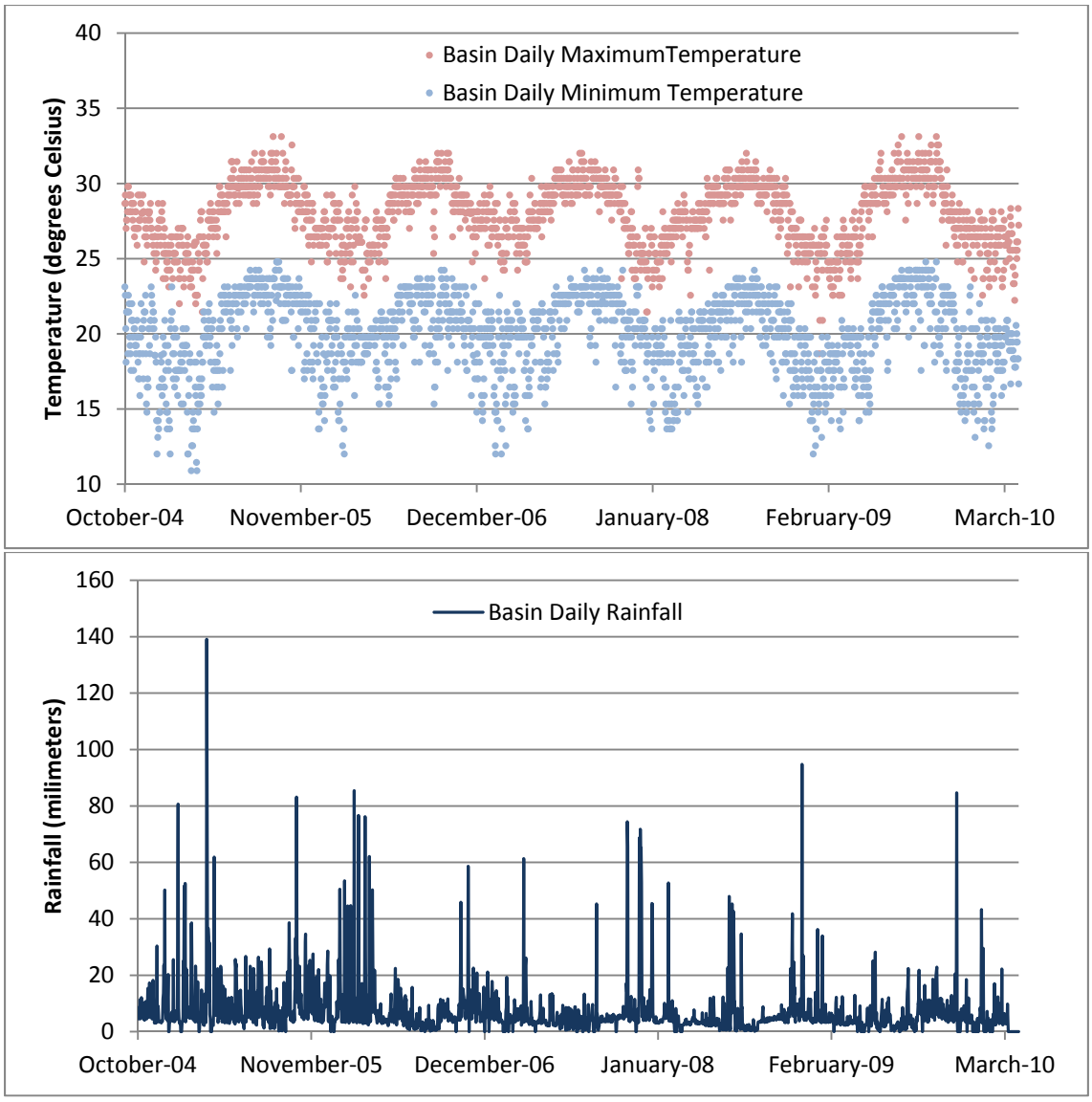

Figure 13. Daily basin maximum temperature, minimum temperature, and rainfall for the Kawela watershed distributed with the *xyz_dist* module.

Daily estimates of potential solar radiation for each HRU are calculated with the *soltab* module. Daily shortwave radiation is estimated using a modified degree-day method using the *ddsolrad* module. Equations for both are described below:

$$Rsp_{HRU}^{m} = sc^{m}(c1_{PSR} + c2_{PSR}),$$

$$c1_{PSR} = sin(DM^{m})\, sin(lat'_{HRU})\, sh_{HRU}^{m}, \qquad and$$

$$c2_{PSR} = \frac{cos(DM^{m})\, cos(lat'_{HRU}) \left[sin\left(ss_{HRU}^{m} + long'_{HRU}\right) - sin\left(sr_{HRU}^{m} + long'_{HRU}\right)\right] 24}{2\pi}$$

Rsp_{HRU}^{m} is the potential solar radiation on the HRU during time step m, in calories per square centimeter per day;

lat'_{HRU} is the latitude of the equivalent-slope surface of the HRU, in radians;

$long'_{HRU}$ is the longitude offset between the equivalent-slope surface and the HRU, in radians;

sc^{m} is the 60-min period solar constant for time step m, in calories per square centimeter per hour;

sh_{HRU}^{m} is the daylight length on the HRU for time step m, in hours;

ss_{HRU}^{m} is the hour angle of sunset on the sloped surface of the HRU for time step m, in radians;

sr_{HRU}^{m} is the hour angle of sunrise on the sloped surface of the HRU for time step m, in radians; and

DM^{m} is the solar declination for time step m, in angular degrees.

$$Rah_{HRU}^{m} = ap_{HRU}^{m} Rsp_{HRU}^{m}, and$$

$$Rasw_{HRU}^{m} = \frac{Rah_{HRU}^{m}}{\cos(tan^{-1}(slope_{HRU}))} pptadj_{HRU}$$

Rah_{HRU}^{m} is the measured or computed as the horizontal plane shortwave radiation on the HRU during time step m, in calories per square centimeter per day;

ap_{HRU}^{m} is the degree-day ratio of actual to potential shortwave radiation for the HRU during time step m, dimensionless;

$Rasw_{HRU}^{m}$ is the computed shortwave radiation on the HRU during time step m, in calories per square centimeter per day;

*$slope_{HRU}$ is the slope of the HRU–parameter **HRU_SLOPE**, dimensionless; and*

$pptadj_{HRU}$ is the precipitation-day adjustment factor to solar radiation, dimensionless.

Precipitation in PRMS can either be intercepted by vegetation, evaporated, or continue to the land surface as throughfall. Interception in PRMS is modeled by the *intcp* module which calculates the amount of rainfall that is intercepted by vegetation, the amount of evaporation of intercepted rain, and the amount net rain throughfall that reaches the soil.

Throughfall precipitation, which is precipitation that is not intercepted by the plant canopy, is computed as:

$$Spca_{HRU}^{m} = (Spcmx_{HRU} - Spc_{HRU}^{m})(A_{HRU}\rho'_{HRU})$$

$$Ptf_{HRU}^{m} = P_{HRU}^{m} - \frac{Spca_{HRU}^{m}}{A_{HRU}\rho'_{HRU}} \quad when\ P_{HRU}^{m} > \frac{Spca_{HRU}^{m}}{A_{HRU}\rho'_{HRU}}$$

$$Ptf_{HRU}^{m} = 0.0\ when\ P_{HRU}^{m} \leq \frac{Spca_{HRU}^{m}}{A_{HRU}\rho'_{HRU}}$$

P_{HRU}^{m} is the precipitation at the HRU during time step m, in inches;

$Spca_{HRU}^{m}$ is the available storage in the plant canopy of the HRU during time step m, in acre-inch;

*$Spcmx_{HRU}$ is the maximum storage in the plant canopy for summer rain and winter rain on each HRU–parameter **SRAIN_INTCP** (summer rain) and **WRAIN_INTCP** (winter rain), in inches;*

Spc_{HRU}^{m} is the storage in the plant canopy (summer or winter) on the HRU during time step m in acre-inch;

*A_{HRU} is the area of the HRU–parameter **HRU_AREA**, in acres;*

*ρ'_{HRU} is the plant canopy density as a decimal fraction of the HRU area–parameter **COVDEN_SUM** (summer) or **COVDEN_WIN** (winter), dimensionless; and*

Ptf_{HRU}^{m} is the precipitation throughfall on the HRU during time step m, in inches.

The precipitation that reaches the ground during time step m is referred to as net precipitation, and is the sum of throughfall and precipitation on the HRU not covered by plants. Net precipitation is calculated according to:

$$Pnet_{HRU}^{m} = P_{HRU}^{m}\left(1.0 - \rho'_{HRU}\right) + \left(Ptf_{HRU}^{m}\rho'_{HRU}\right),$$

$Pnet_{HRU}^{m}$ is the precipitation that reaches the ground during time step m, in inches.

Potential evapotranspiration (PET_{HRU}^{m}) was calculated externally from PRMS with a Java script using the Penman-Monteith daily reference evapotranspiration equations (Snyder and Eching, 2002) and read in as a climate-by-HRU file with the *climate_hru* module. Any rainfall reaching the land surface may then be stored in the impervious zone reservoir, infiltrate into the soil zone, be evaporated, or contribute to surface runoff. The actual ET is then computed by PRMS as a function of the HRU soil type, the water available in the soil zone, and the water-storage capacity of the soil zone. The surface runoff and infiltration for each HRU are computed using the *srunoff_smidx* module, a non-linear variable-source-area method.

If rain throughfall satisfies available retention storage on the impervious parts of the HRU, Hortonian runoff is generated. Hortonian runoff from impervious parts of each HRU is calculated from continuity according to:

$$C_{imper}^{m} = D_{imper}^{m-1} - Dimx_{imper} + Pnet_{HRU}^{m} + ROhup_{HRU}^{m}$$

$$ROh_{imper}^{m} = C_{imper}^{m} \; when \; C_{imper}^{m} > 0$$

$$ROh_{imper}^{m} = 0 \; when \; C_{imper}^{m} \leq 0 \, ,$$

C_{imper}^{m}*is the water available for Hortonian runoff from the impervious part per unit area of the HRU during time step m, in inches;*

ROh_{imper}^{m}*is the Hortonian runoff from the impervious part of the HRU per unit area during time step m, in inches;*

D_{imper}^{m-1} *is the impervious storage, as calculated by the impervious storage equation, for the last iteration of time step m-1, as volume per unit area for the HRU, in inches;*

$Dimx_{imper}$ *is the maximum retention storage for HRU impervious area, in inches; and*

$ROhup_{HRU}^{m}$*is the sum of Hortonian runoff from all upslope contributing HRUs as a volume per unit area of the HRU for time step m, in inches.*

Evaporation from impervious parts of HRUs is computed for each time step by;

$$C1_{imperv}^{m} = PET_{HRU}^{m}$$

$$C2_{imperv}^{m} = D_{imper}^{m-1} + Pnet_{HRU}^{m} + ROhup_{HRU}^{m} - ROh_{imper}^{m}$$

$$Evap_{imper}^{m} = C2_{imperv}^{m} \; when \; C1_{imperv}^{m} \geq C2_{imperv}^{m}$$

$$Evap_{imper}^{m} = C1_{imperv}^{m} \; when \; C1_{imperv}^{m} < C2_{imperv}^{m}$$

$Evap_{imper}^{m}$ *is the evaporation from the impervious part of the HRU for time step m, in inches;*
Storage on the impervious parts of the HRU is calculated according to:

$$D_{imper}^{m} = D_{imper}^{m-1} + Pnet_{HRU}^{m} + ROhup_{HRU}^{m} - ROh_{imper}^{m} - Evap_{imper}^{m}$$

Hortonian runoff from pervious parts of a HRU is related to the area where the throughfall exceeds the soil infiltration rate. This is represented by nonlinear function (module srunoff_smidx) of antecedent soil-moisture content. The nonlinear form of computing the contributing area for pervious runoff can be written as:

$$Smidx_{HRU}^{m} = D_{CPR}^{m-1} + 0.5Pnet_{HRU}^{m}$$

$$C3_{HRU}^{m} = Smc_{HRU} * 10^{(Smex_{HRU}Smidx_{HRU}^{m})}$$

$$Fperv_{HRU}^{m} = C3_{HRU}^{m} \; when \; C3_{HRU}^{m} \leq Fmx_{HRU}$$
$$Fperv_{HRU}^{m} = Fmx_{HRU} \; when \; C3_{HRU}^{m} > Fmx_{HRU}$$

$Fperv_{HRU}^{m}$is the surface-runoff-contributing area of the pervious parts in the HRU for time step m, as a decimal fraction of HRU area, dimensionless;

*Fmx_{HRU} is the maximum possible area contributing to surface runoff, as a decimal fraction of HRU area–parameter **CAREA_MAX**, dimensionless;*

$Smidx_{HRU}^{m}$ is the soil-moisture index of the capillary reservoir for time step m, in inches;

D_{CPR}^{m-1} is the volume per unit area of water in the capillary reservoir at the last iteration of time step m-1, in inches;

*Smc_{HRU} is a coefficient used to calculate decimal fraction of pervious surfaces–parameter **SMIDX_COEF**, dimensionless; and*

*$Smex_{HRU}$ is an exponent used to calculate the decimal fraction of pervious surfaces–parameter **SMIDX_EXP,** in per inch.*

The runoff from the pervious part of an HRU is calculated as:

$$ROh_{perv}^{m} = Fperv_{HRU}^{m}(ROhup_{HRU}^{m} + Pnet_{HRU}^{m})$$

$ROh_{perv}^{m}$is the runoff per unit area from the pervious part of the HRU for time step m, in inches.

Infiltration occurs on the pervious areas of each HRU and includes Hortonian runoff from upslope HRUs and rain throughfall. Hortonian runoff from the HRU is subtracted from the available water for infiltration. Infiltration is calculated as:

$$C4_{HRU}^{m} = ROhup_{perv}^{m}$$
$$qsi_{perv}^{m} = \left(C4_{HRU}^{m} + Pnet_{HRU}^{m} - ROh_{perv}^{m}\right)A_{perv}$$

qsi_{perv}^{m} is the soil infiltration over the pervious part of the HRU for time step m, in acre-inch;

A_{perv} is the pervious area of the HRU in acres.

Once water infiltrates into the soil zone, PRMS uses a conceptual three-reservoir system to model soil-zone water content (Figure 14). Each of these three reservoirs (the capillary, gravity, and preferential-flow reservoirs), are not separate physical spaces but instead are ways for PRMS to represent the different soil-water processes at different soil-water content thresholds. The capillary reservoir models soil water between the wilting-point and field-capacity thresholds. The gravity reservoir models soil-water

content between field capacity and the preferential-flow threshold, and accounts for slow lateral interflow and drainage to the groundwater reservoir. The preferential-flow reservoir also models soil-water content over field capacity, but instead accounts for fast lateral interflow. The *soilzone* module in PRMS computes the inflows and outflows of each soil zone for each HRU. Currently the equations used in the *soilzone* module have only been documented in detail for use in the USGS GSFLOW model (Markstrom et al., 2008).

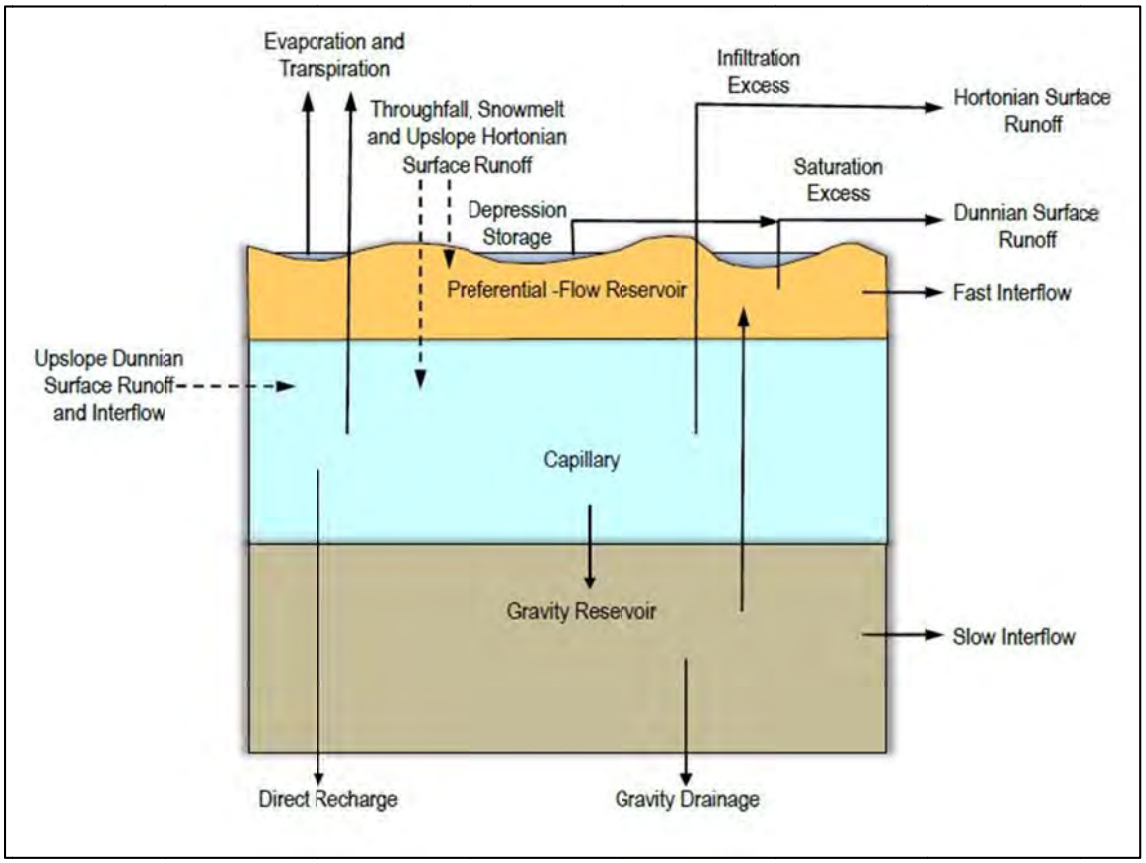

Figure 14. Details of the Precipitation-Runoff Modeling System Soil Zone (Markstrom et al., 2012).

An inflow and outflow component of subsurface flow (interflow) for each HRU subsurface reservoir is computed. When the maximum available water-holding capacity of the soil zone exceeds the maximum quantity of water in the capillary reservoir an

inflow to the subsurface reservoir is computed. The term subsurface reservoir pertains to all three of the conceptual reservoirs used by PRMS to represent the different soil-water processes at different soil-water content thresholds. Using the continuity of mass equation, the subsurface flow over time is computed as the difference between inflows and outflows:

$$ssr_{flow} = ssr_{in} - \frac{d(ssr_{stor})}{dt}$$

ssr_{flow} *is the contribution to streamflow from each subsurface reservoir;*

ssr_{in} *is the total inflow to each subsurface reservoir; and*

ssr_{stor} *is the storage in each subsurface reservoir.*

Outflows from the subsurface reservoir are calculated using two routing coefficients:

$$ssr_{flow} = (ssr_{stor} \cdot ssrcoef_{lin}) + (ssr_{stor}{}^{2} \cdot ssrcoef_{sq})$$

$ssrcoef_{lin}$ *is the linear subsurface routing coefficient routing subsurface storage to streamflow–parameter* ***FASTCOEF_LIN*** *or* ***SLOWCOEF_LIN****; and*

$ssrcoef_{sq}$ *is the non-linear subsurface routing coefficient routing subsurface storage to streamflow–parameter* ***FASTCOEF_SQ*** *or* ***SLOWCOEF_SQ.***

Groundwater in PRMS is simulated with the *gwflow* module using another conceptual reservoir called the groundwater reservoir. Any excess infiltration from the soil zone can directly enter the groundwater reservoir as direct recharge or go through the gravity reservoir and be partitioned into gravity drainage from the soil zone or slow interflow.

$$ssr2gw = ssr2gw\_rate \cdot (\frac{ssr_{stor}}{ssr2gw\_max})^{ssr2gw\_exp}$$

$ssr2gw$ *is the recharge from the subsurface to the groundwater reservoir;*

$ssr2gw\_max$ *is the maximum value for water routed from subsurface to groundwater–parameter* ***SSRMAX_COEF****;*

$ssr2gw\_exp$ *is the exponent in the equation used to compute gravity drainage to groundwater reservoir–parameter* ***SSR2GW-EXP****; and*

$ssr2gw\_rate$ *is the linear coefficient in the equation used to compute gravity drainage to groundwater reservoir–parameter* ***SSR2GW_RATE.***

Base flow for each groundwater reservoir is computed using a reservoir routing coefficient and the groundwater reservoir storage:

$$gwres_{flow} = gwflow\_coef \cdot gwres_{stor}$$

$gwres_{flow}$ *is the amount of base flow;*

$gwflow\_coef$ *is the linear coefficient to route water in groundwater reservoir to streams–parameter* ***GWFLOW_COEF****; and*

$gwres_{stor}$ *is the groundwater reservoir storage.*

Groundwater may leave the groundwater reservoir but stay in the watershed or leave the groundwater reservoir and be specified to leave the system with the **GWSINK_COEF** parameter. In the Kawela PRMS model the **GWSINK_COEF** parameter was used to represent groundwater underflow. A lack of sustained base flow at the Kawela Gulch stream-gaging station indicates that groundwater recharge in the watershed likely discharges directly to the ocean and not as base flow in the stream. Groundwater underflow is computed by multiplying the $gwres_{stor}$ and the **GWSINK_COEF** parameter value.

The PRMS summary module (*basin_sum*) calculates the water and energy balances for each HRU and the total for the watershed and writes the results to the model output files. The computation sequence used by PRMS is shown in Figure 15.

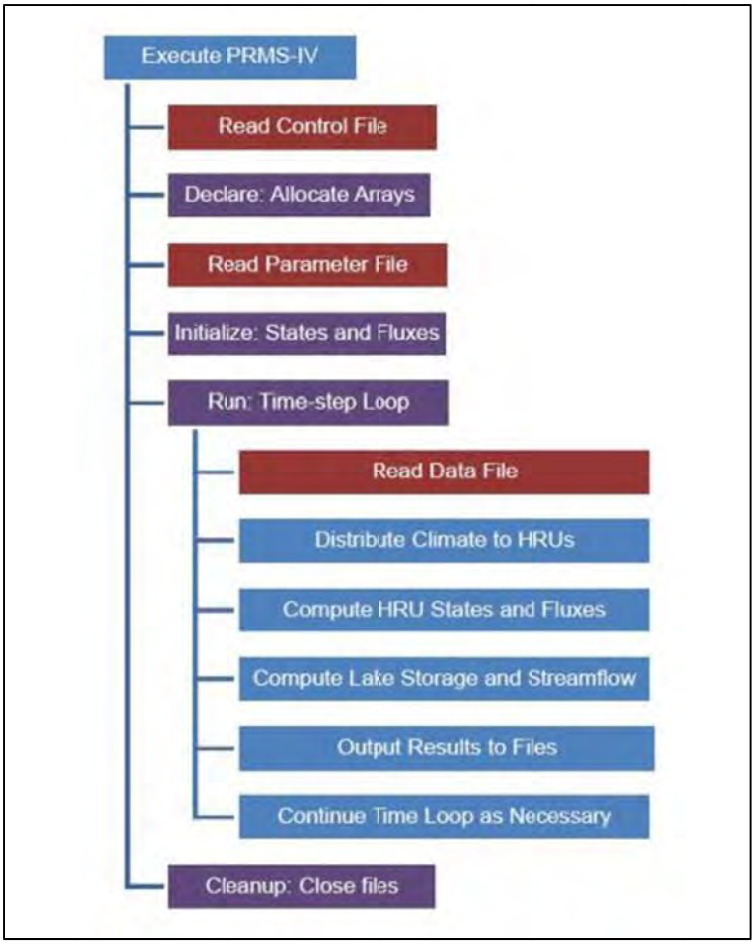

Figure 15. Computational sequence of PRMS-IV (Markstrom et al., 2012).

3.4 Model Calibration and Validation

The model was run for an initial period (10/1/2004-3/31/2006) to allow the model to estimate initial conditions in the watershed before the calibration and validation periods. This period also contained an unusually long period of high amounts of rainfall that was not well correlated (coefficient of determination (R^2) =0.2) to the measured runoff at the Kawela Gulch gaging station making it an undesirable period of data to be used as input to either a calibration or a validation period. PRMS was calibrated and validated using independent time periods within the remaining available dataset. PRMS was calibrated using data from 4/1/2008-3/31/2010 and validated using data from

4/1/2006-3/31/2008. During the calibration phase, the model's simulated streamflow discharge was compared to the measured discharge at the USGS Kawela Gulch stream-gaging station. The calibration process attempts to minimize the differences between the simulated and measured streamflow by altering model parameter values. Model parameter values can either be adjusted manually or using an automatic calibration scheme. Some model parameter values and coefficients have more influence on the amount of simulated runoff. A sensitivity analysis built into the automatic calibration procedure was used to determine which parameters the model is most sensitive to and therefore have the greatest influence on simulating runoff. The calibration process was evaluated by visual comparisons of the measured and simulated hydrographs as well as statistical comparisons of the measured and simulated runoff.

3.4.1 Calibration

Manual calibration of one of the major climatic model coefficients, the monthly rainfall correction factor (**RAIN_ADJ**), was done as a first step to get the general shape of the measured and simulated hydrographs in the calibration period to match and decrease the difference between the simulated and measured total runoff to less than 25 percent. To further minimize the differences between the measured and simulated runoff, an automatic calibration method in the PEST (Parameter ESTimation) program (Doherty, 2010) was used as a second calibration step. PEST is a model independent parameter estimation program that allows the user to systematically approach estimating model parameter values. Only selected parameters and coefficients were calibrated. Measureable physical basin and HRU parameter values were not changed in the calibration.

An initial model run for the Kawela watershed using the un-calibrated parameter values and coefficients resulted in simulated runoff much higher than measured runoff for larger storms and simulated runoff less than measured runoff for smaller more frequent flows. As a result, the **RAIN_ADJ** parameter needed to be decreased to decrease the amount of rainfall for certain months and increased to increase the amount of rainfall for others. The monthly rainfall correction factors used in the PRMS Kawela model are listed in Table 8.

Table 8. Monthly rainfall adjustment coefficient used in the PRMS Kawela model.

MONTH	RAIN_ADJ
January	1.15
February	1.00
March	1.00
April	1.00
May	1.00
June	0.70
July	0.70
August	0.70
September	1.00
October	1.10
November	0.90
December	0.85

A sensitivity analysis and automatic calibration using PEST (Doherty, 2010) was performed after the manual calibration. Within PEST, the model output time-series data are read in, parameters and their boundaries are specified for adjustment, the method for the parameter estimation across the parameter dimension is selected, targets for model calibration are set, and the step-wise order in which the parameters will be calibrated is specified. Singular value decomposition (SVD) and variables appropriate for calibrating surface-water models (RLAMBDA1=25, RLAMFAC=-3, and the Lambda Forgive

option) as described by Doherty (2010) were used in the automatic calibration. An initial run of the PRMS Kawela model in PEST is needed for the initial fit of the model prior to the PEST parameter optimization. A sensitivity run was performed to determine the sensitivities associated with each of the adjustable parameters. The composite sensitivity of each parameter is derived from the Jacobian matrix column magnitude modulated by the weight attached to each observation divided by the number of observations (Doherty, 2010). The Jacobian matrix contains the derivatives of all "model-generated observations" with respect to a particular parameter. Based on the results of the calibration within PEST, the simulated streamflow was the most sensitive to parameters related to subsurface and groundwater flows (**SSR2GW_RATE**, **SLOWCOEF_SQ**, **SLOWCOEF_LIN**, **SOIL2GW_MAX**, **SSR2GW_EXP**). The calibrated values for all of the parameter values and coefficients used in the PRMS Kawela model runoff computations are listed in Tables 9 and 10. The parameter values in Tables 9 and 10 have been converted to the International System of Units (SI units) for this report, however for use within PRMS the parameter values must be transformed back into the units that PRMS requires listed in Table 6.

Certain model parameter values and physical measures, including canopy storage and rooting depth, were estimated using GIS land-cover datasets and the GIS Weasel (Viger and Leavesley, 2007) and these parameter values were compared to values found in the literature for Hawaiian watersheds. The GIS Weasel assigns a summer and winter rain storage in the plant canopy (**SRAIN_INTCP** and **WRAIN_INTCP**) based on the specified land cover. The GIS Weasel assigns 0.00, 0.51, 1.27, or 1.27 mm of interception capacity to bare, grass, shrub, or tree land-cover types respectively. Safeeq and Fares (2012) found that the canopy storage capacity for their study sites with invasive

trees in the Mākaha valley watershed ranged from 1.23 to 1.90 mm. Takahashi et al. (2011) estimated that canopy storage capacity for their study site in Hawai‘i Volcanoes National Park was 0.85 mm for an invaded forest site and 1.86 mm for a native forest site. Therefore, the interception parameter values calculated by the GIS Weasel and used in the PRMS Kawela model are within the range of published canopy storage capacity values for Hawaiian watersheds, but may be slightly underestimating canopy interception in the forested areas of the watershed (Table 9). Rooting depth is used to calculate certain model parameters, including **SOIL_MOIST_MAX** and **SOIL_RECHR_MAX**. The GIS Weasel assigns a rooting depth based on the specified land cover using a reclassification scheme that converts tree species into rooting depths. The rooting depths for bare ground, grass, shrub, or tree land cover were 46, 46, 76, or 76 centimeters (cm) respectively. Izuka et al. (2005) used rooting depths of 15, 51, 30, and 91 cm for bare land, grassland, scrub/shrub, and evergreen forest respectively in a water balance for the Līhu‘e basin, Kaua‘i. Therefore, the rooting depths calculated by the GIS Weasel and the soil-moisture parameter values used in the PRMS Kawela model are similar to published values for Kaua‘i, but may be slightly lower than published values in forested areas and grasslands and slightly higher in shrub and bare areas (Table 9).

The calculated potential-evapotranspiration values for the calibration, validation, and entire periods were also compared to values found in the literature for other Hawaiian watersheds to evaluate the reasonableness of the Penman-Monteith method used. The calculated daily potential evapotranspiration for each HRU for any individual day ranged from 1.52 to 5.84 mm per day for all periods. The mean annual basin potential evapotranspiration for the calibration, validation, and entire periods was approximately 1,360 mm. Measured pan-evaporation data from three sites on the island of Moloka‘i

were available, however all three sites were located on the dry, windy uplands of central and west Molokaʻi with mean annual pan evaporation ranging from 2,057 to 2,997 mm (Ekern and Chang, 1985). These pan-evaporation rates are about 30-40 percent higher than annual rates over the ocean (Ekern and Chang, 1985), and may not be representative of evaporation rates for Kawela watershed. Other measured estimates of potential evaporation ranging from 3.3-6.4 mm per day exist for sites on the leeward slopes of Haleakalā from altitudes of 950 to 2,130 meters (Giambelluca and Nullet, 1992). According to Giambelluca and Nullet (1992) the 950 meter site with 3.3 mm of evaporation per day exhibits evaporation characteristics of areas below the trade-wind inversion or from sea level to about 1,200 meters. Of the sites in this study the 950 meter site is the most comparable to some of the upper areas in Kawela watershed. An annual evapotranspiration of 1,232 mm was measured for a site in the Hawaiʻi Volcanoes National Park on the island of Hawaiʻi, at an altitude of 1,219 meters, where long-term average annual rainfall is about 2,500 mm (Giambelluca et al., 2009). Although this site receives more annual rainfall than the Kawela watershed, the potential evapotranspiration in Giambelluca et al. (2009) is consistent with the Kawela watershed's mean annual potential evapotranspiration for all periods. Therefore, the Penman-Monteith method reasonably calculates estimates of potential evapotranspiration for Kawela watershed.

3.4.2 Validation

Using the calibrated parameters in Tables 9 and 10 the PRMS Kawela model was run using input data from 4/1/2006-3/31/2008 to validate the model's performance with an independent period of data. The model output from the validation period will determine how well the PRMS model can simulate the hydrology of Kawela on a daily time step.

Table 9. Final parameter values and coefficients by hydrologic response unit in the PRMS Kawela model

Parameters are defined in Table 6. *Parameter calibrated in PEST.

Parameter or coefficient	Hydrologic-response unit																
	1	**2**	**3**	**4**	**5**	**6**	**7**	**8**	**9**	**10**	**11**	**12**	**13**	**14**	**15**	**16**	**17**
COVDEN_SUM	0.000	0.044	0.000	0.349	0.399	0.005	0.001	0.000	0.000	0.002	0.000	0.039	0.055	0.163	0.060	0.006	0.192
COVDEN_WIN	0.000	0.012	0.000	0.243	0.220	0.001	0.000	0.000	0.000	0.001	0.000	0.015	0.015	0.081	0.024	0.001	0.082
FASTCOEF_LIN	0.281	0.409	0.324	0.340	0.382	0.387	0.366	0.353	0.420	0.340	0.330	0.393	0.491	0.448	0.458	0.567	0.517
PREF_FLOW_DEN	0.016	0.029	0.021	0.022	0.027	0.027	0.025	0.024	0.031	0.022	0.021	0.028	0.038	0.033	0.035	0.046	0.041
RAD_TRNCF	0.992	0.907	0.992	0.481	0.605	0.979	0.992	0.992	0.992	0.992	0.992	0.992	0.992	0.741	0.992	0.992	0.879
SAT_THRESHOLD (cm)	5.727	6.766	5.623	7.327	7.398	6.733	6.690	6.664	6.809	6.033	6.264	7.136	6.842	7.255	7.269	6.210	6.491
SLOWCOEF_LIN*	0.008	0.009	0.008	0.008	0.009	0.009	0.008	0.008	0.009	0.008	0.008	0.009	0.009	0.009	0.009	0.009	0.009
SOIL_MOIST_MAX (cm)	1.608	3.866	1.381	5.086	5.239	3.795	3.702	3.643	3.960	2.272	2.774	4.671	4.031	4.929	4.961	2.657	3.269
SOIL_RECHR_MAX* (cm)	1.608	3.614	1.381	3.811	4.410	3.750	3.702	3.643	3.960	2.272	2.774	4.671	4.031	4.466	4.961	2.657	3.084
SSR2GW_RATE*	0.700	0.549	0.649	0.630	0.580	0.574	0.599	0.615	0.536	0.630	0.642	0.567	0.451	0.502	0.490	0.361	0.420
SRAIN_INTCP (mm)	0.940	0.721	1.039	1.255	1.240	0.485	1.123	0.851	0.445	1.181	1.128	1.270	0.866	1.270	1.260	0.711	1.229
WRAIN_INTCP (mm)	0.940	0.721	1.039	1.255	1.240	0.485	1.123	0.851	0.445	1.181	1.128	1.270	0.866	1.270	1.260	0.711	1.229

Parameter or coefficient	Hydrologic-response unit																
	18	**19**	**20**	**21**	**22**	**23**	**24**	**25**	**26**	**27**	**28**	**29**	**30**	**31**	**32**	**33**	**34**
COVDEN_SUM	0.005	0.747	0.586	0.027	0.001	0.013	0.000	0.496	0.125	0.515	0.488	0.222	0.000	0.000	0.275	0.000	0.000
COVDEN_WIN	0.001	0.568	0.498	0.009	0.000	0.003	0.000	0.346	0.049	0.498	0.281	0.080	0.000	0.000	0.181	0.000	0.000
FASTCOEF_LIN	0.483	0.365	0.346	0.634	0.538	0.511	0.284	0.442	0.526	0.168	0.468	0.555	0.647	0.301	0.461	0.340	0.732
PREF_FLOW_DEN	0.037	0.025	0.023	0.053	0.043	0.040	0.016	0.033	0.042	0.004	0.036	0.045	0.054	0.018	0.035	0.022	0.063
RAD_TRNCF	0.992	0.266	0.220	0.984	0.992	0.992	0.992	0.358	0.748	0.242	0.472	0.969	0.992	0.992	0.484	0.992	0.992
SAT_THRESHOLD (cm)	6.685	8.215	8.410	6.446	6.219	6.291	5.694	8.037	6.846	8.558	7.349	6.539	5.971	6.487	7.821	6.127	5.871
SLOWCOEF_LIN*	0.009	0.008	0.008	0.010	0.009	0.009	0.008	0.009	0.009	0.007	0.009	0.009	0.010	0.008	0.009	0.008	0.010
SOIL_MOIST_MAX (cm)	3.690	7.016	7.441	3.170	2.677	2.833	1.535	6.630	4.040	7.762	5.134	3.373	2.137	3.259	6.159	2.476	1.921
SOIL_RECHR_MAX* (cm)	3.690	5.009	4.984	3.150	2.677	2.833	1.535	4.993	3.568	4.747	4.079	3.330	2.137	3.259	4.733	2.477	1.921
SSR2GW_RATE*	0.460	0.601	0.623	0.282	0.395	0.427	0.697	0.509	0.410	0.833	0.478	0.375	0.266	0.677	0.486	0.630	0.165
SRAIN_INTCP (mm)	0.643	1.270	1.270	1.153	0.973	0.767	1.158	1.270	1.049	1.270	1.191	1.130	0.579	0.343	1.260	0.155	0.290
WRAIN_INTCP (mm)	0.643	1.270	1.270	1.153	0.973	0.767	1.158	1.270	1.049	1.270	1.191	1.130	0.579	0.343	1.260	0.155	0.290

Table 9. Final parameter values and coefficients by hydrologic response unit in the PRMS Kawela model–Continued.

Parameters are defined in Table 6. *Parameter calibrated in PEST.

Parameter or coefficient	Hydrologic-response unit																
	35	**36**	**37**	**38**	**39**	**40**	**41**	**42**	**43**	**44**	**45**	**46**	**47**	**48**	**49**	**50**	**51**
COVDEN_SUM	0.032	0.645	0.613	0.149	0.000	0.366	0.624	0.000	0.744	0.079	0.000	0.001	0.012	0.000	0.099	0.539	0.452
COVDEN_WIN	0.003	0.645	0.480	0.080	0.000	0.343	0.616	0.000	0.744	0.022	0.000	0.000	0.002	0.000	0.039	0.532	0.177
FASTCOEF_LIN	0.514	0.323	0.416	0.447	0.299	0.514	0.369	0.317	0.410	0.693	0.449	0.657	0.736	0.374	0.783	0.367	0.538
PREF_FLOW_DEN	0.040	0.020	0.030	0.033	0.018	0.040	0.025	0.020	0.029	0.059	0.034	0.055	0.063	0.026	0.068	0.025	0.043
RAD_TRNCF	0.992	0.168	0.247	0.698	0.992	0.373	0.179	0.992	0.128	0.992	0.992	0.992	0.992	0.992	0.992	0.225	0.973
SAT_THRESHOLD (cm)	6.045	8.500	8.231	7.621	5.650	8.504	8.560	5.688	8.496	5.564	5.532	5.652	5.965	5.684	5.044	8.484	7.301
SLOWCOEF_LIN*	0.009	0.008	0.009	0.009	0.008	0.009	0.008	0.008	0.009	0.010	0.009	0.010	0.010	0.008	0.011	0.008	0.009
SOIL_MOIST_MAX (cm)	2.299	7.635	7.050	5.725	1.439	7.644	7.767	1.522	7.627	1.253	1.184	1.444	2.125	1.515	0.123	7.600	5.029
SOIL_RECHR_MAX* (cm)	2.299	4.581	4.946	4.885	1.439	4.790	4.694	1.522	4.576	1.254	1.184	1.444	2.125	1.515	0.123	4.594	4.990
SSR2GW_RATE*	0.424	0.650	0.540	0.503	0.679	0.424	0.596	0.657	0.548	0.211	0.501	0.254	0.160	0.590	0.105	0.598	0.395
SRAIN_INTCP (mm)	0.333	1.270	1.267	1.227	1.186	1.270	1.270	1.001	1.270	0.871	0.315	0.424	0.767	0.523	1.247	1.270	1.234
WRAIN_INTCP (mm)	0.333	1.270	1.267	1.227	1.186	1.270	1.270	1.001	1.270	0.871	0.315	0.424	0.767	0.523	1.247	1.270	1.234

Parameter or coefficient	Hydrologic-response unit																
	52	**53**	**54**	**55**	**56**	**57**	**58**	**59**	**60**	**61**	**62**	**63**	**64**	**65**	**66**	**67**	**68**
COVDEN_SUM	0.351	0.127	0.033	0.009	0.000	0.003	0.000	0.723	0.000	0.009	0.000	0.442	0.719	0.710	0.133	0.110	0.000
COVDEN_WIN	0.113	0.036	0.011	0.001	0.000	0.001	0.000	0.694	0.000	0.001	0.000	0.196	0.719	0.693	0.045	0.041	0.000
FASTCOEF_LIN	0.794	0.727	0.461	0.780	0.265	0.333	0.576	0.640	0.260	0.665	0.373	0.709	0.300	0.248	0.676	0.452	0.346
PREF_FLOW_DEN	0.070	0.062	0.035	0.068	0.014	0.021	0.047	0.053	0.014	0.056	0.026	0.061	0.018	0.013	0.057	0.034	0.023
RAD_TRNCF	0.992	0.992	0.992	0.992	0.992	0.992	0.992	0.150	0.992	0.992	0.992	0.795	0.137	0.148	0.992	0.888	0.992
SAT_THRESHOLD (cm)	5.396	4.991	5.624	5.460	5.707	6.409	5.130	8.700	5.712	5.526	6.325	5.812	8.731	8.287	5.119	6.892	5.747
SLOWCOEF_LIN*	0.011	0.010	0.009	0.011	0.008	0.008	0.010	0.010	0.008	0.010	0.008	0.010	0.008	0.008	0.010	0.009	0.008
SOIL_MOIST_MAX (cm)	0.888	0.025	1.383	1.026	1.564	3.090	0.310	8.071	1.575	1.171	2.908	1.791	8.137	7.172	0.286	4.140	1.652
SOIL_RECHR_MAX* (cm)	0.888	0.025	1.383	1.026	1.564	3.090	0.310	4.986	1.575	1.171	2.908	1.404	4.882	4.373	0.286	3.858	1.652
SSR2GW_RATE*	0.092	0.172	0.487	0.109	0.719	0.639	0.350	0.275	0.725	0.245	0.590	0.192	0.677	0.740	0.231	0.497	0.623
SRAIN_INTCP (mm)	1.074	0.978	1.140	0.460	0.117	0.884	1.219	1.270	0.196	0.399	0.871	1.209	1.270	1.270	1.087	1.019	0.838
WRAIN_INTCP (mm)	1.074	0.978	1.140	0.460	0.117	0.884	1.219	1.270	0.196	0.399	0.871	1.209	1.270	1.270	1.087	1.019	0.838

Table 9. Final parameter values and coefficients by hydrologic response unit in the PRMS Kawela model–Continued.

Parameters are defined in Table 6. *Parameter calibrated in PEST.

Parameter or coefficient	Hydrologic-response unit																
	69	**70**	**71**	**72**	**73**	**74**	**75**	**76**	**77**	**78**	**79**	**80**	**81**	**82**	**83**	**84**	**85**
COVDEN_SUM	0.000	0.771	0.525	0.001	0.770	0.747	0.809	0.002	0.414	0.697	0.814	0.456	0.817	0.022	0.782	0.404	0.670
COVDEN_WIN	0.000	0.771	0.476	0.000	0.770	0.747	0.809	0.000	0.157	0.645	0.814	0.357	0.817	0.008	0.782	0.210	0.670
FASTCOEF_LIN	0.427	0.283	0.320	0.330	0.334	0.380	0.202	0.348	0.685	0.409	0.208	0.387	0.238	0.504	0.197	0.437	0.449
PREF_FLOW_DEN	0.031	0.016	0.020	0.021	0.022	0.026	0.008	0.023	0.058	0.029	0.009	0.027	0.012	0.039	0.007	0.032	0.034
RAD_TRNCF	0.992	0.118	0.242	0.992	0.119	0.126	0.107	0.992	0.947	0.166	0.105	0.367	0.104	0.992	0.115	0.617	0.157
SAT_THRESHOLD (cm)	5.492	8.778	7.879	5.665	8.195	8.682	8.676	5.654	6.338	8.256	8.708	8.120	8.735	5.559	8.705	7.728	8.707
SLOWCOEF_LIN*	0.009	0.008	0.008	0.008	0.008	0.009	0.008	0.008	0.010	0.009	0.008	0.009	0.008	0.009	0.008	0.009	0.009
SOIL_MOIST_MAX (cm)	1.096	8.240	6.285	1.473	6.972	8.031	8.019	1.448	2.936	7.105	8.089	6.809	8.147	1.242	8.082	5.958	8.087
SOIL_RECHR_MAX* (cm)	1.097	4.944	4.051	1.473	4.183	4.819	4.811	1.448	2.835	4.509	4.853	4.797	4.888	1.242	4.849	4.908	4.852
SSR2GW_RATE*	0.527	0.697	0.653	0.641	0.637	0.582	0.794	0.621	0.221	0.548	0.786	0.575	0.751	0.435	0.799	0.515	0.501
SRAIN_INTCP (mm)	0.782	1.270	1.270	0.772	1.270	1.270	1.270	0.747	1.143	1.270	1.270	1.270	1.270	1.189	1.270	1.006	1.270
WRAIN_INTCP (mm)	0.782	1.270	1.270	0.772	1.270	1.270	1.270	0.747	1.143	1.270	1.270	1.270	1.270	1.189	1.270	1.006	1.270

Parameter or coefficient	Hydrologic-response unit													
	86	**87**	**88**	**89**	**90**	**91**	**92**	**93**	**94**	**95**	**96**	**97**	**98**	**99**
COVDEN_SUM	0.805	0.780	0.000	0.033	0.000	0.073	0.003	0.002	0.047	0.229	0.503	0.699	0.601	0.731
COVDEN_WIN	0.805	0.780	0.000	0.013	0.000	0.032	0.000	0.000	0.016	0.082	0.420	0.625	0.598	0.731
FASTCOEF_LIN	0.224	0.153	0.366	0.395	0.369	0.393	0.701	0.866	0.655	0.851	0.544	0.617	0.297	0.314
PREF_FLOW_DEN	0.010	0.003	0.025	0.028	0.025	0.028	0.060	0.077	0.055	0.075	0.043	0.051	0.018	0.019
RAD_TRNCF	0.108	0.115	0.992	0.937	0.992	0.910	0.992	0.992	0.992	0.992	0.279	0.188	0.189	0.132
SAT_THRESHOLD (cm)	8.726	8.718	6.144	6.912	5.634	7.013	5.605	5.161	5.321	5.094	8.275	8.502	8.556	8.572
SLOWCOEF_LIN*	0.008	0.007	0.008	0.009	0.008	0.009	0.010	0.011	0.010	0.011	0.009	0.010	0.008	0.008
SOIL_MOIST_MAX (cm)	8.128	8.109	2.515	4.183	1.405	4.403	1.341	0.376	0.725	0.231	7.147	7.640	7.758	7.791
SOIL_RECHR_MAX* (cm)	4.877	4.865	2.515	4.064	1.405	4.203	1.341	0.376	0.725	0.231	4.834	4.935	4.671	4.675
SSR2GW_RATE*	0.768	0.852	0.599	0.565	0.596	0.567	0.202	0.033	0.257	0.033	0.389	0.302	0.681	0.661
SRAIN_INTCP (mm)	1.270	1.270	1.265	1.217	1.245	1.270	0.333	0.396	1.074	1.163	1.270	1.270	1.270	1.270
WRAIN_INTCP (mm)	1.270	1.270	1.265	1.217	1.245	1.270	0.333	0.396	1.074	1.163	1.270	1.270	1.270	1.270

Table 10. Basin-wide parameters and coefficients in the PRMS Kawela model
Parameters are defined in Table 6. *Parameter calibrated in PEST.

Parameter or coefficient	Basin
GWFLOW_COEF	0.0010
GWSINK_COEF	1.0000
GWSTOR_INIT (cm)	0.0000
SSR2GW_EXP*	0.1524
SSSTOR_INIT (cm)	0.0000
CAREA_MAX*	0.6000
FASTCOEF_SQ	1.0000
IMPERV_STOR_MAX* (cm)	2.5400
SLOWCOEF_SQ*	0.0000
SMIDX_COEF*	0.0001
SMIDX_EXP*	0.2000
SOIL_MOIST_INIT (cm)	2.5400
SOIL_RECHR_INIT (cm)	2.5400
SOIL2GW_MAX* (cm)	0.1283

Chapter 4

REULTS AND DISCUSSION

4.1 Results

Simulation results for the calibration (4/1/2008-3/31/2010), validation (4/1/2006-3.31/2008), and entire (4/1/2006-3/31/2010) periods were evaluated statistically and graphically. Figures 16 and 17 compare the simulated and measured hydrographs for the calibration and validation periods. Figure 18 compares the flow-duration curves of the measured and simulated flows for the calibration, validation, and entire periods. The measured and simulated Q_{90} flows are 0 and 0.01 cubic meters per second (m^3sec^{-1}), respectively, during each of the calibration, validation, and entire periods (Figure 18). The measured and simulated median (Q_{50}) flows are 0 and 0.03 m^3sec^{-1}, respectively, during each of the calibration, validation, and entire periods (Figure 18). Unlike the Q_{90} and Q_{50} flows, the Q_{10} flows are different for each of the periods. The measured Q_{10} flows were 0.09, 0.27, and 0.19 m^3sec^{-1} during the calibration, validation and entire periods, respectively. The simulated Q_{10} flows were 0.07, 0.12, and 0.09 m^3sec^{-1} during calibration, validation and entire periods, respectively (Figure 18). The model tends to overestimate flows lower than about the Q_{20}, and underestimate the higher flows from about the Q_{20} to the Q_1 flow.

To provide a hydrological context for the calibration, validation, and entire periods, long-term rainfall data at two rain gages located on Moloka‘i and the long-term annual rainfall for the Kawela watershed were compared to the study period. Annual rainfall at Moloka‘i Airport rain gage ranged from about 70 to 1,100 mm during the 1975-2012 period, and the average annual rainfall during this period was 640 mm (Figure 19). Annual rainfall at the lower elevation coastal Kaunakakai rain-gage ranged from 13

to 750 mm during the 1975-2012 period, and the average annual rainfall during this period was 370 mm (Figure 19). The average annual rainfall at the Kaunakakai gage during the calibration, validation, and entire periods was about 185, 400, and 295 millimeters, respectively. Rainfall during the calibration and entire period was less than the longer-term (1975-2012) average rainfall at the Kaunakakai gage. The long-term (1978-2007) average annual rainfall determined for Kawela watershed, using data from Giambelluca et al. (2012), is 1,798 mm. The average annual rainfall in Kawela watershed during the calibration, validation, and entire periods was about 1,880, 2,155, and 2,018 mm, respectively. Rainfall during all periods was greater than the longer-term (1978-2007) average annual rainfall determined for Kawela watershed (Giambelluca et al., 2012). The calibration period was a drier period in comparison to the validation period. For the calibration period, measured flows ranged from about 0-2.3 m^3sec^{-1}, whereas for the validation period, measured flows ranged from about 0-4.5 m^3sec^{-1} (Figure 16 and 17). Overall PRMS does a satisfactory job of replicating the measured hydrograph for both the calibration and validation periods. The model visually seems to be simulating flow in the calibration period (Figure 16) better than in the validation period (Figure 17), which is expected. The PRMS Kawela model may not accurately simulate larger fall and winter flow events from 2.3-4.5 m^3sec^{-1}, and tends to miss a few of the smaller spring and summer flow events of 1.4 m^3sec^{-1} or less.

Statistical measures of the accuracy of the daily mean simulated streamflow for the calibration, validation, and entire periods are presented in Table 11. The goodness of fit between the measured and simulated hydrographs was evaluated using the coefficient of efficiency (Nash and Sutcliffe, 1970). The coefficient of efficiency ranges from 1 to negative values. A value of 1 signifies a perfect fit between the measured and simulated

hydrographs; a value of 0 signifies that the mean measured value is equivalent in predictive power to the model; and a negative value signifies that the mean measured value is a better predictor than the model. The coefficient of efficiency is a widely used relative measure of a model's predictive power (Markstrom et al., 2008). A bias percentage was also calculated to determine if the model consistently overestimated or underestimated runoff. A bias of 0 indicates that the model does not have a tendency to either overestimate or underestimate runoff. A positive value indicates a tendency to overestimate runoff, whereas a negative value indicates a tendency to underestimate runoff. The third statistic used to evaluate the PRMS Kawela model is the ratio between the root-mean-square error (RMSE) and observations' standard deviation or RSR. RMSE is a commonly used error index statistic and based on a recommendation by Singh et al. (2005), this statistic was standardized using the observations' standard deviation. The RSR statistic varies from 0 to a large positive value. A RSR value of 0 indicates zero RMSE or residual variation and therefore a perfect model simulation. A smaller value of RSR indicates a better model performance (Moriasi et al., 2007).

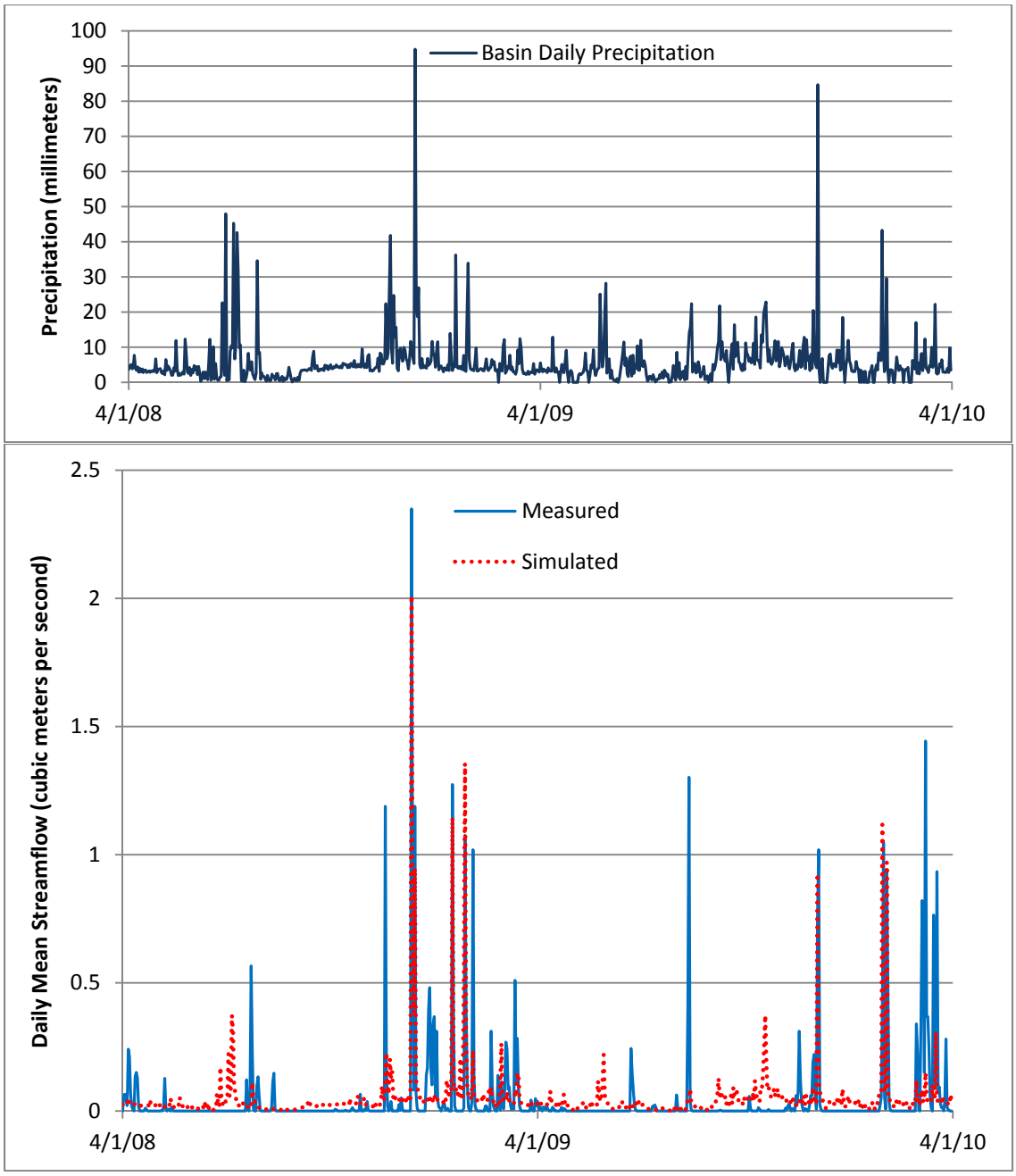

Figure 16. Basin daily precipitation and measured and simulated daily streamflow for the calibration period (4/1/08-3/31/10)

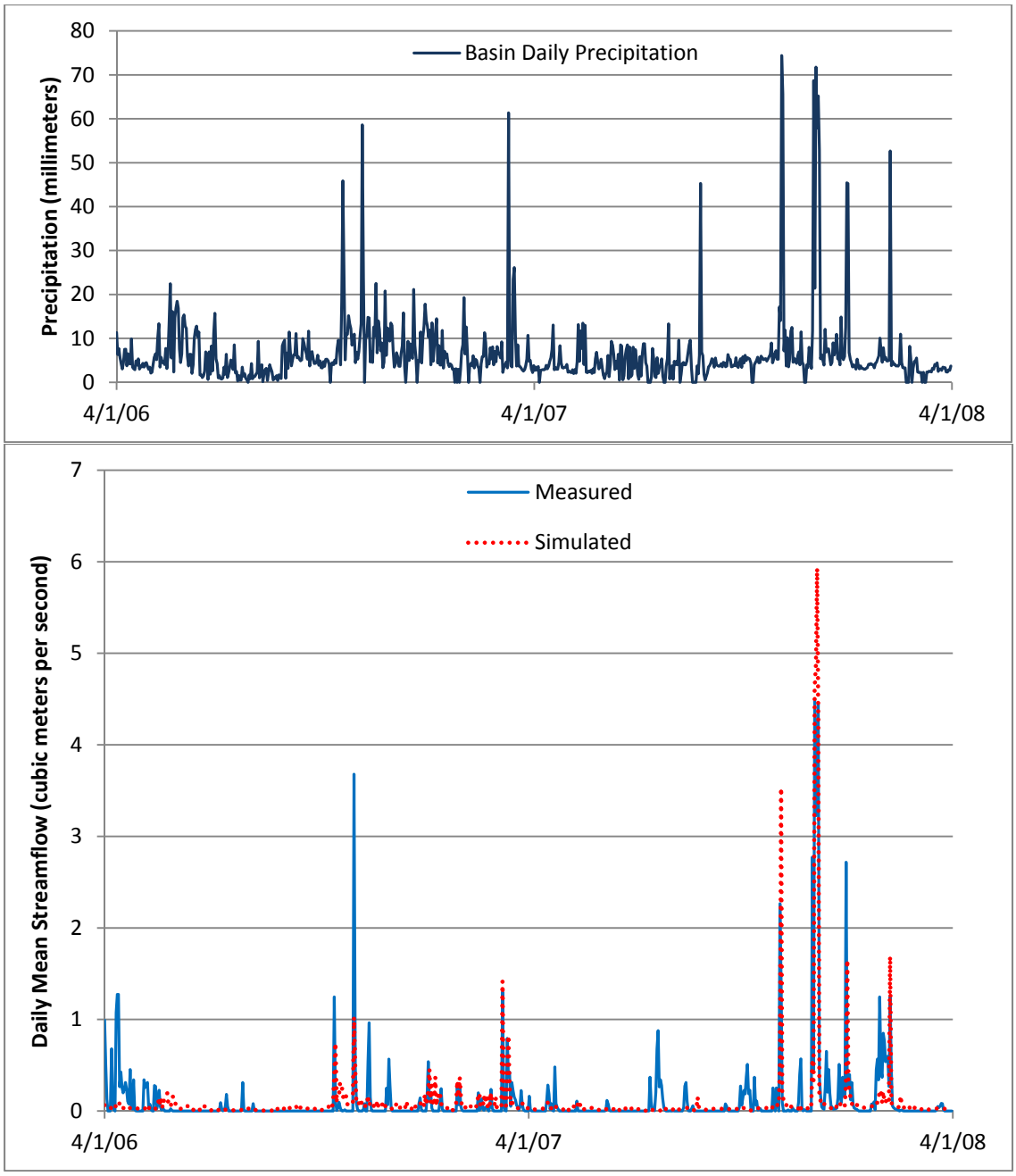

Figure 17. Basin daily precipitation and measured and simulated daily streamflow for the validation period (4/1/06-3/31/08)

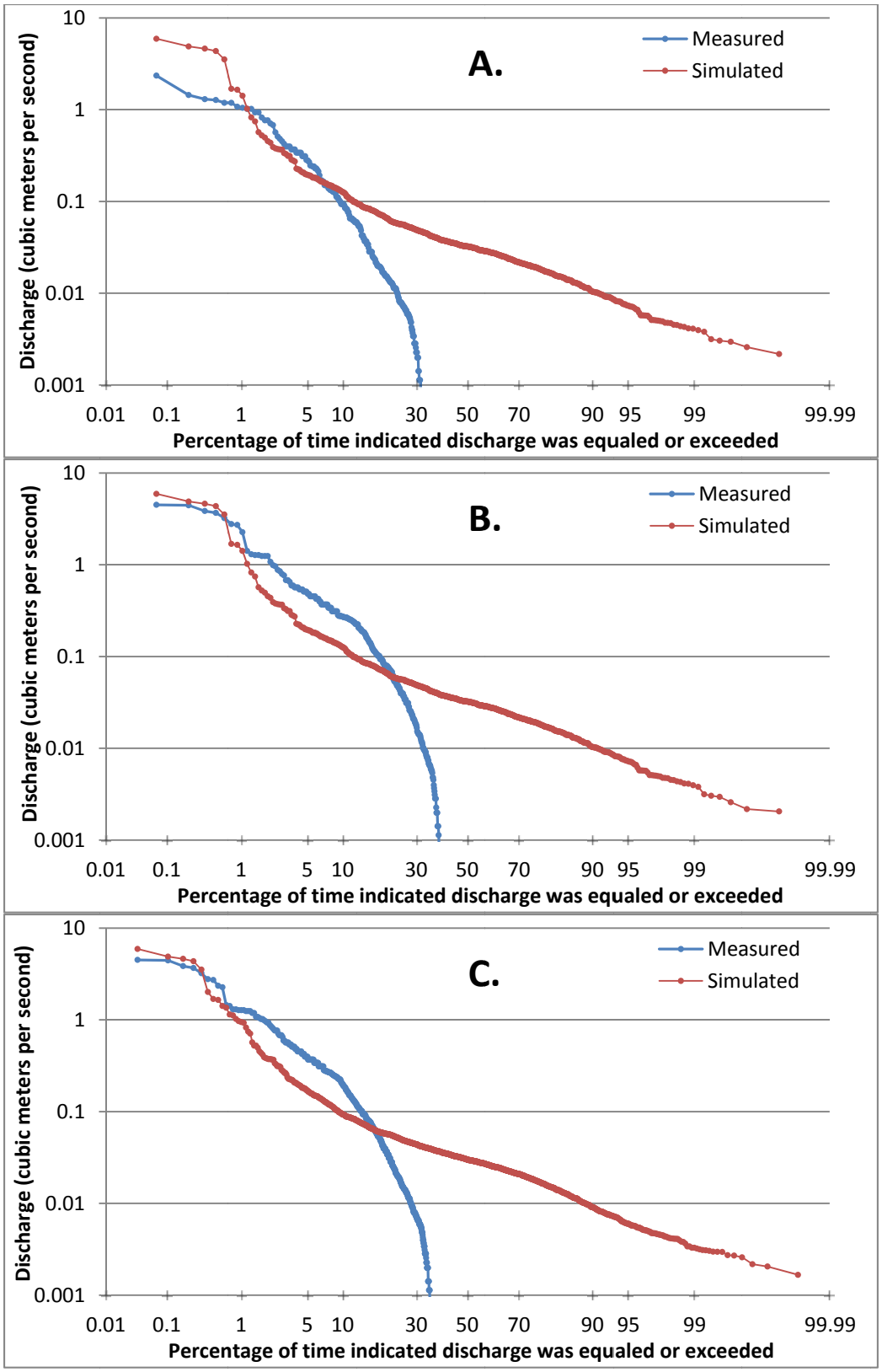

Figure 18. Flow duration curves of the measured and simulated daily flows for the A. calibration B. validation and C. entire period.

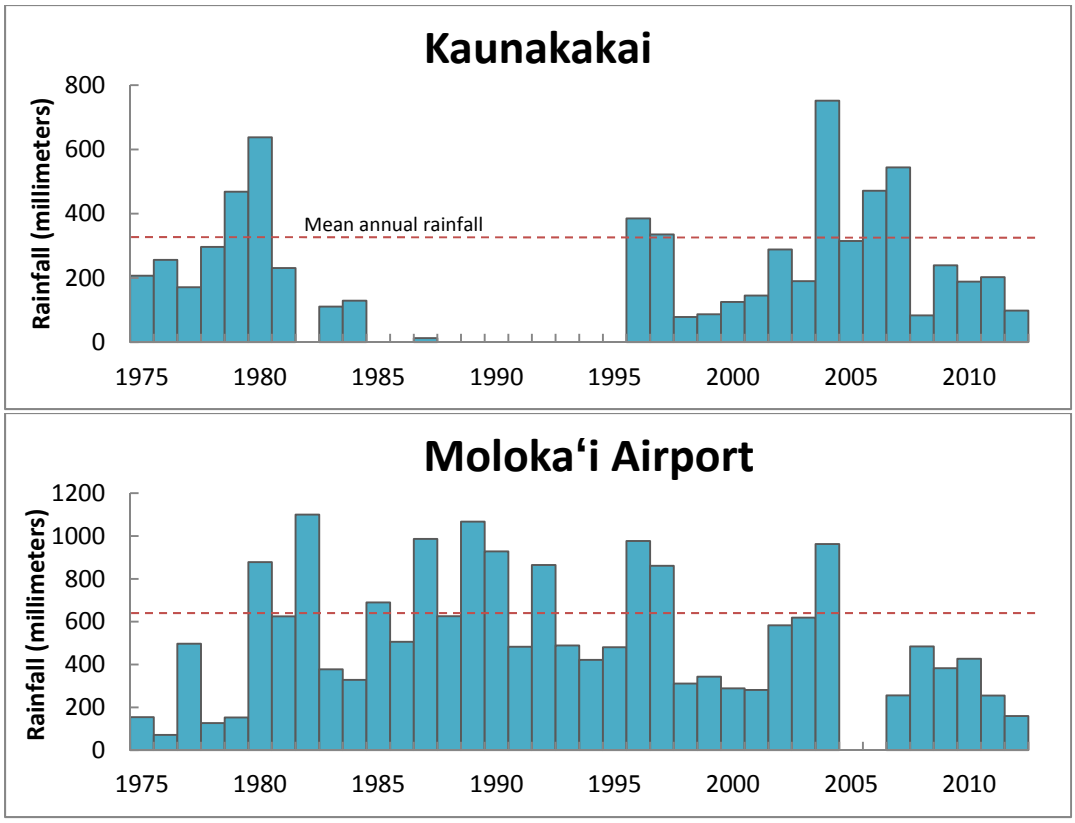

Figure 19. Annual rainfall at selected rain-gaging stations on the Island of Moloka'i, Hawai'i, for the period 1975–2012. Mean annual rainfall values are for 1975–2012 and do not include missing or incomplete years (indicated as zero values). Data from National Climatic Data Center (2013).

The daily coefficient of efficiency ranges from 0.46 for the calibration period to 0.56 for the validation period. These values indicate that the daily PRMS Kawela model's predictive power is greater than using the mean measured value of runoff. Usually the model is expected to perform better in the calibration period and worse in the validation period due to the nature of the calibration process and that particular period being used to optimize the parameter values used in the model. However, PRMS tends to perform better in the wetter validation period and worse in the drier calibration period, which may be related to the use of NEXRAD data. NEXRAD data are primarily used for flood forecasting and therefore may be more favorable to modeling larger flow events. The coefficient of efficiency for the entire period is 0.55, and this value confirms that, overall,

the model's simulated hydrograph reasonably fits the measured hydrograph. Based on the bias statistic, PRMS overestimated runoff in the calibration period (bias=6.34 percent), underestimated runoff in the validation period (bias=-15.37 percent), and, overall, underestimated runoff for the entire period (bias= -8.71 percent). The RSR values indicate that the model performed better in the wetter validation period (RSR=0.66) than the drier calibration period (RSR=0.74). The RSR value for the entire period (RSR=0.62) indicates a satisfactory model performance.

Model-evaluation statistics computed using monthly values (determined from aggregated daily values) generally indicate better performance than statistics computed using the daily values. Monthly model simulations with a coefficient of efficiency equal to or greater than 0.5, a bias between +25 and -25 percent, and an RSR less than 0.7 are commonly rated as having a satisfactory performance. Model simulations with a coefficient of efficiency greater than 0.65, a bias between +15 and -15 percent, and an RSR less than 0.6 are commonly rated as having a good performance. Finally, model simulations with a coefficient of efficiency greater than 0.75, a bias between +10 and -10 percent, and an RSR less than 0.5 are commonly rated as having a very good performance (Moriasi et al., 2007). Statistical measures of the accuracy of the monthly mean simulated streamflow for the calibration, validation, and entire periods are presented in Table 12. The coefficient of efficiency increases and the RSR decreases for both the validation and entire model period at the monthly time scale. However, the coefficient of efficiency decreases slightly and the RSR increases slightly for the calibration period at the monthly time scale. For the entire period, the daily model performance rating of "satisfactory" is upgraded to a "very good" performance rating when daily values are aggregated up to the monthly time scale.

Table 11. Errors in simulated daily mean streamflow, Kawela watershed
[RMSE: Root mean square error]

Period	Coefficient of Efficiency*	Bias (percent)**	RMSE to observations standard deviation ratio (RSR)***
Calibration (04/01/2008-3/31/2010)	0.46	6.34	0.74
Validation (04/01/2006-3/31/2008)	0.56	-15.37	0.66
Entire Period (04/01/2006-04/25/2010)	0.55	-8.71	0.62

$$^{*}Coefficient\ of\ Efficiency = 1 - \left[\frac{\sum_{i=1}^{n}(Y_i^{obs} - Y_i^{sim})^2}{\sum_{i=1}^{n}(Y_i^{obs} - Y^{mean})^2}\right]$$

where,
Y_i^{obs} is the measured streamflow for day *i,*
Y_i^{sim} is the simulated streamflow for day *i,* and
Y^{mean} is the mean measured streamflow for the full simulation period.

$$^{**}Bias = \left[\frac{\sum_{i=1}^{n}(Y_i^{sim} - Y_i^{obs}) * 100}{\sum_{i=1}^{n}(Y_i^{obs})}\right]$$

$$^{***}RSR = \frac{RMSE}{STDEV_{obs}} = \frac{\left[\sqrt{\sum_{i=1}^{n}(Y_i^{obs} - Y_i^{sim})^2}\right]}{\left[\sqrt{\sum_{i=1}^{n}(Y_i^{obs} - Y^{mean})^2}\right]}$$

where,
$RMSE$ is the root-mean-square error,
$STDEV_{obs}$ is the standard deviation of the observations, and
RSR is the root-mean-square error to observations' standard deviation ratio.

Table 12. Errors in simulated monthly mean streamflow, Kawela watershed

[RMSE: Root mean square error]

Period	Coefficient of Efficiency*	Bias (percent)**	RMSE to observations standard deviation ratio (RSR)***
Calibration (04/01/2008-3/31/2010)	0.44	6.35	0.75
Validation (04/01/2006-3/31/2008)	0.85	-15.37	0.38
Entire Period (04/01/2006-04/25/2010)	0.82	-8.71	0.42

$$^{*}Coefficient\ of\ Efficiency = 1 - \left[\frac{\sum_{i=1}^{n}\left(Y_i^{obs} - Y_i^{sim}\right)^2}{\sum_{i=1}^{n}\left(Y_i^{obs} - Y^{mean}\right)^2}\right]$$

where,
Y_i^{obs} is the measured streamflow for day *i,*
Y_i^{sim} is the simulated streamflow for day *i,* and
Y^{mean} is the mean measured streamflow for the full simulation period.

$$^{**}Bias = \left[\frac{\sum_{i=1}^{n}\left(Y_i^{sim} - Y_i^{obs}\right)*100}{\sum_{i=1}^{n}\left(Y_i^{obs}\right)}\right]$$

$$^{***}RSR = \frac{RMSE}{STDEV_{obs}} = \frac{\left[\sqrt{\sum_{i=1}^{n}\left(Y_i^{obs} - Y_i^{sim}\right)^2}\right]}{\left[\sqrt{\sum_{i=1}^{n}\left(Y_i^{obs} - Y^{mean}\right)^2}\right]}$$

where,
$RMSE$ is the root-mean-square error,
$STDEV_{obs}$ is the standard deviation of the observations, and
RSR is the root-mean-square error to observations' standard deviation ratio.

A summary of the measured and simulated runoff volumes for the calibration, validation, and entire periods (Table 13) indicates that most of the overall difference between the measured and simulated flows is associated with the validation period. The model computed the total runoff volume within 8.7 percent over the entire simulation period.

Table 13. Summary of measured and simulated cumulative runoff, Kawela watershed

[Runoff: Measured runoff= total volume of runoff/area of watershed.
Percentage difference=100 x (Simulated - Measured)/Measured]

Period	Measured Runoff (meters)	Simulated Runoff (meters)	Percentage difference
Calibration (04/01/2008-3/31/2010)	0.227	0.242	6.4
Validation (04/01/2006-3/31/2008)	0.514	0.435	-15.4
Entire Period (04/01/2006-04/25/2010)	0.741	0.676	-8.7

Preliminary model runs driven with only rain-gage data, only NEXRAD-derived rainfall data, and calibrated/validated to varying dates were also evaluated. However, these preliminary models did not perform acceptably (Table 14). Therefore, precipitation data estimated from NEXRAD data and corrected with data from the five Kawela area rain gages using the mean-field bias correction were used as input for the final PRMS Kawela model.

Table 14. Errors in simulated daily mean streamflow for preliminary model versions.
[NSE: Nash Sutcliffe coefficient of efficiency, RSR: Root-mean-square error to observations standard deviation ratio]

Model Version	Rainfall Input Used	Action	Period Used	NSE	Bias (percent)	RSR
1	NEXRAD-derived rainfall (uncorrected)	Calibration	2006-2008	0.7	-4	0.54
		Validation	2008-2010	-5.36	195	2.52
2	NEXRAD-derived rainfall (uncorrected)	Calibration	2008-2010	0.42	6	0.76
		Validation	2006-2008	0.25	-48	0.86
3	Rain Gage 4 (Kawela Field Site, Kamiloloa, Kānoa Beach, Kaunakakai)	Calibration	2006-2008	0.76	-39	0.49
		Validation	2008-2010	0.34	-50	0.81
4	Rain Gage 5 (Kawela Field Site, Kamiloloa, Kawela Fan, Kānoa Beach, Kaunakakai)	Calibration	2006-2008	0.73	-19	0.51
		Validation	2008-2010	0.34	6	0.81
5	Rain Gage 5 (Kawela Field Site, Kamiloloa, Kawela Fan, Kānoa Beach, Kaunakakai)	Calibration	2007-2009	0.74	-8	0.5
		Validation	2006	0.6	-22	0.63
		Validation	2010	0.2	-14	0.89
6	Rain Gage 5 (Kawela Field Site, Kamiloloa, Kawela Fan, Kānoa Beach, Kaunakakai)	Calibration	2008-2010	0.39	-3	0.77
		Validation	2006-2008	0.72	-26	0.53

4.2 Applications of the Model

The PRMS Kawela model can be used both as a water and natural-resource management tool to evaluate the hydrological response of the watershed to changes in various conditions. Running the calibrated PRMS Kawela model produces a summary output file of the simulated water budget that can be set to a user-specified frequency (daily, monthly, yearly) and includes basin-weighted averages for net precipitation, evapotranspiration for all sources, storage in all reservoirs, and the simulated and observed flows (Markstrom et al., 2008). The simulated water budget can be used to calculate the amount of groundwater recharge, which can be used for water-availability assessments and as input to groundwater models.

The calibrated PRMS Kawela model's simulated water budget can also be used as a baseline to assess different watershed land-cover change scenarios and evaluate the hydrological system's sensitivity to changes in vegetation. A generalized map of Kawela watershed's vegetation cover before human impacts (Jacobi, 2011b) and simple cover-type conversions of HRUs within the watershed that reflect restoration or degradation were used as land-cover change scenarios. The effectiveness of the restoration scenario or impact of the degradation was assessed by examining the relative change in the partitioned amount of rainfall to simulated runoff and recharge in each scenario from the baseline. Any scenarios that significantly decrease the amount of runoff in the watershed and, by inference, the amount of sediment reaching the nearshore environment, without drastically changing the amount of recharge in the watershed is considered an effective watershed restoration scenario.

4.2.1 Water-Budget Assessment

The fundamental equation used in the PRMS Kawela model to simulate the hydrological cycle within the watershed is the basic continuity equation. The continuity equation simply states that any changes in water storage in the watershed should be equal to the water inputs to the watershed minus the water outputs from the watershed. The inputs and outputs of the simple continuity equation can be expanded into the components of the hydrological cycle modeled by PRMS and rearranged to calculate the amount of estimated groundwater recharge for the watershed.

$$\Delta Storage = (Inputs) - (Outputs) \quad (2)$$

$$\Delta S = (P) - (R + ET + G)$$

$$G = P - R - ET - \Delta S$$

G=Groundwater recharge
P=Precipitation (rainfall plus fog drip)
R=Runoff
ET=Evapotranspiration
ΔS= Change in storage

The water budget of the PRMS Kawela model for the calibration, validation, and entire periods of simulation is listed in Table 15. An average annual water budget for the PRMS Kawela model over the four-year period (04/01/2006-03/31/2010) and the associated ratios of evapotranspiration, runoff, and recharge to precipitation were also calculated so that they may be compared to previous water budgets prepared for the greater Kawela area (Table 16).

Table 15. Water budget for the Kawela watershed (millimeters).
[ET: Evapotranspiration]

Period	Precipitation	ET	Storage	Runoff	Recharge
Calibration (04/01/2008-03/31/2010)	3,760	1,700	20	240	1,810
Validation (04/01/2006-03/31/2008)	4,310	1,810	10	440	2,060
Entire Period (04/01/2006-03/31/2010)	8,070	3,510	20	680	3,870

Table 16. Previous water-budget component estimates for the Kawela area compared to the average annual PRMS Kawela water budget.
[mm: millimeters; ET: Evapotranspiration; %:percent; km^2: kilometers squared]

Study, Area	Precipitation (mm/year)	ET (mm/ year)	Runoff (mm/year)	Recharge (mm/year)	ET/ Precipitation Ratio (%)	Runoff/ Precipitation Ratio (%)	Recharge/ Precipitation Ratio (%)
PRMS Kawela (Avg. Ann.), 13.7 km^2	2,020	870	170	970	43	8	48
State of Hawai‘i (1990), 61.4 km^2	1,220	890	80	250	73	6	21
Shade (1997) (Avg.), 51.3 km^2	990	530	100	360	54	10	36

The results of the PRMS Kawela model over the four-year period (04/01/2006-03/31/2010) indicate that most of the precipitation that falls in the watershed is either partitioned into evapotranspiration (43 percent) or recharge (48 percent). A much smaller percentage of that precipitation is partitioned into runoff (8 percent) that is estimated at the outlet of the watershed at the USGS Kawela stream-gaging station. The instantaneous amount of storage in all of the conceptual PRMS reservoirs calculated at the end of the time period is also shown in Table 15. Figure 20 shows the temporal variability of the simulated components (aggregated to monthly values) of the PRMS Kawela model over the entire simulation period. The figure shows a distinct seasonal pattern in precipitation, evapotranspiration, runoff, and groundwater recharge throughout the simulation period. Generally, more precipitation, runoff, and recharge occur during the winter months. The range of the evapotranspiration estimate is not as wide due to water-availability

limitations in the summer and evaporative energy limits in the winter. Figure 21 shows the spatial variability of actual ET, runoff, and groundwater recharge in the Kawela watershed over the entire simulation period. The majority of the actual ET, runoff, and recharge are generated in the upper forested one third of the watershed where most precipitation occurs. The spatial distribution of the recharge differs slightly from the general pattern near the outlet of the basin. This may be a result of the model attempting to limit the amount of runoff simulated at the outlet. A 15 percent increase in the externally calculated potential ET dataset was applied to determine if changes in potential ET have a greater effect on the runoff or recharge component of the Kawela water budget. The 15 percent increase in potential ET resulted in an 8.1 percent increase in actual ET, 3.4 percent decrease in runoff, and a 6.7 percent decrease in recharge.

This study's water budget calculates a greater percentage of precipitation being partitioned into groundwater recharge compared to two previous water budgets (Table 16) for the greater Kawela area, corresponding to the Kawela "aquifer system" defined by the State of Hawai'i (1990). The same Kawela aquifer-system delineation was used in both studies, but the calculated areas for the previous water budget studies differ by about 10 km^2. It is not known how the area for the State of Hawai'i (1990) was computed. The previous water budgets were constructed using a generalized water-budget model and an accounting procedure that balances moisture input of rainfall, and moisture outputs of runoff, evapotranspiration, and groundwater recharge. The water budget by the State of Hawai'i (1990) was calculated annually for a 61.4 square kilometer Kawela aquifer system using maps of mean annual rainfall for the base period from 1931-1983 from Giambelluca et al. (1986). The study assumes a set evapotranspiration value of 73 percent of rainfall for areas with 1,397 mm or less of annual rainfall, and does not include fog

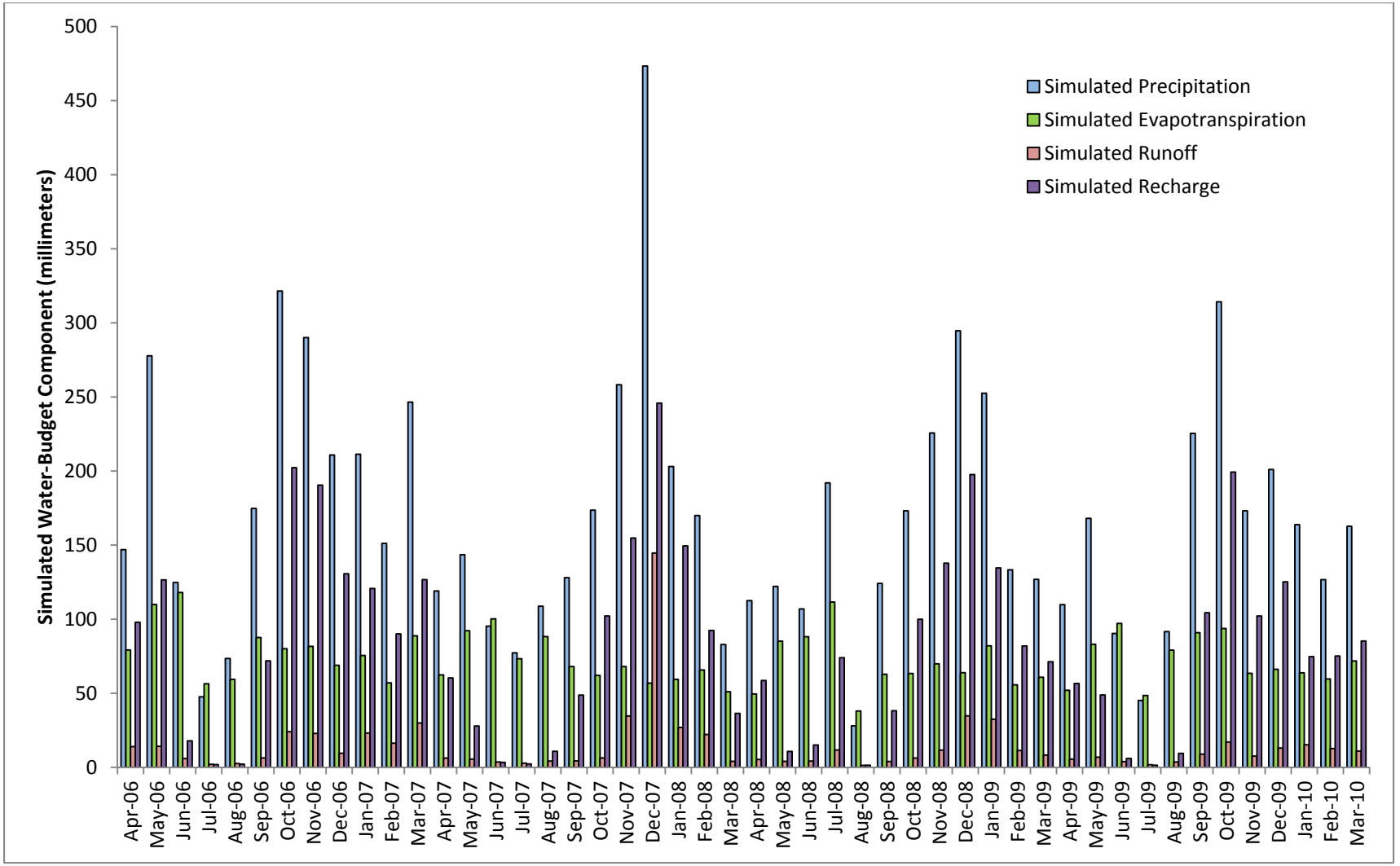

Figure 20. Simulated monthly precipitation, evapotranspiration, runoff, and groundwater recharge for the Kawela watershed over the entire simulation period.

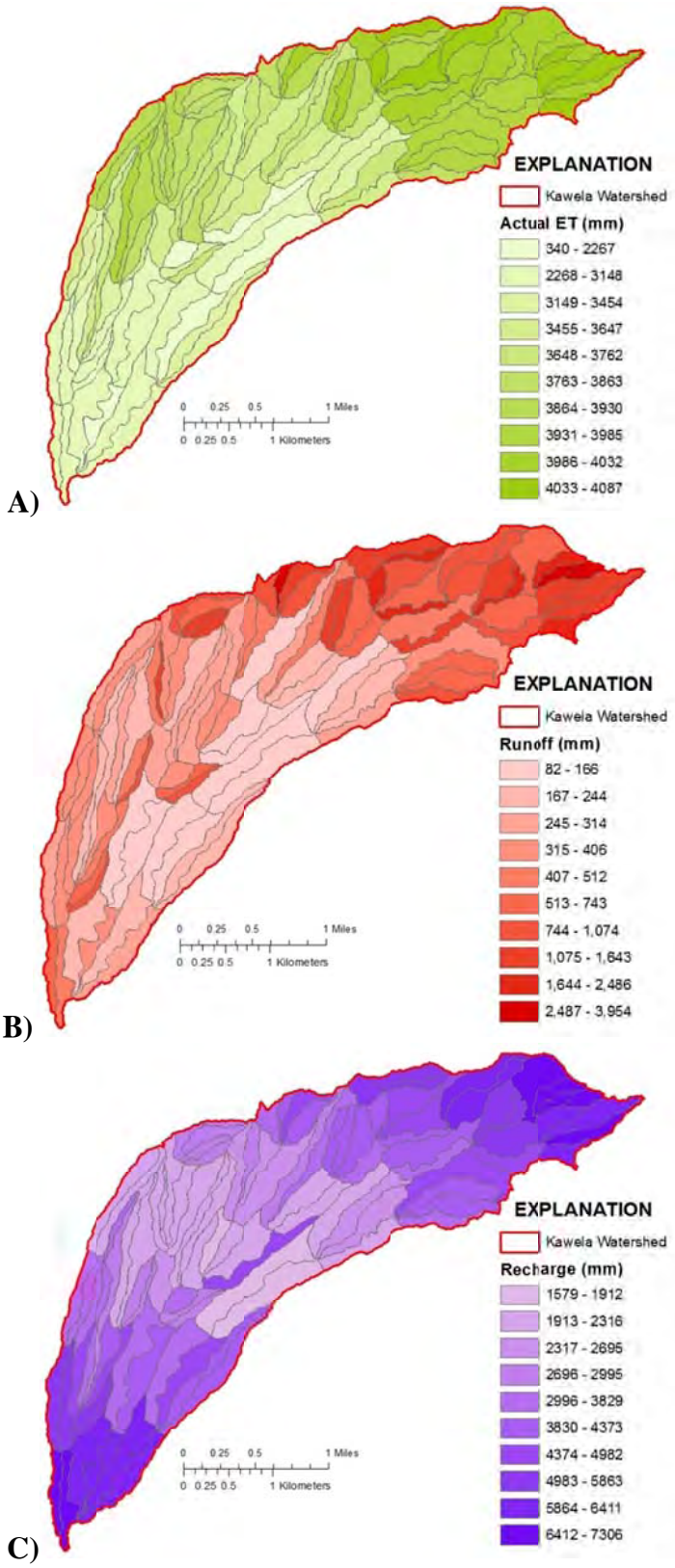

Figure 21. Spatial variability of the A) actual ET, B) runoff, and C) groundwater recharge by HRU for the entire 4-year simulation period.

drip as an added precipitation component to the water budget. The Kawela area recharge estimate of 250 mm/year from the State of Hawai‘i (1990) study is low due to the method used to calculate the evapotranspiration and the exclusion of fog drip. The water budget by Shade (1997) was calculated monthly for a 51.3 square kilometer Kawela aquifer system using maps of mean monthly rainfall from the base period 1931-1983 from Giambelluca et al. (1986). Shade (1997) used two different methods for calculating evapotranspiration and provided an average value by averaging the results of the two accounting methods. The first accounting method allows excess soil moisture to be allocated to groundwater recharge first and the second method allows excess soil moisture to be allocated to evapotranspiration first. The average of the two methods was said to represent a reasonable, although not overly conservative estimate of groundwater recharge (Shade, 1997). Shade also did not account for any added component of fog drip in the water budget. The Kawela area recharge estimate of 360 mm/year from Shade (1997) is also low due to the exclusion of fog drip. Although the average annual water budget from the Kawela PRMS model was derived using data from a different and relatively short period, the ratios of the water-budget components to rainfall are comparable to those calculated by Shade (1997) (Table 16). The increase in the partitioning of rainfall to recharge is partially explained by the greater amount of rainfall and the inclusion of fog-drip in the PRMS Kawela model. Overall the daily, watershed-scale, temporal data used in the PRMS Kawela model can more accurately simulate evapotranspiration, runoff, and groundwater recharge because these components of the water budget are interacting on the order of minutes to hours for smaller watersheds like Kawela.

4.2.2 Land-Cover Change Comparisons

The calibrated PRMS Kawela model's simulated water budget was used as a baseline to assess different watershed land-cover changes and evaluate the hydrological system's sensitivity to changes in vegetation. A generalized map of Kawela watershed's vegetation cover before human impacts (Jacobi, 2011b, Figure 22) and simple cover-type conversions of HRUs within the watershed that reflect some type of restoration or degradation comprised the land-cover change scenarios evaluated. The effectiveness of the restoration scenario and impact of the degradation were assessed by examining the change in the partitioned amount of rainfall to runoff and recharge in each scenario relative to the baseline. Any scenario that decreases the amount of rainfall partitioned to runoff in the watershed and, by inference, the amount of sediment delivered to the nearshore environment, without drastically changing the amount of recharge in the watershed is considered an effective watershed restoration scenario.

Three land-cover change scenarios were simulated by manually changing the vegetation cover and soil-moisture parameter values that are affected by changes of the HRU's cover type and adjusting the fog-drip component of rainfall to fit the new cover-type designation. For two of the three land-cover change scenarios, the cover type of the final calibrated model's HRU was either upgraded or downgraded (Figure 23). For the "Grass to Bare" scenario, all HRUs that were designated as trees, shrubs, and grass were downgraded to shrubs, grass, and bare ground, respectively. For the "Bare to Grass" scenario, all HRUs that were designated as bare ground, grass, and shrubs were upgraded to grass, shrubs, and trees, respectively. These first two scenarios are not meant to represent an actual reconstruction of the land-cover in the watershed, but are simply proposed as possible cover-type conversion scenarios to evaluate either restoration or

degradation in the watershed. For the final "Pre-Human" land-cover scenario, a vegetation map created by Jacobi (2011b) representing the possible pre-human land-cover distribution in the watershed was used to determine the cover type of each HRU (Figure 23).

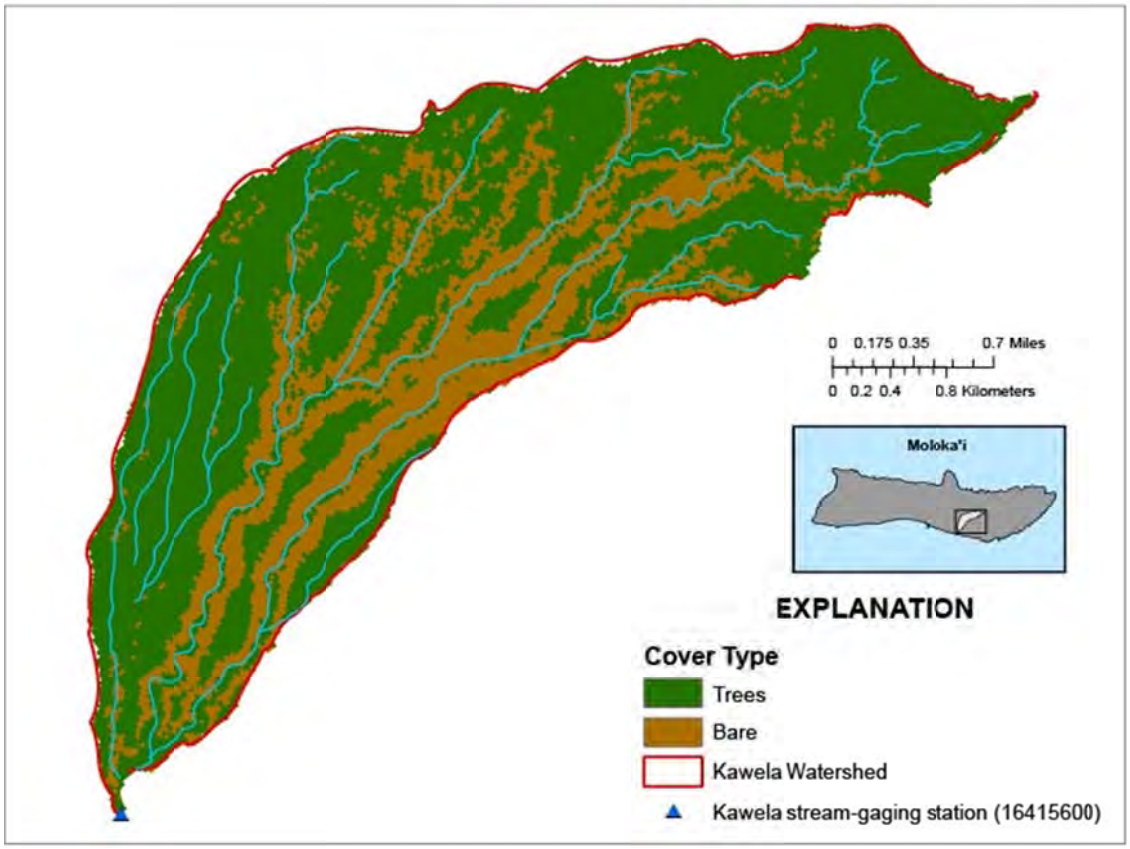

Figure 22. A generalized map of Kawela watershed's vegetation cover before human impacts (modified from Jacobi (2011b)).

Area-weighted averages of the vegetation-cover and soil-moisture parameter values for each cover-type category (bare, grass, shrubs, and trees) were calculated using the values for each HRU with that cover type specified in the final calibrated model. The area-weighted averages of the vegetation-cover and soil-moisture parameter values used in the land-cover change scenarios are summarized in Table 17.

Table 17. Area-weighted average parameter values for each cover type used in each land-cover change scenario
Parameter definitions are shown in Table 6.

	Cover Type			
Parameter	**Bare**	**Grass**	**Shrubs**	**Trees**
COVDEN_SUM	0.000	0.000	0.065	0.607
COVDEN_WIN	0.000	0.000	0.024	0.558
SRAIN_INTCP (mm)	0.117	0.281	0.874	1.259
WRAIN_INTCP (mm)	0.117	0.281	0.874	1.259
SOIL_MOIST_MAX (cm)	1.564	3.000	2.084	7.187
SAT_THRESHOLD (cm)	5.707	6.368	5.946	8.294
SOIL_RECHR_MAX (cm)	1.564	2.868	2.041	4.645
RAD_TRNCF	0.992	0.992	0.971	0.245

In areas of the watershed where the root depths and therefore soil-moisture parameter values were limited by the presence of rock beneath thin soil zones, the area-weighted average parameter values of the original land-cover type specified in the final model were used as input to the new land-cover type for the land-cover change scenario. For example, much of the watershed is covered by HRU's originally categorized as shrub, and many of those shrub HRU's have underlying geological constraints that restricts the rooting depth well above the shrub's potential rooting depth (as well as above the lesser potential rooting depth of grass). Therefore, when the cover type is switched from shrub to grass, the soil-moisture parameter values must still be limited by the original rooting depth constraints regardless of the potential rooting depth of the new cover type. In this example, the shrub soil-moisture parameter values were retained whereas the cover type and other vegetation parameter values were changed to the new area-weighted averages for grass.

A new fog adjustment was calculated with the same equation used in the final calibrated model that multiplies a fog interception-to-rainfall ratio and a fog-catch efficiency for the specified land-cover type within the HRU. The same 0.02, 0.12, and

0.21 fog interception-to-rainfall ratios were used in the fog-drip calculation for HRUs located in the following elevation ranges 762-914 meter, 915-1,219 meter, and 1,220-1,524 meter altitude ranges, respectively. HRUs with a tree land-cover classification were assigned a fog-catch efficiency of 1 and HRUs with shrubs were assigned a fog-catch efficiency of 0.5, reflecting the lower stature of shrubs relative to trees. All other HRU vegetation types were assumed to have zero fog-drip contribution. The calculated fog-drip adjustments for each of the relevant HRUs within the watershed for the three land-cover change scenarios are summarized in Table 18.

The results of the land-cover change scenarios using the area-weighted average values of vegetation and soil-moisture parameter values derived from the final calibrated model and the new fog-drip adjustments are summarized in Table 19.

In the "Grass to Bare" or more denuded vegetation scenario (Figure 23, plate B.) the amount of precipitation that is partitioned into runoff increases from 8 to 9 percent and the overall amount of precipitation in the water budget decreases by 4.4 percent due to a decrease in fog-drip contributions. In the "Bare to Grass" or more vegetated scenario (Figure 23, plate C.) the amount of precipitation partitioned into runoff decreases from 8 to 7 percent and the overall amount of evapotranspiration increases by 11.6 percent due to the increased area of the tree cover type. The amount of precipitation in the water budget increased by only 0.2 percent due to additional fog drip, because much of the additional tree-covered HRUs are below the cut-off altitude for fog-drip formation. In the "Pre-Human" land-cover change scenario (Figure 23, plate D.) the same amount of precipitation is partitioned into runoff as the baseline case. However, more precipitation is partitioned into evapotranspiration (47 percent) and less into recharge (45 percent) due to the increase in tree cover.

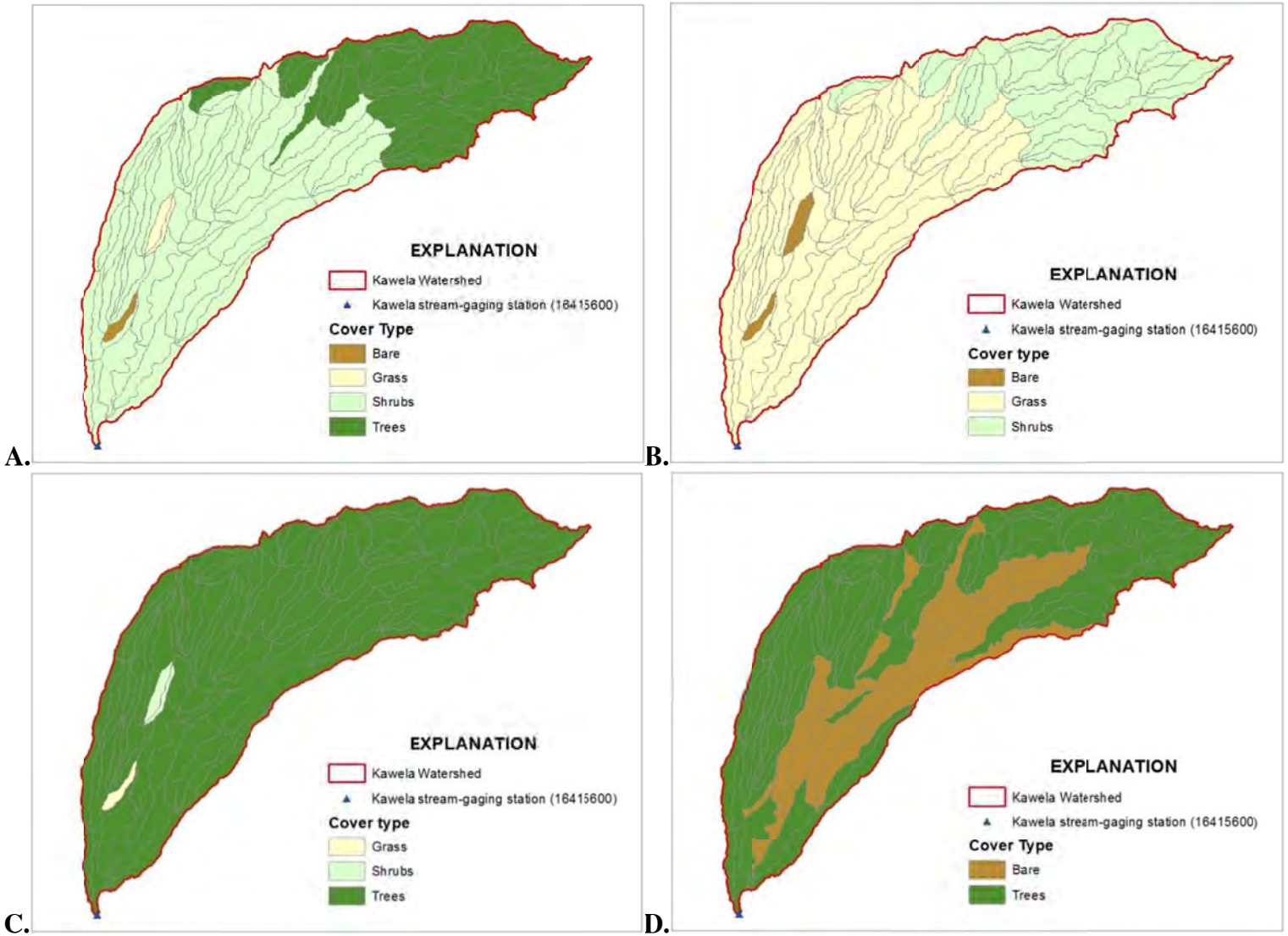

Figure 23. Cover types for each of the modeled HRUs in the A. Final calibrated model B. Grass to Bare scenario C. Bare to Grass scenario and D. Pre-human scenario

Table 18. Calculated fog-drip adjustment for relevant HRUs within the Kawela watershed for the final calibrated model and the three land-cover change scenarios.

HRU	Final Calibrated Model	Grass to Bare	Bare to Grass	Pre-Human
4	0.02	0.01	0.02	0.02
5	0.02	0.00	0.02	0.02
12	0.01	0.01	0.02	0.02
14	0.06	0.00	0.02	0.02
15	0.01	0.06	0.12	0.12
16	0.01	0.00	0.12	0.12
17	0.01	0.06	0.12	0.12
19	0.12	0.06	0.12	0.12
20	0.12	0.00	0.02	0.02
21	0.01	0.00	0.02	0.00
25	0.12	0.06	0.12	0.12
26	0.01	0.00	0.02	0.02
27	0.12	0.00	0.02	0.02
28	0.02	0.06	0.12	0.12
29	0.01	0.06	0.12	0.12
32	0.12	0.01	0.02	0.00
36	0.12	0.06	0.12	0.12
37	0.12	0.00	0.02	0.02
38	0.12	0.06	0.12	0.12
40	0.12	0.06	0.12	0.12
41	0.12	0.06	0.12	0.12
43	0.12	0.06	0.12	0.12
47	0.01	0.00	0.02	0.00
50	0.12	0.00	0.12	0.00
51	0.06	0.00	0.02	0.00
52	0.01	0.11	0.21	0.21
55	0.01	0.06	0.12	0.12
59	0.12	0.06	0.12	0.00
63	0.01	0.11	0.21	0.21
64	0.12	0.00	0.02	0.00
65	0.21	0.00	0.02	0.02
67	0.01	0.06	0.12	0.00
70	0.12	0.06	0.12	0.00
71	0.12	0.06	0.12	0.12
73	0.12	0.00	0.02	0.02
74	0.12	0.06	0.12	0.12
75	0.21	0.00	0.02	0.00
75	0.21	0.11	0.21	0.00
77	0.01	0.11	0.21	0.21
78	0.12	0.11	0.21	0.21
79	0.21	0.11	0.21	0.21
80	0.12	0.06	0.12	0.12
81	0.21	0.11	0.21	0.21
83	0.21	0.11	0.21	0.21
84	0.12	0.06	0.12	0.12
85	0.21	0.06	0.12	0.00

Table 18. Calculated fog-drip adjustment for relevant HRUs within the Kawela watershed for the final calibrated model and the three land-cover change scenarios–Continued.

HRU	Final Calibrated Model	Grass to Bare	Bare to Grass	Pre-Human
86	0.21	0.06	0.12	0.12
87	0.21	0.06	0.12	0.12
96	0.12	0.06	0.12	0.12
97	0.12	0.11	0.21	0.21
98	0.21	0.11	0.21	0.21
99	0.21	0.11	0.21	0.21

Table 19. Water budget for the final model and for each of the land-cover change scenarios (4/1/2006-3/31/2010).
[mm: millimeters; ET: Evapotranspiration]

Scenario	Precipitation (mm)	ET (mm)	Storage (mm)	Runoff (mm)	Recharge (mm)	ET/ Precipitation Ratio (%)	Runoff/ Precipitation Ratio (%)	Recharge/ Precipitation Ratio (%)
Final Model	8,070	3,510	20	680	3,870	43	8	48
Grass to Bare	7,720	3,390	10	660	3,660	44	9	47
Bare to Grass	8,090	3,920	50	570	3,560	48	7	44
Pre-Human	8,000	3,750	30	610	3,610	47	8	45

To provide insight into sediment transport to the nearshore environment, the top ten daily peak flows for the entire period were compared for each of the land-cover change scenarios (Figure 24). Although daily peak flows underestimate the instantaneous peak flows within a day, daily peak flows may be a useful indicator of potential sediment transport (Figure 25). Most of the sediment transported to the nearshore environment likely occurs during larger storms. Four of the top ten peaks for the entire period are from a December 2007 event. The largest simulated peak of 5.93 m^3sec^{-1} on December 6, 2007 was reduced to 5.42 m^3sec^{-1} with the Pre-Human scenario, reduced to 5.35 m^3sec^{-1} with the Bare to Grass scenario, and increased to 5.98 m^3sec^{-1} with the Grass to Bare scenario

(Figure 24). Overall, the Pre-human and Bare to Grass scenarios reduced the top ten peak flows by 8.7 and 16.6 percent, respectively. The Grass to Bare scenario increased the top ten peak flows by 42.6 percent.

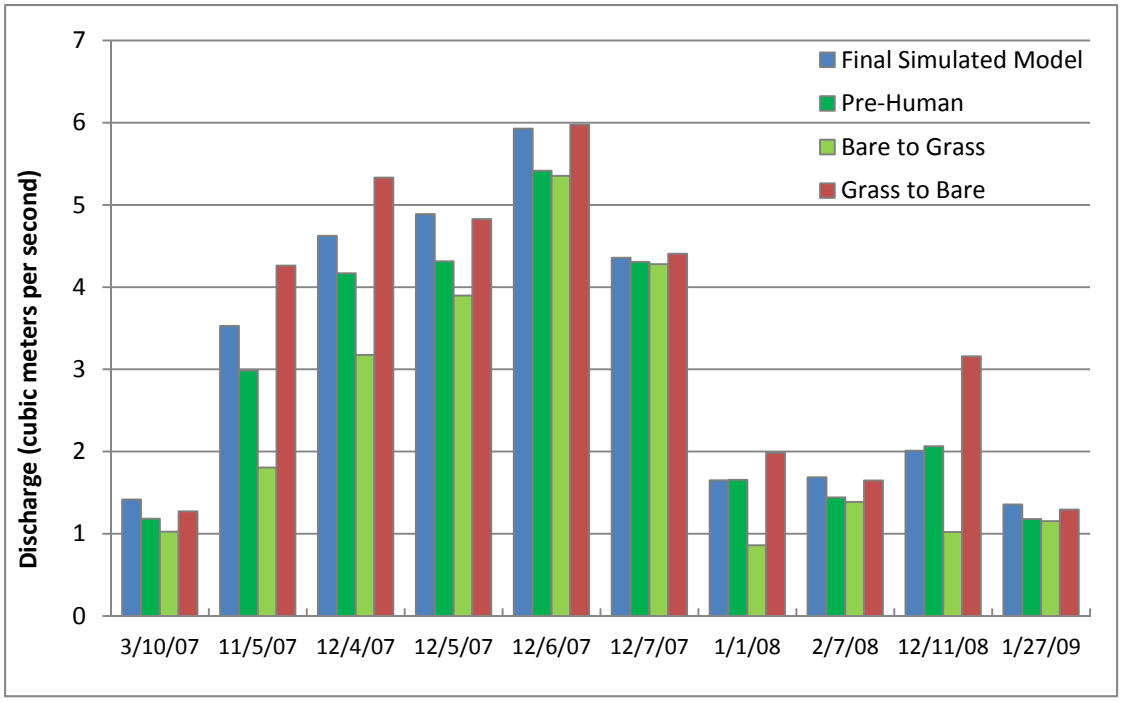

Figure 24. Top ten peak flows for the entire period for each land-cover change scenario compared to the final simulated model.

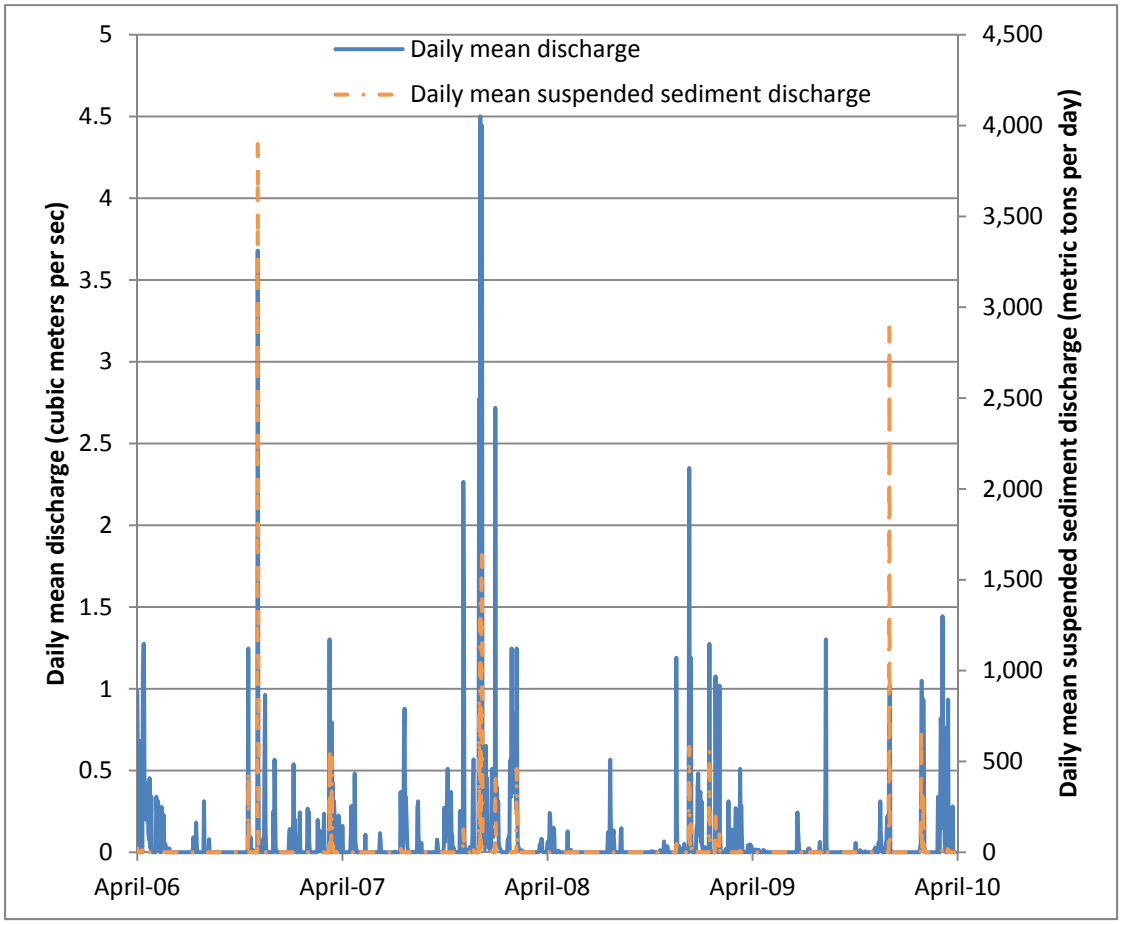

Figure 25. Daily mean discharge and daily mean suspended-sediment discharge for the entire period.

Although the results here are presented for hypothetical, simplified conditions of land-cover changes, PRMS can be used to evaluate the watershed's hydrological response to accurately defined changes in basin characteristics. The "Grass to Bare" scenario provides an example of how further vegetation denudation in Kawela watershed affects the water budget by decreasing the overall precipitation in the watershed and increasing the amount of runoff, and therefore sediment, that reaches the nearshore environment. The other "Bare to Grass" land-cover change scenario provides an example of how a restoration effort could affect the water budget by successfully reducing the amount of runoff reaching the nearshore environment.

4.3 Model and Data Limitations

PRMS is a practical tool that makes it possible to simplify complex natural systems through sets of mathematical equations representing the major components of the hydrological cycle and hydrological processes involved. Due to the assumptions and simplifications that must be made, error and uncertainty are built into the model. In PRMS, the delineated HRUs are assumed to be homogeneous with respect to both their parameter values and computations of storage and flow (Markstrom et al., 2008). Even though the 99 HRUs in the PRMS Kawela model capture some of the heterogeneity of the watershed characteristics, these characteristics still must be simplified into these assumed homogenous units. Models in general are also limited by errors associated with the input data. The quality and accuracy of time-series data for precipitation, temperature, runoff, and potential evapotranspiration impact the accuracy of the simulation results. Calibration and validation were done for a specific time period and range of streamflow and therefore it is uncertain how the model will perform under different conditions.

Much of the error and uncertainty associated with the rainfall input data used for the daily mean-field bias correction has been described by Rotzoll and El-Kadi (2012). The NEXRAD-derived rainfall estimates corrected with data from the five Kawela area rain gages using the daily mean-field bias were used to create a rainfall dataset with the spatial variability of the radar data and the quality of rain-gage observations. However, without a rain gage near the headwaters of the watershed, the corrected NEXRAD-derived rainfall is uncertain in the upper reaches of the watershed.

Watersheds are dynamic systems and the physical parameters specified in PRMS are static. Physical HRU parameter values derived from the 2011 vegetation map (Jacobi,

2011a) using 2004 QuickBird imagery represent the modeled period well. However, the cover-density information derived from the 2001 National Land Cover Data set and impervious-surface data produced by the Multi-Resolution Land Characteristics Consortium (Multi-Resolution Land Characteristics Consortium, 2001) may not as accurately represent the current condition of the watershed. Physical soil properties for the model were derived from the U.S. General Soil Map (STATSGO2) (Natural Resources Conservation Service, 2006) and the large 1:250,000 scale limits the extent to which PRMS can represent the actual hydrological system. Modeling errors can also be associated with the parameter-estimation process during the calibration procedure. Calibrated parameter values were constrained using an upper and lower limit during the automatic PEST calibration so that no physical relations were violated in the optimization process. Finally, the model was only calibrated to the measured streamflow at the USGS Kawela Gulch stream-gaging station, and runoff only accounted for 8 percent of precipitation partitioned into the simulated water budget components. Ideally, the model should have also been calibrated to measured datasets of potential ET and solar radiation, but those datasets for the study area were not available.

The model does not represent low flows well, which may be a problem for estimating water availability for some instream uses. PRMS has both surface water and groundwater components, but it lacks the capabilities to adequately simulate surface water and groundwater interactions. Therefore, losing streams (channel seepage losses) are not well represented in PRMS. The model may also be overestimating low flows due to persistent rainfall in the NEXRAD-derived rainfall dataset.

The inferences related to sediment discharge are also limited by the fact that the model is not an event based model. The model predicts a daily mean streamflow which underestimates the instantaneous peak flow within a day, therefore inferences related to sediment discharge are uncertain.

4.4 Recommended Future Research

PRMS has adequately modeled the hydrology and land-cover change effects on a small, leeward Hawaiian watershed on a daily time step using rain-gage corrected NEXRAD-derived rainfall. However, research should continue to improve the NEXRAD-derived rainfall dataset, so that the corrected NEXRAD-derived rainfall dataset will more accurately reflect smaller rainfall events and days without rain in the watershed. PRMS could also be modified to better simulate losing streams, or perhaps the GSFLOW model (Markstrom et al., 2008), which couples PRMS and the USGS' Modular Groundwater Flow model (MODFLOW), and which more realistically simulates surface water and groundwater interactions could be evaluated for application in leeward Hawaiian watersheds.

Future research should evaluate whether PRMS can also be applied in larger, windward Hawaiian watersheds on a daily time step using rain-gage corrected NEXRAD-derived rainfall. By coupling PRMS to a suitable sediment-transport model, it will be possible to evaluate the potential of PRMS to predict sediment loads from Hawaiian watersheds. When climate-change datasets to drive PRMS become available for Hawai‘i, PRMS' performance in modeling climate-change scenarios should also be evaluated for Hawaiian watersheds.

Chapter 5

SUMMARY AND CONCLUSIONS

The Precipitation-Runoff Modeling System software developed by the USGS (Leavesley et al., 1983) was used to construct a watershed model for Kawela, southern Moloka‘i, Hawai‘i, and this model was used to evaluate the effects of land-cover changes on runoff and groundwater recharge.

PRMS was run in “daily mode” using daily datasets for Kawela watershed. Daily streamflow data from the USGS Kawela Gulch stream-gaging station (16415600) were used to calibrate the model. Daily minimum and maximum temperature data from four climate stations across the island, rainfall data estimated from NEXRAD data and corrected with data from the five Kawela-area rain gages using a mean-field bias correction, and potential evapotranspiration calculated externally from PRMS with a Java script using the Penman-Monteith daily reference evapotranspiration equations were used as input for the final Kawela model. Fog interception was incorporated as an added precipitation input for HRUs that are located at altitudes of 762 meters or higher and with land-cover designations of either trees or shrubs. The watershed boundary and HRUs were delineated using the automated delineation procedure in the GIS Weasel (Viger et al., 2007). Physical distributed parameter values for each HRU were based on the USGS DEM, the 2001 National Land Cover Data set, and the STATSGO soils dataset using the parameterization methods in the GIS Weasel (Viger et al., 2007). The *xyz_dist* module, which uses a three-dimensional multiple-linear regression based on latitude, longitude, and altitude of climate stations, was used to distribute temperature and precipitation data to each HRU.

The model was run for an initial period (10/1/2004-3/31/2006) to allow the model to estimate initial conditions in the watershed. The model was calibrated using data from 4/1/2008-3/31/2010 and validated using data from 4/1/2006-3/31/2008. Simulation results for the calibration, validation, and entire (4/1/2006-3/31/2010) periods were evaluated both statistically and graphically. The coefficient of efficiency for the daily PRMS Kawela model ranges from 0.46 for the calibration period to 0.56 for the validation period. Both values indicate that the daily PRMS Kawela model's predictive power is greater than using the mean measured value of runoff. The coefficient of efficiency for the entire period is 0.55, and this value confirms that overall the model's simulated hydrograph reasonably fits the measured hydrograph. The bias statistic indicated that the PRMS Kawela model overestimated runoff in the calibration period (bias=6.3 percent) and underestimated runoff in the validation period (bias=-15.4 percent). Overall, the model computed the total runoff volume within 8.7 percent over the entire simulation period. The lower root-mean-square error to standard deviation of the observation ratio (RSR) indicated that the model performed better in the wetter validation period (RSR=0.66) than the drier calibration period (RSR=0.74). Overall, the RSR value for the entire period (RSR=0.62) indicates a satisfactory model performance.

The simulated water budget was then used to calculate groundwater recharge in the watershed and the percentage of precipitation that was partitioned into evapotranspiration, runoff, and recharge. Simulation results for the four year period (04/01/2006-03/31/2010) indicate that most of the precipitation that falls on the watershed is either partitioned into evapotranspiration (43 percent) or groundwater recharge (48 percent). A much smaller percentage of rainfall is partitioned into runoff (8 percent) that is measured at the outlet of the watershed.

The calibrated PRMS Kawela model's simulated water budget was then used as a baseline to assess different watershed land-cover changes and evaluate the hydrological system's sensitivity to changes in vegetation. A generalized map of Kawela watershed's vegetation cover before human impacts (Jacobi, 2011b) and simple cover-type conversions of HRUs within the watershed that reflect restoration or degradation were used as land-cover change scenarios. Compared to the current land cover, the tested land-cover change scenario of vegetation denudation resulted in a smaller component of fog-drip, which translated to a 4 percent decrease in precipitation and consequently only a 1 percent increase in the amount of precipitation partitioned into runoff. However, vegetation restoration decreases runoff by 16 percent, which, by inference, would lead to reduced sediment loading of the nearshore environment. The amount of precipitation partitioned into recharge changed by less than 5 percent in both scenarios.

The original contributions of this study included creating the first rainfall-runoff model for a Moloka‘i watershed, using a unique approach to correct NEXRAD-derived rainfall data and then using the corrected dataset as input to a rainfall-runoff model of a Hawaiian watershed, and evaluating the performance of the USGS' PRMS software for use in a small, leeward Hawaiian watershed. The PRMS Kawela model can serve as a management tool for stewards of this watershed and others that are hydrologically similar. Eventually, although not in the scope of this project, the calibrated and validated model could be coupled with a sediment-transport model to accurately determine the effect of different land-cover change scenarios on reducing the amount of sediment transported to the nearshore reef environment. PRMS' performance should also be evaluated in larger, windward Hawaiian watersheds, and for modeling climate-change scenarios once these datasets become available for Hawai‘i.

References

Apple, M., 2008, Applicability of the Hydrological Simulation Program-Fortran (HSPF) for modeling runoff and sediment in Hawaii watersheds: MS Thesis, Honolulu, HI, University of Hawai‘i.

Bae, D.H., Jung, I.W., and Chang, H., 2008, Long-term trend of precipitation and runoff in Korean river basins: Hydrological Processes, v. 22, p. 2644–2656.

Barnhardt, W.A., Richmond, B.M., Grossman, E.E., and Hart, P., 2005, Possible modes of coral-reef development at Molokai, Hawaii, inferred from seismic-reflection profiling: Geo-Marine Letters, v. 25, no. 5, p. 315–323.

Bicknell, B.R., Imhoff, J.C., Kittle, J.L., Jobes, T.H., and Donigian, A.S., 2005, Hydrologic Simulation Program-FORTRAN (HSPF) Version 12.2, User’s Manual: Aqua Terra Consultants, Mountain View, CA.

Bingner, R.L., and Theurer, F.D., 2005, AnnAGNPS Technical Processes Documentation, Version 3.2: USDA-ARS and USDA-NRCS, Available at http://www.ars.usda.gov/Research, March.

Bothner, M.H., Reynolds, R.L., Casso, M.A., Storlazzi, C.D., and Field, M.E., 2006, Quantity composition and source of sediment collected in sediment traps along the fringing coral reef off Molokai, Hawaii: Marine Pollution Bulletin, v. 52, no. 9, p. 1034–1047.

Calhoun, R.S., and Field, M.E., 2008, Sand composition and transport history on a fringing coral reef, Moloka‘i, Hawai‘i: Journal of Coastal Research, v. 24, p. 1151–1160.

Carr, R.S., and Nipper, M., 2003, Toxicity testing of sediments from Molokai and Maui, Hawaii: Report prepared for U.S. Geological Survey, Pacific Science Center, Coastal and Marine Geology Program, Santa Cruz, California, 17 p.

Chang, H. J., and Jung, I. W., 2010, Spatial and temporal changes in runoff caused by climate change in a complex large river basin in Oregon: Journal of Hydrology (Amsterdam), v. 388, p. 186–207.

Cheng, C.L., 2007, Evaluating the Performance of AnnAGNPS and N-SPECT for Tropical Conditions: MS Thesis, Honolulu, HI., University of Hawai‘i.

Christensen, J.H., Hewitson, B., Busuioc, A., Chen, A., Gao, X., Held, I., Jones, R., Kolli, R.K., Kwon, W.-T., Laprise, R., Magaña Rueda, V., Mearns, L., Menéndez, C.G., Räisänen, J., Rinke, A., Sarr, A., and Whetton, P., 2007, Regional Climate Projections. In: Climate Change 2007: The Physical Science Basis. Contribution of Working Group I to the Fourth Assessment Report of the Intergovernmental Panel on Climate Change [Solomon, S., Qin, D., Manning, M., Chen, Z., Marquis, M., Averyt, K.B., Tignor, M., and

Miller, H.L. (eds.)]. Cambridge University Press, Cambridge, United Kingdom and New York, NY, USA.

Chu, P.S., and Chen, H., 2005. Interannual and interdecadal rainfall variations in the Hawaiian Islands: Journal of Climate. v. 18, p. 4796–4813.

Dawdy, D.R., Lichty, R.W., and Bergmann, J.M., 1972, A rainfall-runoff simulation model for estimation of flood peaks for small drainage basins: U.S. Geological Survey Professional Paper 506–B, p. 1-28.

DHI, 2003, MIKE SHE Flow Modules Manual: Danish Hydraulic Institute, Denmark.

Doherty, J., 2010, PEST: Model-Independent Parameter Estimation: User Manual: 5th Edition, Watermark Numerical Computing, Brisbane, Australia, 336 p.

Ekern, P.C., and Chang, J.-H., 1985, Pan evaporation; State of Hawai‘i, 1894–1983: Hawai‘i Department of Land and Natural Resources Report R74, 172 p.

Engels, M.S., Fletcher, C.H., III, Field, M.E., Storlazzi, C.D., Grossman, E.E., Rooney, J.B., Conger, C.L., and Glenn, C., 2004, Holocene reef accretion; southwest Molokai, Hawaii, U.S.A.: Journal of Sedimentary Research, v. 74, no. 2, p. 255–269.

Engott, J.A., 2011, A water-budget model and assessment of groundwater recharge for the Island of Hawai‘i: U.S. Geological Survey Scientific Investigations Report 2011–5078, 53 p.

Fares, A**.** 2008. Overview of the hydrological modeling of coastal watershed in small tropical islands. In Fares, A. and El-Kadi, A.I. (ed.) Coastal Watershed Management, WIT Press, Southampton, UK, 438 p., ISBN:978-1-84564-091-0.

Field, M.E., Cochran, S.A., Logan, J.B., and Storlazzi, C.D., eds., 2008, The coral reef of south Moloka’i, Hawai’i — portrait of a sediment-threatened fringing reef: U.S. Geological Survey Scientific Investigations Report 2007–5101, 180 p.

Giambelluca, T.W., Chen, Q., Frazier, A.G., Price, J.P., Chen, Y.-L., Chu, P.-S., Eischeid, J.K., and Delparte, D.M., 2012, Online Rainfall Atlas of Hawai‘i: Bull. Amer. Meteor. Soc., doi: 10.1175/BAMS-D-11-00228.1.

Giambelluca, T. W., Diaz, H. F., and Luke, M. S. A., 2008, Secular temperature changes in Hawai‘i: Geophysical Research Letters, v. 35, L12702, doi:10.1029/2008GL034377.

Giambelluca, T.W., Nullet, M.A., and Schroeder, T.A., 1986, Rainfall atlas of Hawai‘i: Hawai‘i Department of Land and Natural Resources Report R76, 267 p.

Giambelluca, T.W., and Nullet, M.A., 1992, Evaporation at high elevations in Hawaii: Journal of Hydrology, v. 136, p. 219-235.

Giambelluca, T.W., Martin, R.E., Asner, G.P., Huang, M., Mudd, R.G., Nullet, M.A., DeLay, J.K., and Foote, D., 2009, Evapotranspiration and energy balance of native wet montane cloud forest in Hawai‘i: Agricultural and Forest Meteorology, v. 149, p. 230-243.

Goode, D.J., Koerkle, E.H., Hoffman, S.A., Regan, R.S., Hay, L.E., and Markstrom, S.L., 2010, Simulation of runoff and reservoir inflow for use in a flood-analysis model for the Delaware River, Pennsylvania, New Jersey, and New York, 2004–2006: U.S. Geological Survey Open-File Report 2010–1014, 68 p.

Izuka, S.K., Oki, D.S., and Chen, C., 2005, Effects of irrigation and rainfall reduction on ground-water recharge in the Lihue Basin, Kauai, Hawaii: U.S. Geological Survey Scientific Investigations Report 2005–5146, 48 p.

Jacobi, J.D., 2011a, Generalized Moloka‘i RTR Vegetation Map [computer file]. Honolulu, HI: U.S. Geological Survey Pacific Islands Ecosystems Research Center.

Jacobi, J.D., 2011b, Generalized Moloka‘i Original Vegetation Map [computer file]. Honolulu, HI: U.S. Geological Survey Pacific Islands Ecosystems Research Center.

Juvik, J.O., and Ekern, P.C., 1978, A climatology of mountain fog on Mauna Loa, Hawai‘i Island: University of Hawai‘i Water Resources Research Center Technical Report no. 118, 63 p.

Juvik, J.O., and Juvik, S.P., 1998, Atlas of Hawai‘i (3rd ed.): Hilo, University of Hawai‘i Press, 352 p.

Leavesley, G.H., Lichty, R.W., Troutman, B.M., and Saindon, L.G., 1983, Precipitation-runoff modeling system–User’s manual: U.S. Geological Survey Water-Resources Investigations Report 83–4238, 207 p.

Leavesley, G.H., and Stannard, L.G., 1995, The precipitation-runoff modeling system PRMS, in Singh, V.P., ed., Computer Models of Watershed Hydrology: Highlands Ranch, CO, Water Resources Publications, p. 281–310.

Legesse, D., Vallet-Coulomb, C., and Gasse, F., 2003, Hydrological response of a catchment to climate and land use changes in Tropical Africa: case study

South Central Ethiopia. Elsevier Ltd, Oxford, UK, Journal of Hydrology, v. 275, 1/2, p. 67–85.

Mair, A., and Fares, A., 2010, Throughfall characteristics in three non-native Hawaiian forest stands: Agricultural and Forest Meteorology Journal. v. 150, p. 1453–1466.

Markstrom, S.L., Niswonger, R.G., Regan, R.S., Prudic, D.E., and Barlow, P.M., 2008, GSFLOW—Coupled ground-water and surface water flow model based on the integration of the Precipitation-Runoff Modeling System (PRMS) and the Modular Ground-Water Flow Model (MODFLOW-2005): U.S. Geological Survey Techniques and Methods 6-D1, 240 p.

Markstrom, S.L., Regan, R.S., Hay, L.E., Viger, R.J., Webb, R.M.T., and Payne, R.A., 2012, PRMS-IV, the Precipitation-Runoff Modeling System, Version 4: U.S. Geological Survey Techniques and Methods Draft, accessed January 11, 2013.

Mink, J.F., and Lau, L.S., 1992, Aquifer identification and classification for Moloka'i: Groundwater protection strategy for Hawai'i: University of Hawai'i Water Resources Research Center Technical Report 187, 31p.

Monteith, J.L., 1965, Evaporation and environment In: Proceedings of the 19th Symposium of the Society for Experimental Biology Cambridge University Press, New York, NY, p. 205–233.

Moriasi, D. N., Arnold, J.G., Van Liew, M.W., Bingner, R.L., Harmel, R.D., and Veith, T.L., 2007, Model evaluation guidelines for systematic quantification of accuracy in watershed simulations: Transactions of the ASABE, v. 50, no. 3, p. 885–900.

Multi-Resolution Land Characteristics Consortium (MRLC), 2001, National land cover database: accessed October 20, 2010, at http://www.mrlc.gov/nlcd.php.

Nash, J.E., and Sutcliffe, J.V., 1970. River flow forecasting through conceptual models. Part 1- A discussion of principles: Journal of Hydrology, v. 10, p. 282–290.

National Climatic Data Center, 2007, Quality controlled local climatological data: accessed October 20, 2010, at http://cdo.ncdc.noaa.gov/qclcd/QCLCD?prior=N.

National Climatic Data Center, 2013, Quality controlled local climatological data: accessed March 01, 2013, at http://www.ncdc.noaa.gov/cdo-web/quickdata.

National Oceanic and Atmospheric Administration (NOAA), 2004, Nonpoint Source Pollution and Erosion Comparison Tool (N-SPECT) Technical Guide: NOAA Coastal Service Center.

National Weather Service, Hydrology Laboratory, NOAA, 2010, WSR-88D Rainfall Estimation, Publications and Papers: accessed October 25, 2010, at http://www.nws.noaa.gov/oh/hrl/papers/papers.htm#wsr88d.

Natural Resources Conservation Service, 2006, U.S. General Soil Map (STATSGO2): Natural Resources Conservation Service, accessed October 20, 2010, at http://soils.usda.gov/survey/geography/statsgo/.

Notter, B., MacMillan, L., Viviroli, D., Weingartner, R., and Liniger, H., 2007, Impacts of environmental change on water resources in the Mt. Kenya region: Journal of Hydrology(Amsterdam), v. 343, no. 3/4, p. 266–278.

Ogston, A.S., Storlazzi, C.D., Field, M.E., and Presto, M.K., 2004, Sediment resuspension and transport patterns on a fringing reef flat, Molokai, Hawaii: Coral Reefs, v. 23, no. 4, p. 559–569.

Oki, D.S., 1997, Geohydrology and Numerical Simulation of the Ground-Water Flow System of Molokai, Hawaii: U.S. Geological Survey Water-Resources Investigations Report 97–4176, 62 p.

Oki, D.S., 2004, Trends in Streamflow Characteristics at Long-Term Gaging Stations, Hawaii: U.S. Geological Survey Scientific Investigations Report 2004–5080, 120 p.

Oki, D.S., 2006, Numerical simulation of the hydrologic effects of redistributed and additional ground-water withdrawal, Island of Molokai, Hawaii: U.S. Geological Survey Scientific Investigations Report 2006–5177, 57 p.

Polyakov, V., Fares, A., Kubo, D., Jacobi, J., and Smith, C., 2007, Evaluation of a non-point source pollution model, AnnAGNPS, in a tropical watershed: Environmental Modeling and Software, v. 22, p.1617-1627.

Presto, M.K., Ogston, A.S., Storlazzi, C.D., and Field, M.E., 2006, Temporal and spatial variability in the flow and dispersal of suspended-sediment on a shallow fringing reef flat, Molokai, Hawaii: Estuarine, Coastal and Shelf Science, v. 67, no. 1-2, p. 67–81.

Price, J., Gon III, S. M, Jacobi, J. D., and Matsuwaki, D., 2007, Mapping Plant Species Ranges in the Hawaiian Islands: Developing a Methodology and Associated GIS layers. Hawai‘i Cooperative Studies Unit Technical Report HCSU-008. University of Hawai‘i at Hilo. 58 p.

Price, J., Jacobi, J., Mehrhoff, L., Wagner, W., Lucas, M., and Row, B., In review, 2009, Digital Atlas of the Hawaiian Biota. (Presented as a poster at the Hawai‘i Conservation Conference, July 2009, Honolulu).

Roberts, L.M., 2001, Historical land use, coastal change, and sedimentation on south Molokai reefs, in Saxena, N.K., ed., Recent advances in marine science and technology, 2000: Honolulu, PACON International, p. 167–176.

Rodgers, K.S., Jokiel, P.L., Smith, W.R., Farrell, F., and Uchino, K., 2005, Biological survey in support of the USGS turbidity and sediment baseline survey on south Moloka‘i reef flat, April 2005: U.S. Geological Survey Open-File Report 2005–1361, 35 p.

Rotzoll, K., and El-Kadi, A.I., 2012, Application of Radar imagery as input to a rainfall-runoff model for the Kawela Watershed, Molokai: WRRC, University of Hawaii, Final Report, 6 p.

Safeeq, M., and Fares, A., 2012, Hydrologic effect of groundwater development in a small mountainous tropical watershed: Journal of Hydrology, v. 428–429, p.51–67.

Safeeq, M., and Fares, A., 2011, Hydrologic response of a Hawaiian watershed to future climate change scenarios: Hydrological Processes, v.26, p.2745–2764.

Sahoo, G.B., Ray, C., and De Carlo, E. H., 2006, Calibration and validation of a physically distributed hydrological model, MIKE SHE, to predict streamflow at high frequency in a flashy mountainous Hawaii stream: Journal of Hydrology, v. 327, p.94–109.

Shade, P.J., 1984, Hydrology and sediment transport, Moanalua Valley, Oahu, Hawaii: U.S. Geological Survey Water-Resources Investigations Report 84–4156, 54 p.

Shade, P.J., 1997, Water budget for the Island of Molokai, Hawaii: U.S. Geological Survey Water-Resources Investigations Report 97–4155, 20 p.

Sherrod, D. R., Sinton, J. M., Watkins, S. E., Brunt, K. M., Geologic Map of the State of Hawai‘i; 2007. U.S. Geological Survey Open-File Report 2007–1089.

Singh, J., Knapp, H., Vernon., Arnold, J.G. and Demissie, M., 2005, Hydrological modeling of the Iroquois river watershed using HSPF and SWAT: Journal of the American Water Resources Association, 41: 343–360. doi: 10.1111/j.1752-1688.2005.tb03740.x.

Smith, J. A., Baeck, M. L., Villarini, G., Welty, C., Miller, A. J., and Krajewski, W. F., 2012, Analyses of a long-term, high resolution radar rainfall data set for the Baltimore metropolitan region: Water Resour. Res., 48, W04504, doi: 10.1029/2011WR010641.

Snyder, R.L., and Eching, S., 2002, Penman-Monteith daily (24-hour) Reference evapotranspiration equations for estimating ET_0, ET_r and HS ET_0 with daily data. Regents of the University of California, Sacramento, CA.

State of Hawai‘i, 1990, Water resources protection plan, volumes I and II, Hawaii Water Plan: State of Hawai‘i, Commission on Water Resource Management.

Stearns, H.T., and Macdonald, G.A., 1947, Geology and ground-water resources of the island of Molokai, Hawaii: Hawaii Division of Hydrography Bulletin 11, Territory of Hawaii, 113p.

Stock, J.D. and Tribble, G., 2010, Erosion and sediment loads from two Hawaiian watersheds, Joint Federal Interagency Conference, accessed October 30, 2010, at http://acwi.gov/sos/pubs/2ndJFIC/Contents/11D_Stock_02_28_10.pdf

Stock, J.D., Hanshaw, M.N., Rosener, M., Schmidt, K. M., Brooks, B. A., Tribble, G., and Jacobi, J., 2009, Hillslope-channel coupling in a steep Hawaiian catchment accelerates erosion rates over 100-fold: Eos Trans. AGU, 90(52), Fall Meet. Suppl., Abstract EP53E-04.

Storlazzi, C.D., Ogston, A.S., Bothner, M.H., Field, M.E., and Presto, M.K., 2004, Wave- and tidally-driven flow and sediment flux across a fringing coral reef; South-central Molokai, Hawaii: Continental Shelf Research, v. 24, no. 12, p. 1397–1419.

Takahashi, M., Giambelluca, T.W., Mudd, R.G., DeLay, J.K., Nullet, M.A., and Asner, G.P., 2011, Rainfall partitioning and cloud water interception in native forest and invaded forest in Hawai‘i Volcanoes National Park: Hydrological Processes, v. 25, p.448-464.

U. S. Geological Survey, 2010 a, National Water Information System: USGS Water Data for Hawai‘i: accessed October 24, 2010, at http://waterdata.usgs.gov/hi/nwis/nwis

U. S. Geological Survey, 2010 b, National Elevation Database: accessed October 20, 2010, at http://ned.usgs.gov.

Viger, R.J., and Leavesley, G.H., 2007, The GIS Weasel user's manual: U.S. Geological Survey Techniques and Methods, book 6, chap. B4, 201 p.; http://pubs.usgs.gov/tm/2007/06B04/

Ward-Garrison, C., Markstrom, S.L., and Hay, L.E., 2009, Downsizer—A graphical user interface-based application for browsing, acquiring, and formatting time-series data for hydrologic modeling: U.S. Geological Survey Open-File Report 2009–1166, 27 p.

Weisler, M., and Kirch, P.V., 1985, The structure of settlement space in a Polynesian chiefdom: New Zealand Journal of Archaeology, v. 7, p. 129-158.

Wigmosta, M.S., Lettenmaier, D.P., and Vail, L.W., 1994, A distributed hydrology vegetation model for complex terrain: Water Resources Research, v.30, p.1665–1679.

Yeung, C.W., 2004, Rainfall-runoff and water-balance models for management of the Fena Valley Reservoir, Guam: U.S. Geological Survey Scientific Investigations Report 2004–5287, 52 p.